324

THE 515NM ELECTROCHROMIC ABSORPTION CHANGE AND PHOTOSYNTHETIC ELECTRON TRANSPORT

LINDA BEATRICE GIORGI

A thesis submitted to the University of London
for the degree of Doctor of Philosophy

January 1984
Imperial College
Department of Pure and Applied Biology
London

ABSTRACT

The factors controlling the generation of the fast (phase a) and slow (phase b) rises of the flash-induced 515nm electrochromic absorption change (ΔA_{515}) in chloroplasts have been investigated.

Redox potentiometric titrations indicate that phase a (complete in < ms) is apparent over the redox potential span of the initial photochemical reactions of photosystems 1 and 2. Three waves in the low potential titration of phase a with $E_{m,7.5}$ of +60mV, -190mV and < -400mV can be detected. From the insensitivity to the inhibitor DCMU, it is proposed that the species with $E_{m,7.5}$ of -190mV and < -400mV are both related to photosystem 1. A much slower phase, which occurs in the millisecond time domain, can be detected at positive redox potentials. It is enhanced in amplitude over the +100mV redox potential range, in which the plastoquinone pool is chemically reduced, but is attenuated at redox potentials in which the cytochrome b-563 is reduced. Changes in the amplitude of both phase a and phase b are incurred upon the destacking of the thylakoid grana.

To determine the underlying mechanism generating phase b, flash-induced studies of the ΔA_{515} and of the cytochrome b-563 and cytochrome f redox reactions, have been carried out, using different reductants and under different salt conditions. These indicate that phase b can be correlated with cytochrome b-563 reoxidation, via a Q-cycle type mechanism. This conclusion is further supported by studies of the effect of electron transfer inhibitors on phase b, and their effect on cytochrome redox changes and proton uptake/release.

ACKNOWLEDGEMENTS

I would like to thank Prof. James Barber, my supervisor, for introducing me to the fascinating world of photosynthesis, for his help and encouragement throughout the course of this work, and for his constructive comments during the preparation of this thesis.

I am indebted to Dr. Nigel Packham for many useful and stimulating discussions, for his time and interest and for his constant encouragement. I would also like to thank him for his many constructive comments on the manuscript.

I am grateful for many other useful discussions with various members of the ARC Photosynthesis group but in particular I would like to thank Drs. Lars Olsen, Alison Telfer, Bob Ford and Barry Rubin. I also acknowledge the invaluable technical support of John De-Felice and Kathy Wilson.

I thank my family and David for their constant encouragement throughout the course of this project and for their patience during the writing up period.

My thanks to Lyn Barber for her help with the diagrams and to Patrizia Stanzione for her careful typing of the manuscript.

Finally, I would like to thank the University of London for their financial support.

CONTENTS

Abstract 2

Acknowledgements 3

List of figures 7

List of tables 11

Symbols and Abbreviations 12

1 Introduction 15

1.1 The overall concept 15
1.2 Structure and function of the photosynthetic membrane 17
1.2.1 Components of the thylakoid membrane 17
1.2.2 Organization of components within the thylakoid membrane 21
1.2.3 Functional consequences resulting from the organization of the thylakoid membrane 24
1.3 Electron transport mechanisms involving the cytochrome $\underline{b}_6/\underline{f}$ complex 26
1.3.1 Properties of quinol oxidation 26
1.3.2 The Q-cycle and the alternative b-cycle 32
1.3.3 Inhibitors 37
1.3.4 Cyclic electron transport 39
1.4 Measurement of the electric field by electrochromism 40
1.4.1 Detection by electrochromism 40
1.4.2 Kinetic and spectral characteristics of flash-induced electrochromic absorption changes 41
1.4.3 Consequences of simple electrochromic theory 45
1.4.4 Electrochromic absorption changes induced by steady-state light 48
1.4.5 Electrochromic absorption changes induced by extrinsic electric field transients 51
1.4.6 Calibration of the flash-induced electric field 52
1.4.7 Limitations of the electrochromic method 53
1.5 Electrical events indicated by the flash-induced electrochromic absorption change: the fast phase 55
1.6 Electrical events indicated by the flash-induced electrochromic absorption change: the slow phase 58

1.6.1 Properties of the slow phase 58

1.6.2 Conditions required for the generation of the slow phase 60

1.6.3 Possible interpretations of the slow phase 61

1.7 Objectives of this thesis 64

2 Materials and Methods 66

2.1 Chloroplast preparation 66

2.1.1 Preparation of Class I intact chloroplasts 66

2.1.2 Determination of chlorophyll 67

2.2 Flash-induced absorption measurements 68

2.2.1 Apparatus 68

2.2.2 Flash-induced 515nm electrochromic absorption changes 70

2.2.3 Flash-induced cytochrome and P700 absorption changes 71

2.2.4 Redox titrations of the flash-induced 515nm absorption change 71

2.2.5 Flash-induced proton uptake from the outer aqueous phase 77

2.2.6 Flash-induced proton release into the inner aqueous phase 78

2.3 Steady state chlorophyll fluorescence measurements 79

3 The electrochromic properties of the 515nm absorption change 81

3.1 Physical features of the 515nm absorption change 81

3.2 Evidence for the electrochromic nature of the ΔA_{515} 83

3.3 Localized and delocalized electric fields 91

3.4 Discussion 94

4 Redox potentiometric titrations of the 515nm absorption change 97

4.1 The salt dependence of the 515nm electrochromic shift 97

4.2 Redox potential titrations of phase a 101

4.3 Redox potential titrations of phase b 111

4.4 Discussion 113

5	The electrochromic absorption change related to electron transport	123
5.1	A comparative study of the ΔA_{515} with different reductants	123
5.2	Dithionite induced electron transport	128
5.3	Ferredoxin/NADPH induced electron transport	143
5.4	Durquinol induced electron transport	150
5.5	Ascorbate/DCPIP induced electron transport	153
5.6	Discussion	155
6	The electrochromic absorption change related to proton uptake/release	163
6.1	The effect of pH on the ΔA_{515} and cytochrome absorption changes	163
6.2	Flash-induced proton uptake	166
6.3	Flash-induced proton release	172
6.4	Discussion	179
7	Inhibitor studies	183
7.1	Inhibitor effects on the ΔA_{515}	183
7.2	Inhibitor effects on cytochromes b-563 and f	185
7.3	Inhibitor effects on proton uptake/release	191
7.4	Discussion	195
8	Summary and final discussion	201
References		215

LIST OF FIGURES

1.1 The Z-scheme 16

1.2 Schematic representation of the protein complexes of photosynthesis arranged as required for electron and proton transport 18

1.3 A model for the distribution of the thylakoid complexes within the thylakoid membrane 23

1.4 Six of the nine possible redox and protonation states of quinones in solution 27

1.5 Possible mechanisms of reduction of cytochrome c by quinols: the electron- and proton - transfer mechanisms 28

1.6 Possible schemes for the Q- and b-cycles 33

1.7 Schematic representation of the principle of electrochromism 42

1.8 Time course of the field-indicating absorption change; and scheme of the electric events on the thylakoid membrane, with the electrical analogue 44

1.9 Schematic drawing of the electric potentials of the thylakoid membrane before and after steady illumination 50

1.10 Topology of electrogenic and protolytic reactions in chromatophores 57

2.1 Schematic diagram of the single-beam flash spectrophotometer 69

2.2 The Nernst curves for one- and two-electron redox couples; and the theoretical E_m/pH relationship 75

3.1 Flash-induced ΔA_{515} under pseudocyclic conditions, with dithionite as reductant: to resolve the extent and kinetics of phase a and phase b 82

3.2 Semilogarithmic plots of the kinetics of phase a and phase b 84

3.3 To induce phase a and phase b of the flash-induced ΔA_{515} with dithionite, in DCMU-treated chloroplasts 86

3.4 Spectra of phase a and phase b of the flash-induced ΔA_{515} 88

3.5 Titrations of the flash-induced ΔA_{515} with valinomycin, and at different actinic light intensities 89

4.1 The salt-induced fluorescence increase 98

4.2 The effect of different salt concentrations on the flash-induced ΔA_{515}, under pseudocyclic conditions with dithionite as reductant 100

4.3 Redox titrations of the flash-induced ΔA_{515}, detected at 3ms, for stacked thylakoid membranes 102

4.4 pH dependence of the E_m for the low potential component of phase a 106

4.5 Redox titrations of the flash-induced ΔA_{515}, detected at 3ms, for unstacked thylakoid membranes 108

4.6 Redox titration of the flash-induced ΔA_{515}, detected at 10ms, for stacked thylakoid membranes 112

4.7 Redox titrations of phase b, under different conditions 114

4.8 pH dependence of the E_m for the high potential and low potential components of phase b 116

5.1 The flash-induced ΔA_{515} obtained in the presence of different reductants 124

5.2 Titration of the flash-induced ΔA_{515} with dithionite 129

5.3 The effect of different concentrations of MV on the flash-induced ΔA_{515} obtained under pseudocyclic conditions, with dithionite as reductant 130

5.4 Spectra of phase a and the delayed slow rise of the flash-induced ΔA_{515} 131

5.5 The effect of different salt concentrations on the flash-induced ΔA_{515}, under conditions for a delayed slow rise 132

5.6 Flash-induced spectra through the cytochrome α-band region, under pseudocyclic conditions, with dithionite as reductant, and at different MV concentrations 134

5.7 Flash-induced electrochromic and cytochrome ΔA, under pseudocyclic conditions, with dithionite as reductant, and for stacked/unstacked thylakoid membranes 139

5.8 Flash-induced ΔA_{515} under pseudocyclic conditions, with Fd/NADPH as reductant, for stacked/unstacked thylakoid membranes, and in the absence and presence of MV 144

5.9 Flash-induced electrochromic and cytochrome ΔA, under the conditions of Fig. 5.8 146

5.10 The effect of pH on the flash-induced electrochromic and cytochrome ΔA under pseudocyclic conditions, with Fd/NADPH as reductant, and in the presence of MV 148

5.11 Flash-induced ΔA_{515} under pseudocyclic conditions, with DQH_2 as reductant (at different concentrations) and for stacked/unstacked thylakoid membranes 151

5.12 Flash-induced electrochromic and cytochrome ΔA under the conditions of Fig. 5.11 152

5.13 Flash-induced electrochromic and cytochrome ΔA under pseudocyclic conditions, with Asc/DCPIP as reductant 154

5.14 Flash-induced electrochromic and cytochrome ΔA under pseudocyclic conditions, with DQH_2 as reductant, and in the presence of Asc/DCPIP 156

6.1 pH titration of the flash-induced ΔA_{515} under pseudocyclic conditions, with dithionite as reductant 164

6.2 The effect of pH on the flash-induced electrochromic and cytochrome ΔA, under the conditions of Fig. 6.1 165

6.3 Flash-induced proton uptake ΔA, under various conditions 167

6.4 pH titration of the calibrated extent of the proton uptake ΔA, and estimated H^+/P700 ratios 170

6.5 Flash-induced P700 ΔA, under various conditions 171

6.6 Flash-induced proton release ΔA: the effect of imidazole and nigericin 173

6.7 Flash-induced proton release ΔA in the presence of the reductant Fd/NADPH 174

6.8 Flash-induced proton release ΔA in the presence of the reductant DQH_2 178

7.1 The effect of inhibitors on the flash-induced ΔA_{515} under pseudocyclic conditions, with DQH_2 as reductant 184

7.2 Titration of the flash-induced ΔA_{515}, under the conditions of Fig. 7.1, with UHDBT 186

7.3 Titration of the flash-induced ΔA_{515}, under the conditions of Fig. 7.1, with antimycin 187

7.4 The effect of inhibitors on the flash-induced cytochrome b-563 ΔA, under the conditions of Fig. 7.1 188

7.5 The effect of inhibitors on the flash-induced cytochrome f ΔA, under the conditions of Fig. 7.1 189

7.6 The effect of inhibitors on the flash-induced proton uptake ΔA, under similar conditions to those of Fig. 7.1 192

7.7 The effect of inhibitors on the flash-induced proton release ΔA, under similar conditions to those of Fig. 7.1 193

8.1 A modified Q-cycle mechanism in chloroplasts 211

LIST OF TABLES

1.1 Estimated E_o values for couples of plastoquinol-1 in ethanol 30

SYMBOLS AND ABBREVIATIONS

Asc	ascorbate
ATP	adenosine triphosphate
BChl	bacteriochlorophyll
BSA	bovine serum albumin
Chl	chlorophyll
C.R.	cresol red
cyt.	cytochrome
DAD	2,3,5,6-tetramethyl-p-phenylenediamine
DBMIB	2,5-dibromo-3-methyl-6-isopropyl-p-benzoquinone
DCMU	3-(3,4-dichlorophenyl)-1,1-dimethylurea
DCPIP	2,6-dichlorophenolindophenol
DNP-INT	2-iodo-6-isopropyl-3-methyl-2',4,4'-trinitrodiphenyl ether
DQH_2	duroquinol
ΔA	absorption change
$\Delta \varepsilon$	extinction coefficient
E_h	ambient redox potential

$E_{m,7.5}$	midpoint redox potential (at pH 7.5)
Fd	ferredoxin
FeS	iron-sulphur centre
HEPES	N-2-hydroxyethylpiperazine-N'-2-ethanesulphonic acid
HQNO	2-heptyl-4-hydroxyquinoline N-oxide
λ	wavelength
MES	2-(N-morpholino)ethanesulphonic acid
MV	methyl viologen
$NADP^+$	nicotinamide adenine dinucleotide phosphate
NADPH	reduced $NADP^+$
N.R.	neutral red
P680	reaction centre of PS2
P700	reaction centre of PS1
PC	plastocyanin
PQ, PQH_2, $PQH^{\bullet}$, $PQH^{\bullet -}$	plastoquinone, plastoquinol, plastosemiquinone, anionic plastosemiquinone
PS	photosystem (1 or 2)
RFeS	Rieske iron-sulphur centre
Tricine	N-tris(hydroxymethyl)methylglycine

Tris	tris(hydroxymethyl)methylamine
UHDBT	5-(n-undecyl)-6-hydroxy-4,7-dioxobenzothiazole

CHAPTER 1

Introduction

1.1 The overall concept:

Photosynthesis is the process by which plants and bacteria convert light energy to chemical energy. During the light-driven reactions of green plants, which take place in and across the chloroplast thylakoid membrane, oxygen is evolved from water, $NADP^+$ is reduced and ATP is synthesized. These reactions are followed by a second series of reactions, which are independent of light, during which NADPH and ATP are used to power the assimilation and reduction of carbon dioxide to the level of carbohydrate.

The current understanding of the light reactions of photosynthesis has developed from the concept of two photosystems interacting in series to drive electrons and protons from water to $NADP^+$. This idea was originally proposed by Hill and Bendall (1960). Their scheme, the familiar Z-scheme, is based on the relationship of the various photosynthetic components in terms of their redox potentials and has received considerable support from a very wide range of experimental data. An updated version of the Z-scheme is given in Fig. 1.1

A modification of the Z-scheme, which takes into account the organization of the components within the thylakoid membrane, was required in the chemiosmotic hypothesis of Mitchell (1961). This hypothesis provides a logical explanation for the mechanism by which photosynthetic electron flow is coupled to photophosphorylation.

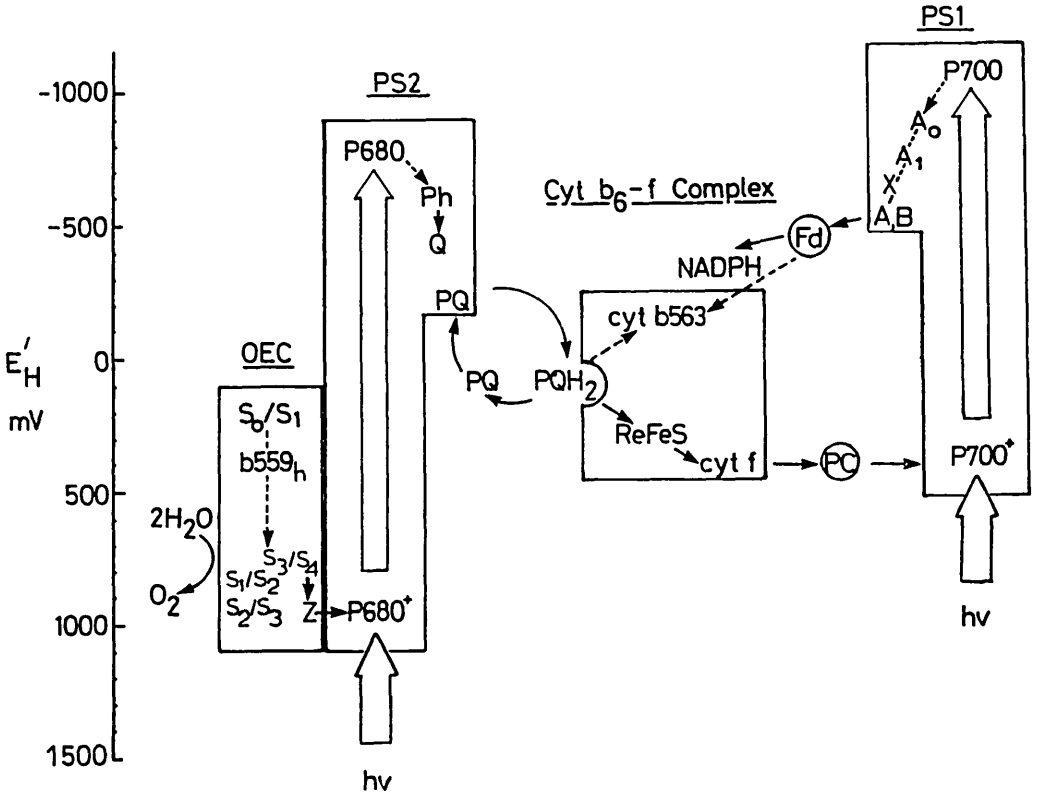


Fig. 1.1. The Z-scheme, in which the components of photosynthetic electron transport are placed on a redox scale. The major protein complexes involved are drawn as blocks. OEC, oxygen evolving complex; PS2, photosystem 2 complex; cyt b_6-f complex, cytochrome $\underline{b_6}$-$\underline{f}$ complex; PSI, photosystem I complex; s_o, s_I, s_2, s_3, s_4, s-states for water oxidation; b-559_h, high potential cytochrome $\underline{b}$-559; Ph, pheophytin; A_o, A_I, X, postulated PSI electron acceptors of unidentified chemical identity; A, B, iron-sulphur centres; other symbols as in Symbols and Abbreviations.

Of importance is that the electron transport components are necessarily assymmetrically located across the thylakoid membrane such that their cooperative interactions not only bring about the reduction of $NADP^+$, but also cause a vectorial transport of protons. The electrochemical potential gradient thus generated is then able to power the synthesis of ATP, via the coupling factor enzyme.

The work presented in this thesis is concerned with the light reactions of photosynthesis. It concentrates particularly on the electric field generated across the chloroplast thylakoid membrane, due to the vectorial charge separation at the reaction centre of each photosystem, upon light activation. Detailed analyses of the properties of the electric field (Witt, 1971; 1979) have already led to a considerable amount of information concerning the distribution of molecules within the membrane, proton translocation and photophosphorylation. In this study, the properties of the electric field are further examined in order to probe, and hence elucidate more clearly, the mechanism and control of the photosynthetic electron transport chain.

1.2 Structure and function of the photosynthetic membrane:

1.2.1 Components of the thylakoid membrane:

The components involved in light-harvesting, electron transport and proton translocation can be arranged into five major membrane-spanning complexes, three of which are directly involved in electron transport, see Fig. 1.2

The photosystem 2 (PS2) complex contains the reaction centre chlorophyll P680, together with a core of antenna chlorophyll a (Anderson, 1980).

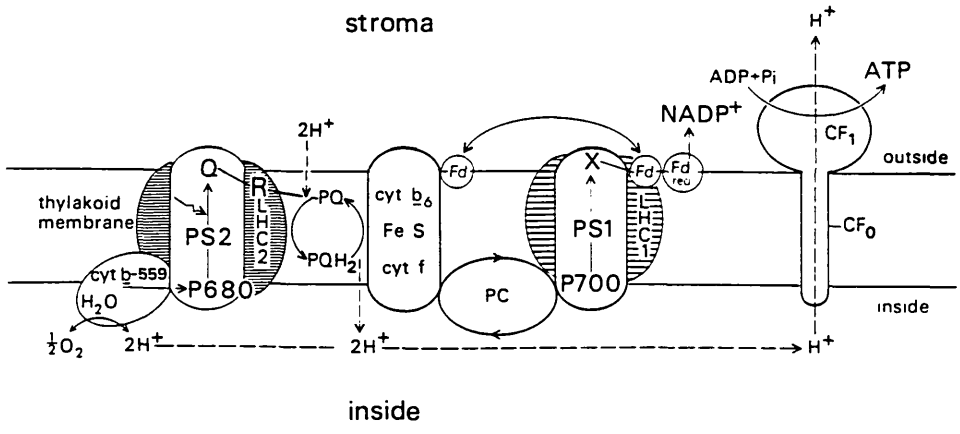


Fig. 1.2. Schematic representation of the protein complexes of photosynthesis, arranged as required for electron flow and proton translocation. (Taken from Anderson and Andersson, 1982).

The electron donor associated with this complex is the oxygen evolving system coupled with a series of intermediate donors (Radmer and Cheniae, 1977; Bouges-Bocquet, 1980a). The primary stable electron acceptor within this complex is the specialized quinone Q_A (Stiehl and Witt, 1969); the secondary acceptor is also a quinone molecule, Q_B, but which acts as a two electron accumulator (Bouges-Bocquet, 1973; Velthuys and Amesz, 1974). Also associated with this complex is the high potential cytochrome b-559 (Satoh, 1981) and a herbicide-binding polypeptide of mol. wt. 32,000 (Mullet and Arntzen, 1981).

The photosystem 1 (PS1) complex contains the reaction centre chlorophyll P700, and its antenna chlorophyll a (Anderson, 1980; Mullet et al 1980). A series of electron acceptors is also associated with this complex, including the primary acceptors A_1 and A_2, as well as two iron-sulphur centres (see Parson and Ke, 1982).

Between these two complexes is the recently isolated cytochrome b_6/f complex (Hurt and Hauska, 1981). It acts as a plastoquinol-plastocyanin oxidoreductase, and is strikingly similar in composition, redox properties and function to the cytochrome b-c_1 complexes of mitochondria and photosynthetic bacteria (see Bendall, 1982; Hauska et al, 1983). The isolated thylakoid complex is comprised of one cytochrome f, two cytochrome b-563, one Rieske iron-sulphur centre and a variable content of bound quinone. The two cytochrome b-563 haems can be distinguished by their redox forms: the $E_{m,7}$ values are -170mV (b_l) and -50mV (b_h), both components exhibiting a pH dependence between pH 6.0 and 9.0 (Hauska et al, 1983).

These three complexes are linked by the mobile electron carriers plastoquinone, plastocyanin and ferredoxin. Electron transport through both photosystems results in the reduction of $NADP^+$ and the transport

of protons from the outside to the intrathylakoid space. This proton gradient is used by a fourth complex, the ATPase complex, for making ATP. This complex consists of a hydrophobic component CF_0 , which acts as a proton conducting channel across the membrane, and a peripheral coupling factor CF_1 (see McCarty and Carmeli, 1982).

The fifth complex, the light-harvesting chlorophyll protein (LHCP) complex, has no catalytic activity itself; its primary function is to capture solar energy and efficiently transfer the excitation energy to the specialized membrane bound chlorophyll reaction centre. It contains up to half the total chlorophyll a and nearly all the chlorophyll b molecules (Thornber, 1975; Thornber and Barber, 1979). Since it is specifically associated with PS2, it is termed LHCP2. Recent evidence, however, suggests that another form of light-harvesting complex, with low chlorophyll b content, is associated with PS1 (Woolman and Bennoun, 1982); this has been designated LHCP1 (Brauman et al, 1982).

These supramolecular complexes are highly organized within the fluid lipid bilayer of the thylakoid membrane. An important feature of these thylakoid membranes is that they are arranged in such a way as to have distinguishable inner and outer surfaces: this is essential for the production of electrical and chemical gradients across their structure in order to drive the synthesis of ATP. A further important feature of the thylakoid membrane is that it differentiates into stacked (granal or appressed) and unstacked (stromal or non-appressed) regions (Coombs and Greenwood, 1976). The outer membrane surfaces of the two regions are thus different: only the stroma thylakoids and the end membranes and margins of the grana stacks are in direct contact with the chloroplast stroma while the closely appressed membranes of the grana have

limited contact with the stroma. As will be discussed below, such a structural differentiation is accompanied by a functional differentiation.

1.2.2 Organization of components within the thylakoid membrane:

Much of the information concerning the organization of components within the thylakoid membrane has been obtained from fractionation studies. The stromal lamellae and granal stacks can be separated by mechanical and detergent fractionation procedures (Anderson and Boardman, 1966; Boardman, 1970). Analyses of these fractionated membranes, together with freeze-fracture studies and fluorescence studies of excitation energy distribution between the two photosystems, has led to a variety of models for the organization of components within the thylakoid membrane (Seely, 1973; Thornber, 1975; Butler, 1978). However, only recently, with the introduction of an aqueous polymer two-phase partition technique for separating fragmented thylakoid membranes (Andersson et al, 1981), has concrete experimental evidence been provided for the lateral and transverse organization of components within the thylakoid membrane. The technique resolves out two membrane vesicle populations from thylakoid membranes: one exhibiting normal right-side-out properties while the other is turned inside-out, as judged by reversed proton and electrical gradients and by freeze-fracture electronmicroscopy (Andersson et al, 1981). In order to explain how the inside-out vesicles had been formed, Andersson (1978) has argued that they are specifically derived from the appressed membranes of the grana.

Analysis of these inside-out vesicles, in combination with electrophoretic methods, (Andersson and Anderson, 1980) has indicated that most of the photosystem 2 and light-harvesting complexes are located in the stacked thylakoid membrane regions. On the other hand, studies using right-side-out vesicles (Andersson and Haehnel, 1982), have provided evidence that

these vesicles, which are derived from stroma exposed thylakoids contain mainly photosystem 1 and ATP synthetase complexes. An extreme lateral separation of PS2 from PS1 had also been suggested by Barber (1980, 1982) based on considerations of electrical surface charge differences between appressed and non-appressed lamellae and on a detailed analysis of salt induced chlorophyll fluorescence changes.

The location of the cytochrome $\underline{b_6}/\underline{f}$ complex, within the thylakoid membrane, has been more controversial. Fragmentation studies suggest that, in contrast to the lateral assymmetry of the two photosystems and the ATP synthetase, the cytochrome $\underline{b_6}/\underline{f}$ complex is uniformly distributed between the two different thylakoid regions (Cox and Andersson, 1981). Recently, however, another possible site for its location has been suggested. In view of the electrical charge properties of both the cytochrome $\underline{b_6}/\underline{f}$ complex itself and particular thylakoid membrane regions, it has been suggested (Barber, 1983a) that the complex is located at the boundaries between the appressed and non-appressed regions. Support for this model also derives from the recent detergent-aided isolation of partition membranes (Berthold *et al*, 1982) which have high O_2-evolving capacity but contain no cytochrome $\underline{b_6}/\underline{f}$ complex. A model for the distribution of the thylakoid complexes between appressed and stroma-exposed thylakoids, with the cytochrome $\underline{b_6}/\underline{f}$ complex located at the boundaries, as discussed above, is depicted in Fig. 1.3.

Initial evidence for the vectorial arrangement of electron transport carriers, within the thylakoid membrane (see Fig. 1.2), resulted from analyses of the properties of the light-induced electric field (Witt, 1975). It was suggested that the electron donor sites for both PS1 and PS2 were located towards the inner thylakoid surface and the electron

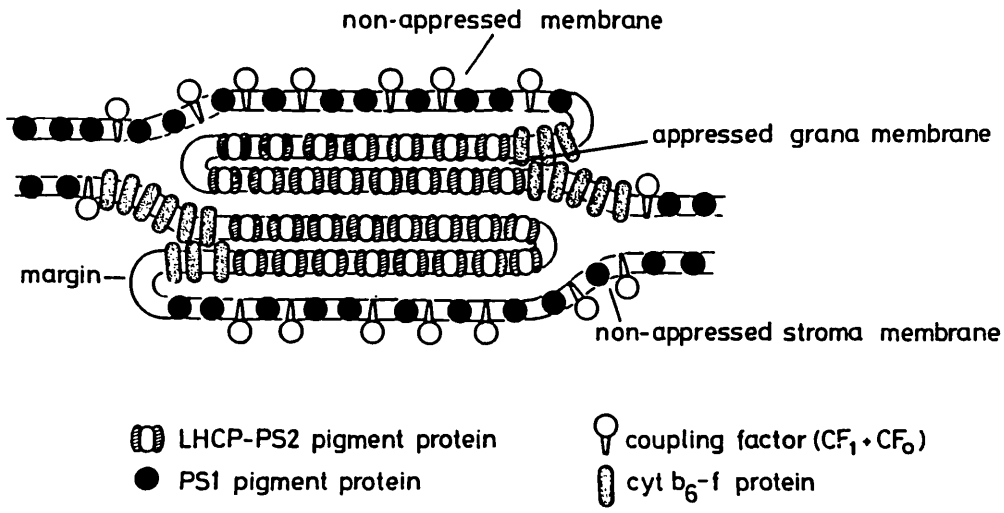


Fig. 1.3. A model for the distribution of the thylakoid complexes between appressed and stroma-exposed thylakoid membranes, with the cytochrome $\underline{b}_6/\underline{f}$ complex located at the boundaries between the appressed and non-appressed regions. (Taken from Barber, 1983a).

acceptors at the outer surface. Such an orientation is required to explain vectorial electron transport by each photosystem and the inward direction of proton pumping.

Recently, however, further evidence for this transverse assymmetry has resulted from studies using both inside-out and right-side-out thylakoid membrane vesicles. Reconstitution studies and analyses of the accessibility of specific reductants and inhibitors (Andersson et al, 1981) have provided further evidence in support of the hypothesis that the water-splitting enzyme is located at the inner thylakoid surface. Also, it has been shown that the extrinsic protein plastocyanin is loosely bound to the inner thylakoid membrane (Haehnel et al, 1981) and that the light-harvesting chlorophyll protein complex is indeed a membrane-spanning complex (Andersson et al, 1982).

1.2.3 Functional consequences resulting from the organization of the thylakoid membrane:

There are two main functional consequences resulting from the extreme lateral assymmetry of the protein complexes between appressed and stroma exposed thylakoids. One involves electron transport between laterally separated components and the other transfer of light energy between the two photosystems.

Since the protein complexes involved in electron transport are not uniformly distributed between appressed and non-appressed regions, this emphasizes the necessity of long range diffusional processes for electron transport to occur. It has thus been proposed (Anderson, 1982; Anderson and Andersson, 1982) that plastoquinone acts as the mobile carrier in

transporting electrons from the photosystem 2 complex to the cytochrome $\underline{b_6}/\underline{f}$ complex. The transfer of electrons from the cytochrome $\underline{b_6}/\underline{f}$ complex, whether it be located in the non-appressed or appressed regions, to nearby photosystem 1 complexes in the non-appressed thylakoids, is suggested to be facilitated by the extrinsic protein plastocyanin, possibly by diffusing laterally while attached to the inner membrane surface (Anderson, 1982; Anderson and Andersson, 1982; Haehnel, 1982). Cyclic electron flow around PS1 involving the cytochrome $\underline{b_6}/\underline{f}$ complex would require the diffusion of ferredoxin along the outer membrane surface. Changes in the lateral spatial relationship of these protein complexes (Barber, 1980) could result in an alteration of the balance between cyclic and non-cyclic electron flow. Also, changes in the fluidity of the lipid matrix of the thylakoid membrane could affect the rate of electron transport by affecting the diffusional rates of the mobile electron carriers (Ford and Barber, 1983).

Concerning the transfer of light energy between the two photosystems, the large distances separating the complexes tends to hinder efficient energy transfer. One possible mechanism to regulate this distribution of light energy between the two photosystems has recently been suggested by Barber (1982; 1983a; 1983b). Phosphorylation of some of the PS2 light-harvesting complexes (Bennett, 1977; Allen *et al*, 1981) would increase their net negative charge, thereby causing them to move from the appressed to the non-appressed membrane regions. This would affect the relative distribution of light to the two photosystems by allowing more of the light harvesting complex to interact with the photosystem 1 complex. Recent evidence suggests (Haworth *et al*, 1982; Horton, 1983) that during the phosphorylation process, *in vivo*, movement of the light-harvesting chlorophyll $\underline{a}/\underline{b}$ protein

does occur. Hence, lateral separation of the two photosystems, in combination with phosphorylation, would be one way for the controlled regulation of light energy distribution between the two photosystems.

1.3 Electron transport mechanisms involving the cytochrome b_6/f complex:

1.3.1 Properties of quinol oxidation:

Quinols play an essential role in the reduction of cytochromes *in vivo*. The reduced and oxidized forms of the quinol/quinone couple differ by two electrons and two protons. This inevitably means that semiquinones (resulting from single electron redox reactions) are involved in the reaction mechanism, as well as a variety of protonated species. Of the nine theoretically possible species in the quinol/quinone system (see Rich and Bendall, 1979), the six shown in Fig. 1.4 are of most importance in biochemical systems. Determination of the characteristic potentials of these redox couples enables definition of equilibrium positions, and can often be useful in the determination of rates of redox reactions (Rich and Bendall, 1980b). With this, extensive studies have been carried out to determine the mechanism of quinol oxidation by cytochromes (Yamazaki and Ohnishi, 1966; Rich and Bendall, 1979; 1980b). At low pH, it has been found (Rich and Bendall, 1979; 1980b) that the oxidation of benzoquinol by mammalian cytochrome *c* can take place by two possible mechanisms: the electron transfer mechanism or the H-atom transfer mechanism, depicted in Fig. 1.5 (a) and (b), respectively. In both mechanisms, the rate-limiting step is the transfer of the first reducing equivalent from the quinol to cytochrome *c*, with the transfer of a second equivalent from the semiquinone following rapidly. By examining the effect of ionic strength on the reaction rate of each mechanism (one of the reactants is uncharged in the case of the H-atom

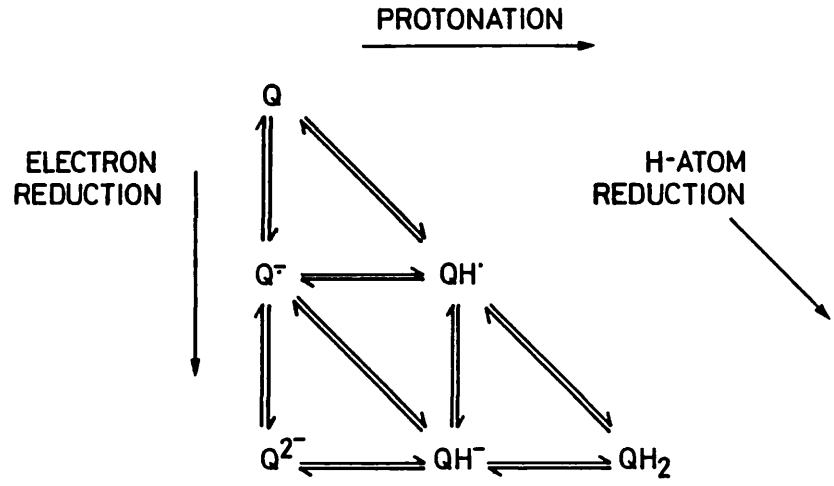


Fig. 1.4. Six of the nine possible redox and protonation states of quinones in solution. Each reaction involves the addition or removal of one electron, one proton or one hydrogen atom. (Redrawn from Rich and Bendall, 1979).

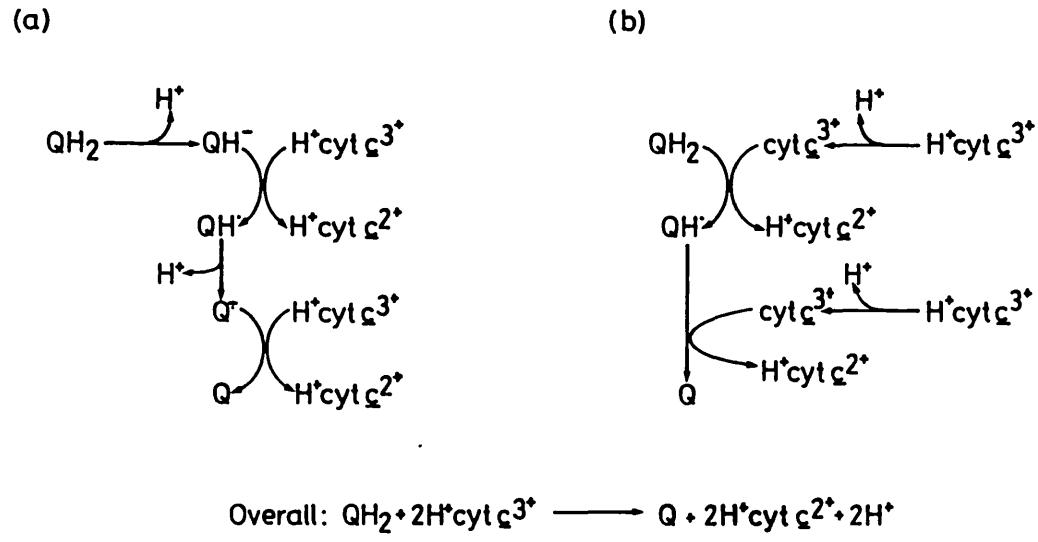
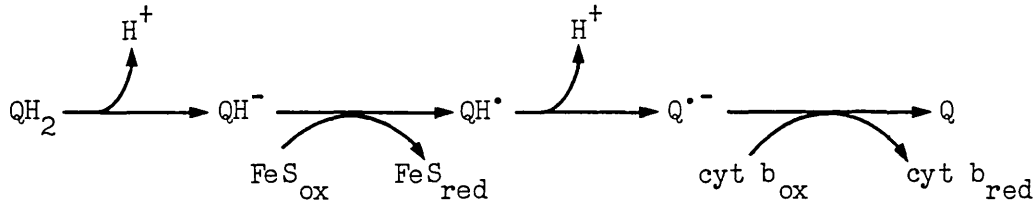


Fig. 1.5. Possible mechanisms of reduction of cytochrome c by quinols at acid pH. (a) Electron-transfer mechanism. (b) H-atom transfer mechanism. Mechanism a is preferred, as discussed in the text. (Redrawn from Bendall, 1982).

transfer) it was found that the electron transfer mechanism was most favoured.

Other possible evidence that such an electron transfer mechanism, rather than an H-atom transfer, operates for quinol oxidation in chloroplasts, comes from a comparison of the midpoint redox potential, E_o, values of the various quinol/quinone couples shown in Table 1.1, with the $E_{m,7}$ values of cytochrome b-563 and the Rieske FeS centre, -100mV (Rich and Bendall, 1980a) and +290mV (Malkin and Aparicio, 1975), respectively. This indicates that it is the E_o values of the $QH^{\bullet}/QH^{-}$ and $Q/Q^{\bullet -}$ couples that correlate with the E_m values of the Rieske FeS centre and cytochrome b-563, respectively. Thus, a possible scheme for quinol oxidation in chloroplasts, which incorporates an electron-transfer mechanism, is as shown below. The species involved in H^+ release are also indicated.



Experimentally, $Q^{\bullet -}$ has been detected by EPR in mitochondrial preparations, thus suggesting the couples involved in electron transport to be $Q/Q^{\bullet -}$ and $QH_2/Q^{\bullet -}$ (Ohnishi and Trumpower, 1980). Note, the work done by Rich and Bendall (1979, 1980b) has been carried out in protonic solvents where $Q^{\bullet -}$ stability would be poor.

Apart from these mechanistic features of quinol oxidation, the degree to which quinol/quinone molecules are bound or mobile is also of importance. Classically, models for mitochondrial electron flow based upon the presence of a diffusible pool of ubiquinone molecules were proposed (Kröger and Klingenberg, 1973). More recently, however,

Couple	n	E_o(mV)
Electron Transfers		
$Q/Q^{\cdot -}$	1	-165
$Q^{\cdot -}/Q^{2-}$	1	-196
Q/Q^{2-}	2	-181
$QH^{\cdot}/QH^{-}$	1	+239
H-atom transfer		
$Q/QH^{\cdot}$	1	+190
$Q^{\cdot -}/QH^{-}$	1	+575
Q/QH^{-}	2	+383
$QH^{\cdot}/QH_2$	1	+870
Q/QH_2	2	+530

Table 1.1 Estimated E_o values for couples of plastoquinone-1 in ethanol (sources of data are given in Rich and Bendall, 1980b).

evidence has suggested, instead, a role for large numbers of protein bound quinone (Yu and Yu, 1981). In line with this, Bouges-Bocquet (1981a) has proposed, in chloroplasts, that both the primary acceptor of PS2, Q_A, and the secondary acceptor Q_B are bound quinone molecules. Also, Bouges-Bocquet (1981b) has proposed the existence of a third bound form of quinone, U, that acts as the immediate donor to the cytochrome $\underline{b_6}/\underline{f}$ complex, in a fashion analogous to that of component Z postulated in the cyclic electron transport system of bacterial chromatophores (Prince and Dutton, 1977; Dutton and Prince, 1978): she suggests that direct electron flow can occur more rapidly between two bound quinones, namely Q_B and U, than via the diffusible plastoquinone pool.

A way of reconciling these two extreme views on the degree of binding of quinol/quinone molecules has been suggested by Rich (1981). In his model, the pool contains a relatively large number of mobile diffusible quinone and quinol molecules. The electron donor and acceptor molecules may possess quinone or quinol molecules which are loosely bound, in the manner of enzyme-substrate intermediates: these molecules then equilibrate with the pool by association or dissociation reactions. Experimental evidence for such a dissociable intermediate has come from investigations of the inhibition properties of DCMU and other herbicides (Velthuys, 1981; Bowes & Crofts, 1981). These led to the proposal that the mechanism of inhibition was that of competition at the site of the secondary acceptor of PS2, Q_B, between Q_B and the inhibitor, thus invoking Q_B as a dissociable intermediate. The primary acceptor Q_A, on the other hand, probably remains firmly bound, and has a highly stabilized semiquinone: although quinones

usually display two electron redox reactions,when associated with the reaction centre iron, their redox reactions are modified such that they display only single electron reduction. Concerning the immediate donor of the cytochrome $\underline{b}_6/\underline{f}$ complex, U, and in view of the model proposed by Rich (1981) above, it has been suggested (Bendall, 1982) that U could be regarded as an intermediate enzyme substrate complex as well. The rate-limiting step in plastoquinol oxidation would then be the binding of quinol to an acceptor site, possibly the Rieske FeS protein (see Trumpower, 1981),to form U. Oxidation of U would be relatively rapid provided an oxidized acceptor was available. The only problem with this suggestion, though, is whether the semiquinone subsequently formed, would need to be released from its binding site in order to reduce cytochrome b-563. Such PQ binding sites on the cytochrome $\underline{b}_6/\underline{f}$ complex have indeed been identified by photoaffinity labelling studies (Oettmeier et al, 1982).

1.3.2 The Q-cycle and the alternative b-cycle:

Various models have been put forward to explain both (a) the mechanism by which quinol oxidation occurs with the concomitant release of protons into the inner membrane space and (b) the involvement of a quinone species, nominally a semiquinone, in both the reduction and oxidation of a b-type cytochrome.

The model which has received most attention to date is Mitchell's (1976) "protonmotive quinone cycle" or "Q-cycle". However, an alternative model to this is Wikström's "b-cycle" (Wikström and Krab, 1980; Wikström et al, 1981). Versions of both of these models are depicted in Fig. 1.6 (a) and (b), respectively. Supportive evidence for the role of such a cycle comes from the observation of the oxidant-induced reduction of cytochrome b. This reaction was initially observed in

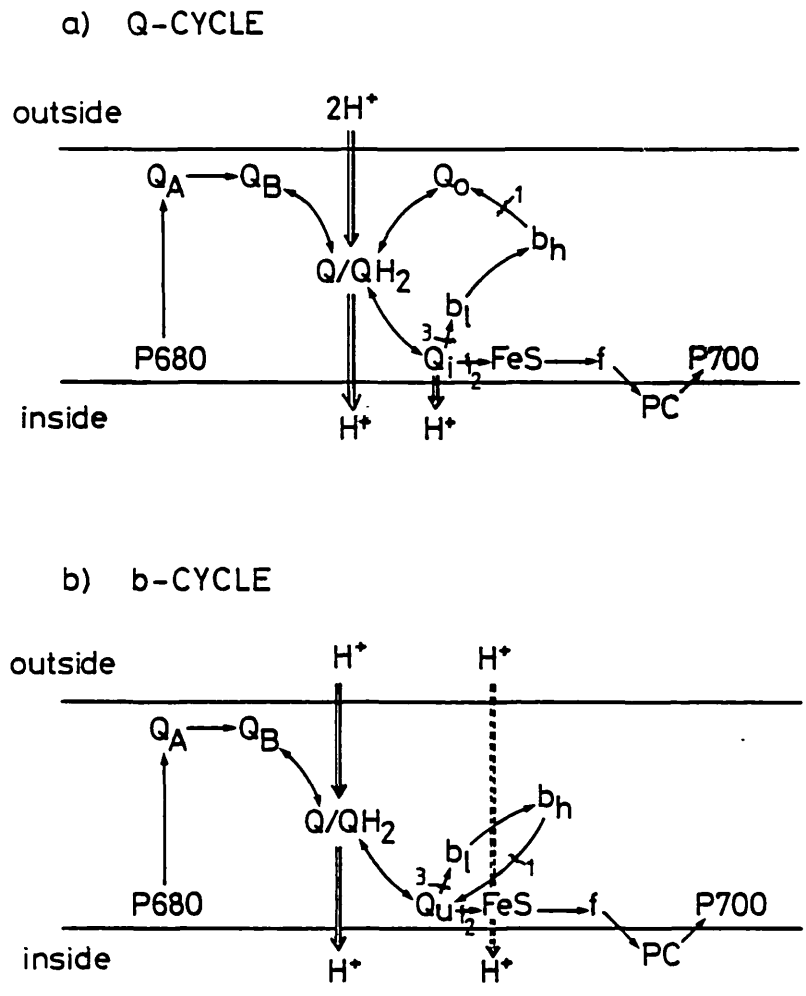


Fig. 1.6. Possible schemes for the (a) Q-cycle and (b) b-cycle. Q_A, Q_B, Q_i, Q_o, Q_u represent bound forms of plastoquinone; Q/QH_2, the plastoquinone pool; b_l, low potential cytochrome b-563; b_h, high potential cytochrome b-563; FeS, the Rieske iron-sulphur centre; f, cytochrome f; PC, plastocyanin. Single headed arrows, electron or proton transfer; double-headed arrows, binding, dissociation and diffusion of quinone/quinol molecules. Site i, site of unstable semiquinone; site o, site of stable quinone. Numbers indicate site of inhibitor action (see section 1.3.3).

mitochondria but has also been observed in bacteria and chloroplasts, and, using the respective isolated cytochrome b-c complexes, in conjunction with reconstitution studies.

The main differences between the above models is the number of reaction sites for the quinol/quinone system. In the Q-cycle there are two sites, while in the b-cycle there is only one, but which reacts in two different modes according to the reduction state of the b-cytochromes. The consequence of such a difference is in the mechanism by which oxidant-induced reduction of cytochrome b takes place. This, in turn, is closely linked with differences in the mechanism of quinol oxidation and in the predicted number of protons (H^+) translocated across the membrane.

In the Q-cycle, quinol oxidation takes place via an electron transfer mechanism (see also section 1.3.1): quinol oxidation at site i is strictly concerted, blocking the thermodynamically favourable reaction of the semiquinone with the Rieske FeS centre, the semiquinone reacting instead with cytochrome b_l. Quinone reduction at site o is thought not to be concerted, with the possibility of both electrons for quinol formation being provided for by cytochrome b_h. The two b-cytochromes thus function between quinol/quinone forms which have relatively unstable (site i) and stable (site o) semiquinone intermediates. This allows energy for an extra H^+ translocation, in addition to that proton that results from the quinone loop functioning between the reaction centre and the cytochrome complex. The Q-cycle would thus predict a H^+/e^- ratio of 2.

In the b-cycle, quinol oxidation takes place via an H-atom transfer (see also section 1.3.1) and hence conformational changes are implicit: the semiquinone formed in the oxidation of the first quinol by the Rieske FeS centre reduces cytochrome b_l, while the semiquinone formed at

the same site from a second quinol, oxidizes cytochrome $\underline{b}_h$. The extra H^+ that would have been translocated in a Q-cycle, is instead, intimately associated with the cytochrome b redox reactions. The b-cycle would thus predict a H^+/e^- ratio of 1. The b-cycle, however, would yield a H^+/e^- ratio of 2 if a specific mechanism, by which an extra H^+ could be pumped across the membrane, were incorporated: one possibility would be the involvement of the b-cytochromes with their redox-linked pK changes (von Jagow and Engel, 1980; Wikström and Krab, 1980; Wikström et al, 1981).

The main argument in favour of the Q-cycle mechanism has already been given in the discussion of section 1.3.1, where the electron transfer mechanism, which is operative in a Q-cycle,is favoured for quinol oxidation. The initial experimental requirement to explain the observed H^+/e^- ratio of 2 in mitochondria (Wikström et al, 1981) would favour both a Q-cycle and a b-cycle, in which an extra site of H^+ translocation had been incorporated. However, even so, in favour of the Q-cycle is that it exhibits a clear concept of how the extra H^+ is translocated.

The use of a H^+/e^- ratio of 2 as a criterion for deciding which is the more suitable model is, however, dubious, since, experimentally, clarification of H^+/e^- ratios is still required. Evidence for a H^+/e^- ratio of 2 has been provided both for mitochondria (Papa et al, 1975; Wikström et al, 1981) and for photosynthetic bacteria (Petty et al, 1977; 1979). This has also been the case for chloroplast electron transport, from plastoquinol to plastocyanin, (Fowler and Kok, 1976; Olsen and Cox, 1979; Velthuys, 1980). Other authors (Olsen et al, 1980), however, could not demonstrate the extra proton translocation in chloroplasts, at all, and hence a b-cycle mechanism, with no extra site of H^+ translocation, was suggested.

A prediction made by the Q-cycle, and by the b-cycle in which a mechanism for extra H^+ translocation is incorporated, is that of an additional charging of the membrane by an electrogenic step, during oxidant-induced reduction of cytochrome b, which is relatively slow compared to the charging by the reaction centres. In the case of a Q-cycle, this slow electrogenic step would be the result of an electron moving outwardly across the membrane, while for a b-cycle, it would be the result of the inward translocation of the (extra) proton. An extra slow electrogenic step has indeed been observed both in bacterial chromatophores (Prince and Dutton, 1977; Crofts et al, 1983) and in chloroplasts (Joliot and Delosme, 1974; Velthuys, 1978; Crowther and Hind, 1980; Bouges-Bocquet, 1981b). Experimental evidence that this slow electrogenic step is indeed indicative of a Q-cycle mechanism, has been well documented for bacterial chromatophores, although, modifications of such a mechanism have been proposed (Crofts et al, 1983). In the case of chloroplasts, however, although various modified Q-cycles and b-cycles have been put forward to explain the slow electrogenic step, alternative interpretations have also been suggested (see section 1.6.3). Further evidence in favour of the predicted electrogenic step comes from recent reconstitution studies in which the isolated cytochrome b_6/f complex is reincorporated into lipid vesicles and has been found to be an electrogenic proton translocator (Hurt et al, 1982), as is the mitochondrial b-c complex (Guerrieri and Nelson,1975; Leung and Hinkle, 1975).

One other criterion that has been used as evidence of a Q- or b- type cycle operating, rather than a straightforward linear electron transport scheme between quinol and cytochrome f, is that the kinetics for the reduction of cytochrome b-563 should match those of the re-

reduction of cytochrome f. However, kinetic studies of the flash-induced cytochrome redox changes show that cytochrome b-563 reduction is considerably faster than the rereduction of cytochrome f (Dolan and Hind, 1974; Velthuys, 1979; Crowther and Hind, 1980). The situation is similar in bacterial chromatophores (Crofts et al, 1974; Prince and Dutton, 1975; 1977). This was thought to be incompatible with a Q-cycle/b-cycle type mechanism, until more recently the presence of the Rieske FeS centre, delaying electron flux from quinol to cytochrome f, was taken into account.

1.3.3 Inhibitors:

As indicated in Fig. 1.6, three different sites of oxidoreductase inhibition can be discerned, giving rise to three different types of inhibitors: type 1 inhibitors block the reoxidation of cytochrome b; type 2 block at the Rieske FeS centre and type 3 block the reduction of cytochrome b.

Antimycin and HQNO are type 1 inhibitors. Their effect is to inhibit the reoxidation of cytochrome b and hence cause an apparent increased extent in its oxidant-induced reduction. As such, antimycin is very effective in mitochondria (Wikström and Berden, 1972; Erecinska et al, 1972) and photosynthetic bacteria (Dutton and Prince, 1978; Gabellini et al, 1982). Although antimycin is not so effective in chloroplasts (Hurt and Hauska, 1981; Bendall, 1982), it does inhibit, albeit at higher concentrations, cyclic electron flow around PS1 (Huber and Edwards, 1977), which also involves the oxidoreductase. However, the site of action of antimycin here is probably not equivalent to that in

mitochondria and photosynthetic bacteria, since, although cytochrome f rereduction and cytochrome b-563 reoxidation are inhibited (Slovacek et al, 1979), in accordance with a type 1 inhibitor, inhibition of the extent of oxidation of cytochrome f and of reduction of cytochrome b-563 was also observed.

UHDBT, DBMIB and DNP-INT are all type 2 inhibitors. They bind, in some form, to the Rieske FeS centre, thus inhibiting its reduction. UHDBT is a hydroxyquinone which was introduced by Folkers (see Roberts et al, 1979). It is an efficient inhibitor of all the quinol/cytochrome c (plastocyanin) oxidoreductases (see Hauska et al, 1983). DBMIB, which is also a quinone analogue, and DNP-INT, which is structurally related to DBMIB, were introduced by Trebst et al (1970; 1978) as inhibitors of plastoquinol oxidation in chloroplasts. Both are highly efficient inhibitors of the isolated plastoquinol-plastocyanin oxidoreductase (Hurt and Hauska, 1981) and also inhibit oxidant-induced reduction of cytochrome b-563 (Hurt and Hauska, 1982). Although some inhibitory effect has been observed with DBMIB in mitochondria (Trumpower, 1981) and in photosynthetic bacteria (Baltscheffsky, 1974), this might rather be explained in terms of DBMIB rapidly diverting electrons from transiently formed ubisemiquinone (Surkov and Konstantinov, 1980). DNP-INT, which has no redox properties, is as efficient as DBMIB in the chloroplast system, but is inert in the bacterial system.

Myxothiazol is a type 3 inhibitor. It is highly efficient in blocking the reduction of cytochrome b in both mitochondria (von Jagow and Engel, 1981) and photosynthetic bacteria (Meinhardt and Crofts, 1982; Gabellini and Hauska, 1983). Like antimycin, however, it is ineffective in the chloroplast system (Hauska et al, 1983).

1.3.4 Cyclic electron transport:

Cyclic electron flow occurs when an electron is returned from the reduced to the donor side of PS1, via a suitable "cofactor", to three possible sites: (a) plastoquinone (e.g. with the natural cofactor ferredoxin), (b) plastocyanin (with permeant cofactors such as 2,3,5,6 - tetramethyl-p-phenylenediamine) and (c) P700 (with the cofactor phenazine methosulphate). When only the plastoquinone input site for electrons from PS1 is considered, more than one type of cofactor can be used. With the natural cofactor ferredoxin, phosphorylation and electron flow are characterized by being antimycin sensitive (Binder and Selman, 1980), being associated with the slow phase of the electrochromic effect (Slovacek and Hind, 1978; Crowther et al, 1979) and being inhibited by DBMIB (Hauska et al, 1974) , the latter effect indicating the involvement of plastoquinone. Anthraquinone-2-sulphonate is an alternative cofactor, which in some ways is similar to ferredoxin in that it is non-permeant and its reaction is sensitive to DBMIB, but on the other hand, its reaction is insensitive to antimycin (Hauska et al, 1974; Binder and Selman, 1980; Robinson and Yocum, 1980).

A crucial question is how electrons pass back to a carrier within the membrane from non-permeant cofactors. Although plastoquinone is involved in the cyclic pathway, the nature of the primary acceptor, and the role of the pool are uncertain. Concrete evidence that ferredoxin can reduce the pool has recently been obtained. NADPH and ferredoxin were shown to reduce both C-550 (Arnon and Chain, 1975) and the fluorescence quencher Q_A (Mills et al, 1979).

Initially, it was thought that the direct acceptor of electrons, from ferredoxin, was cytochrome b-563 (Cramer and Butler, 1967; Böhme and Cramer, 1972). However, recently, this has been shown not to be the case,

since ferredoxin does not cause an acceleration of the very slow reduction of cytochrome b-563 by dithionite (Cox, 1979). Non-permeant mediators (anthraquinone-2-sulphonate) are similarly ineffective, whereas permeant mediators (anthraquinone, methyl viologen) do cause an acceleration: thus, the cytochrome seems to be buried in the hydrophobic phase of the membrane and hence is inaccessible to hydrophilic reagents.

On thermodynamic grounds, ferredoxin would be expected to reduce plastoquinone at a reasonable rate, but in practice the direct reaction is slow, probably through lack of accessibility. It seems more likely that the membrane contains an unidentified ferredoxin-plastoquinone oxidoreductase , denoted "V",(Bouges-Bocquet, 1980b; Crowther and Hind, 1980) located on the outer side of the thylakoid membrane. This enzyme probably works as a two-electron accumulator, similar to the Q_B protein of PS2: these two proteins are not identical since DCMU does not inhibit cyclic phosphorylation. Inhibitor studies suggest that the flavoprotein ferredoxin-NADP oxidoreductase mediates electron flow between ferredoxin and the plastoquinone reductase (Shahak et al, 1981), even though a flavoprotein antiserum does not inhibit cyclic electron flow (Böhme, 1977). Cyclic electron flow with other non-permeant cofactors, however, does not necessarily follow the same route as that of ferredoxin: for example, with anthraquinone-2-sulphonate as cofactor, electrons may be donated to plastoquinone directly,thus by-passing V (see Bendall, 1982).

1.4 Measurement of the electric field by electrochromism:

1.4.1 Detection by electrochromism:

Detection of voltages across the thylakoid as well as the bacterial chromatophore membranes, such as those set up by the primary charge se-

paration upon light activation, has been possible by spectrophotometric measurements of electrochromic absorption changes. The term "electrochromism" describes the influence of strong electric fields, light-induced or otherwise, on the absorption spectra of pigments, which results in an almost homogeneous shift of the absorption band.

Fig. 1.7 shows, in a simplified form, the principle of electrochromism (a more detailed discussion of its consequences is given later; for theoretical descriptions see Liptay, 1969 and Reich and Sewe, 1977). Absorption of light transforms a pigment molecule from its ground state to an excited state. If an electric field is applied, and if the ground or excited state either have a different permanent dipole moment or a different polarizability, then the energy difference between these states will be altered. Such a change in transition energy, which is dependent on the magnitude of the electric field, results in a shift of the absorbance maximum and hence a shift of the whole absorbance band. This band-shift causes "field-indicating absorbance changes", ΔA. Such absorbance changes were initially used by Junge and Witt (1968) to provide the first experimental evidence for the existence of an electric field across the functional membrane of photosynthesis.

1.4.2 Kinetic and spectral characteristics of flash-induced electrochromic absorption changes:

The flash-induced field-indicating absorption change is characterized by a rise time shorter than 20ns (Wolff et al, 1969) and a decay time in the range of 10ms to 1s, depending on the membrane permeability and pH gradient.

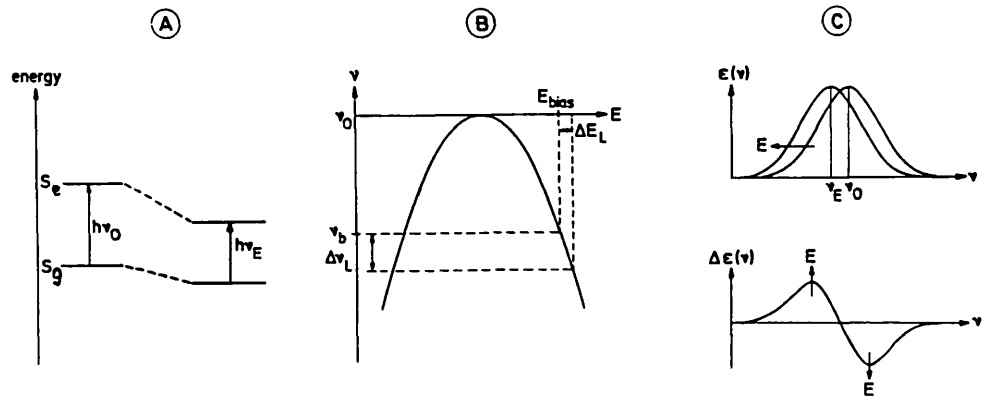


Fig. 1.7. Schematic representation of the influence of high electric field strength on the absorption spectrum of a dye. (A) Shifts of the energy of the excited (subscript e) and the ground state (g) of the dye and in consequence modification of the resonant frequency for the light absorption (ν_o changed into ν_E). (B) Dependency of the resonant frequency on the electric field strength. It is assumed that second-order effects prevail. If the dye is exposed to a strong biasing field the second-order dependence may become pseudo-first order with respect to the smaller variable component (E_L). (C) The electrochromic band shift (above) and its difference spectrum (below). The extent of the difference in extinction ($\Delta\varepsilon$) is proportional to the electric field strength. (Taken from Junge, 1977).

A typical time-course for this absorption change is shown in Fig. 1.8 left. The fast initial rise is interpreted as the electrical charging of the membrane at the primary reaction centres (Junge and Witt, 1968), while the decay has been analysed as the discharging of this field by ionic currents. The decay can be accelerated by treatments which are known to increase the permeability of the membrane (e.g. ageing, osmotic shock, treatment with solvents and ion-transporting antibiotics). From such studies with thylakoids it has been found (Junge and Witt, 1968) that just one molecule of gramicidin per thylakoid sac is required to produce an acceleration of the decay; similar observations have also been made in bacterial chromatophores (Jackson and Crofts, 1971; Saphon et al, 1975). This has led to the proposal that these conductivity-sensitive absorption changes represent an electric field that is delocalized over a large area of the thylakoid or chromatophore surface. There is evidence that this delocalization of the initial localized electric field can take place in less than 1μs (Junge, 1974; Witt, 1979).

A scheme of these electric events in the thylakoid membrane of chloroplasts is depicted in Fig. 1.8 bottom right. An electrical analogue is depicted in Fig. 1.8 top right. The light reaction, which shifts electrons across the membrane is symbolized by a generator which charges the membrane capacitor. The electrochromic effect of the bulk pigments (Chl-a, -b and carotenoids) indicates the electric potential changes, which are represented by a voltmeter. The discharge of the membrane capacitor occurs by ion fluxes through different channels: these are shown as resistors.

The spectrum of these conductivity-sensitive absorption changes is complicated, but exhibits a large maximum in the visible region at about 515nm for both thylakoids (Emrich et al, 1969) and bacterial chromatophores (Jackson and Crofts, 1969). It was found that the spectrum for

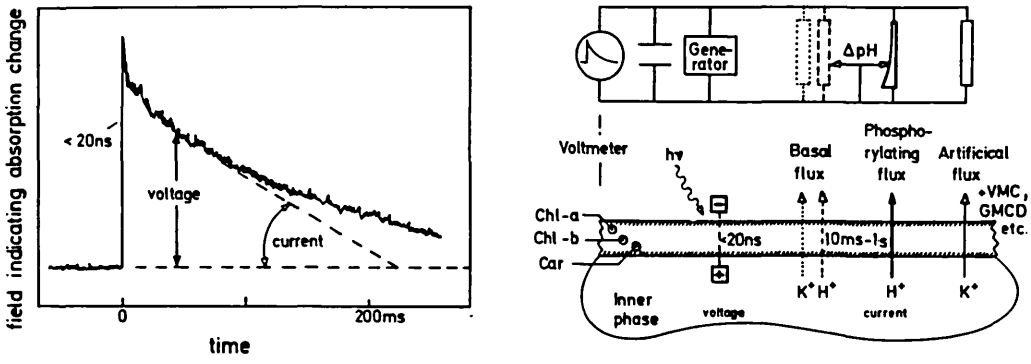


Fig. 1.8. Left. Time course of the field-indicating absorption change. Right. Scheme of the electric events on the thylakoid membrane of chloroplasts, with the electrical analogue. (Taken from Witt, 1979).

thylakoids could be approximately mimicked by the electrochromic difference spectra of isolated carotenoids and chlorophylls, measured in microcapacitors (Schmidt et al, 1971a; also see Witt, 1975); a similar reconstruction compared even more accurately with the chromatophore absorption changes (see Schmidt et al, 1971b; Witt, 1975). These studies clearly showed that it was the carotenoids that were the pigments sensitive to the transmembrane electric field and that gave rise to the absorbance changes. However, from further detailed spectral analyses in chromatophores (de Grooth and Amesz, 1977b; Symons et al, 1977) and chloroplasts (Sewe and Reich, 1977; de Grooth et al, 1980), it was found that only a small fraction of the total carotenoid pool in membranes was electrochromically sensitive. Experiments suggest that the sensitive carotenoids in thylakoids are associated mainly with the PS2 complex: this has been inferred from the involvement of chlorophyll b (Sewe and Reich, 1977) and indirectly from the low temperature behaviour of the electrochromic response (Conjeaud et al, 1976). In chromatophores, the sensitive carotenoids have been suggested to be associated with only one of the two light-harvesting pigment-protein complexes, either the B870 complex or the B800-850 complex: selective removal of the B800-850 complex (Matsuura et al, 1980; Webster et al, 1980) results in the loss of the electrochromic absorption change.

1.4.3 Consequences of simple electrochromic theory:

A simplified equation which describes the theory of electrochromism (Reich and Sewe, 1977) is as follows:

$$\Delta\lambda_m = \frac{\lambda_m^2}{hc}\left[(\underline{\mu}_g - \underline{\mu}_e).\ \underline{E} + \tfrac{1}{2}(\alpha_g - \alpha_e)\,E^2\right]$$

λ_m is the absorption peak (m) in the absence of the field, h is Planck's constant (6.63×10^{-34} Js), c is the speed of light (3×10^8 ms^{-1}),

$\underline{\mu}_g$ and $\underline{\mu}_e$ are the permanent dipole moments in the ground and excited states (C m), α_g and α_e are the polarizabilities of the ground and excited states ($C\,m^2V^{-1}$) and $\underline{E}$ is the electric field (Vm^{-1}). For molecules which have a permanent dipole, the main effect is a linear shift in the absorbance maximum to the red with change in field strength. For molecules with no permanent dipole, the main effect is a quadratic relationship between the extent of the shift and the field strength. This arises from a linear effect of the field on the induced dipole $(\alpha_g - \alpha_e).\ \underline{E}$, which results from the polarizing effect of the field. The scalar product contains the dependence on the angle between the permanent dipole and that of the field.

There are three effects which can be predicted from the above simplified electrochromic theory: (1) the carotenoids, which have no permanent dipole moment but which are polarizable, should exhibit a quadratic shift with respect to the applied electric field; (2) the red-shift of the carotenoid absorption should be small (of the order of a few tenths of a nanometer for typical field strengths of 10^5 V cm^{-1}) and hence the magnitude of the electrochromic absorption change should also be small; and (3) the carotenoid absorption peak will shift progressively along the wavelength axis with increasing field strength.

Using several independent techniques, in both thylakoids and chromatophores (Jackson and Crofts, 1969; Witt and Zickler, 1974; Schapendonk and Vredenberg, 1977), it has been found that the carotenoids exhibit a linear shift with applied electric field, rather than the expected quadratic shift. To explain this discrepancy, the following hypothesis has been proposed (Reich and Sewe, 1977; Sewe and Reich, 1977). The electrochromically sensitive carotenoids are contained in an environment in which they experience a strong local field (E_1 in Fig. 1.7), possibly as the result of complex formation with neighbouring

chlorophyll molecules. The effect of this local field is to polarize the carotenoids giving them an induced dipole of $(\alpha_g - \alpha_e)\ \underline{E}_l$ and hence shift their spectrum to the red by $(\alpha_g - \alpha_e)\ E_l^2$. The small additional field due to a membrane potential ($\underline{E}_m$) now gives rise to a linear shift of $(\alpha_g - \alpha_e)\ \underline{E}_l \cdot \underline{E}_m$. Thus, the constant background polarization of the carotenoids, by the chlorophyll molecules, results in a pseudolinear relation between the absorption change and the electric field transient (see middle of Fig. 1.7).

Attempts to observe a progressive shift of the carotenoid absorption spectrum with increasing field strength have been successful with single turnover flashes (Crofts et al, 1974; Holmes and Crofts, 1977). A small but clearly resolved progressive shift to the red in the isosbestic point of the difference spectrum can be observed on successive flashes: the change represents a shift of approximately 0.7nm. When similar attempts were initially made to measure this shift using continuous illumination, no progressive change could be detected. However, recently, by cooling chromatophore suspensions to -35°C and promoting electron transport with redox dyes, de Grooth and Amesz (1977a; b) have been able to observe both an unusually large carotenoid absorption change and a clear shift of its spectrum, as expected, to longer wavelengths, and which was proportional to the change in amplitude of the difference spectrum. This difference spectrum, however, had its initial inflection point several nanometers towards the red of the main absorption band. Their interpretation of these results was that (1) the carotenoid undergoing a change has a spectrum already shifted to the red with respect to the expected carotenoid absorption spectrum, and (2) the bulk spectrum is due to overlapping contributions from this red-shifted population and a population with a λ_{max} to the blue of the bulk spectrum, which results from the contribution of the non-responding

carotenoids. Such a hypothesis complements rather well with that of Reich, above, which would also predict a red shift in the spectrum of the electrochromically sensitive carotenoids.

1.4.4 Electrochromic absorption changes induced by steady-state light:

Under continucus illumination, the 515nm electrochromic absorption change, ΔA_{515}, exhibits a different time course to that observed upon flash activation (Gräber and Witt, 1974). Initially, the electrochromic change rises up to a relatively high level: it reaches between two and four times higher values than that under single flash excitation. Under the influence of this large electric potential difference, cations move outwards and anions move inwards. Simultaneously, the protolytic reactions, which occur as a result of the induced electron transport, cause an active inward translocation of protons. This results in a decrease in the pH of the internal phase and a subsequent increase in the field-driven proton efflux (see Gräber and Witt, 1976): in the steady state, the proton efflux fully compensates the active, inward proton pumping. The internal acidification also causes a retardation of the electron transport. This latter effect, together with the increase in proton efflux, leads to a decrease of the initial high electric field towards a relatively low steady-state value.

During the time course of these events, changes in the bulk potential ($\Delta\Psi_b$) and surface potential ($\Delta\Psi_s$) also occur (Rumberg, 1977): the bulk potential can be calculated from the Nernst-Planck relation while the surface potential can be calculated from the Gouy-Chapman theory. These potentials are of importance since the electric field strength within the membrane is proportional to their sum:

$$E = \frac{\Delta\Psi_{tr}}{d} = \frac{(\Delta\Psi_b + \Delta\Psi_s)}{d}$$

where $\Delta\Psi_{tr}$ is the transmembrane potential and d is the thickness of the membrane (see Fig. 1.9).

Under steady state light illumination, the bulk potential is small. However, the continuous inwardly directed proton pumping may lower the internal pH to such an extent that the negatively charged groups on the inner membrane surface become neutralized. If the external pH remains high, well above the pK of the external surface negative charges, then an electrical gradient will be created across the membrane, in addition to that created by electrogenic or ionic diffusion processes (Barber, 1982). This would then result in a large surface potential difference between the inner and outer side of the membrane. Hence, under steady state conditions, the transmembrane potential difference may contain a large contribution from the surface potential difference (Witt, 1979; Huber et al, 1980). In fact calibration of the electric field in thylakoids and under continuous illumination, as measured by the electrochromic method, does yield a large value of 100mV, positive inside (Gräber and Witt, 1974). This particular method senses the electric field within the membrane and hence is proportional to the transmembrane potential, which includes the large surface potential contribution. Calibration by alternative methods which are only sensitive to the electric potential difference between the bulk phases e.g. microelectrodes (Bulychev and Vredenberg, 1976) yields a low value of 10mV. Similar discrepancies have also been found for the steady state value of the chromatophore membrane potential (see Jackson and Crofts, 1969; Michels and Konings, 1978). Such surface potential differences are negligible in studies of flash-induced voltage changes.

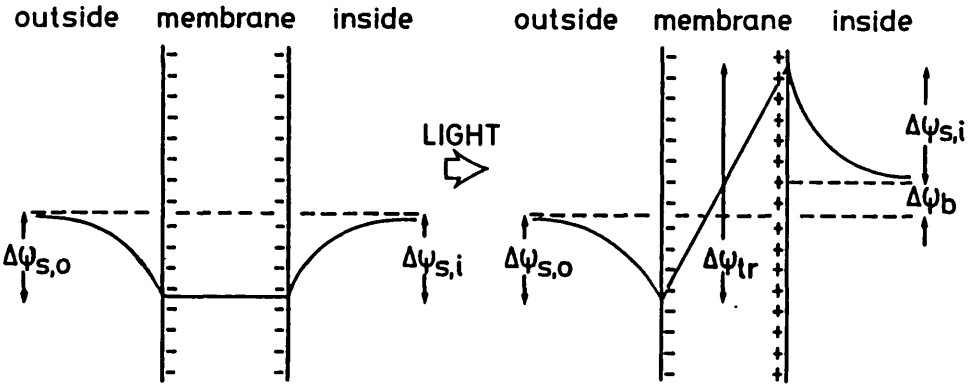


Fig. 1.9. Schematic drawing of the thylakoid membrane before and after steady state illumination, with the electric potentials in the bulk phases (Ψ_b), at the surfaces (Ψ_s) and the potential difference across the membrane ($\Delta\Psi_{tr}$). It has been assumed that initially, the surface potentials are the same and that, under steady illumination, the internal acidification creates a small positive surface potential on the thylakoid interior.

1.4.5 Electrochromic absorption changes induced by extrinsic electric field transients:

In bacterial chromatophores, electrochromic absorption changes have been induced by the exposure of the vesicles to "salt jumps" in the presence of cations (or anions) and specific ionophores (Jackson and Crofts, 1969): this results in a diffusion potential being set up across the membrane. The extent of the resulting absorption change can be linearly related to the extent of the diffusion potential, calculated assuming a Nernst-Planck relation to be valid:

$$\Delta\Psi = -\frac{RT}{ZF} \ln \frac{[I]_i}{[I]_o} \quad \text{..... 1.1}$$

where [I] is the concentration of the permeable ion on the inner (i) and outer (o) side of the membrane. Similar attempts with thylakoids have been hampered by the pronounced light-scattering changes of (the much larger) thylakoids (Strichartz and Chance, 1972). Elimination of these light-scattering transients has, however, also allowed salt-jump induced absorption changes in thylakoids to be observed (Schapendonk and Vredenberg, 1977). These exhibit the expected spectral properties of a field-induced electrochromic absorption change and yield the expected linear relation between the absorption change and the calculated diffusion potential. The use of this technique has led to the calibration of the flash-induced electrochromic absorption change (see later).

An alternative method of inducing electrochromic absorption changes is that of exposing the membranes to an externally applied electric field (de Grooth *et al*, 1980; Schlodder and Witt, 1980). Large, swollen thylakoid vesicles, called "blebs", (see de Grooth *et al*, 1980) have often been used in these studies since large electric fields can be induced across their membranes with comparatively small (by a factor of

10^{-3}) external electric fields (Ellenson and Sauer, 1976; Witt et al, 1976). In contrast to the light-driven membrane voltage, where the polarity is always positive inside, the externally induced voltage drop across these blebs is outwardly directed in 50% of the membrane area and inwardly directed in the other 50%. The linear and pseudolinear electrochromic effects thus cancel in the observed ensemble, while the quadratic effects remain visible. Thus, the observed electrochromic absorption change, induced by an external electric field, is proportional to the square of the transmembrane potential difference: it thus results from that population of carotenoids that do not respond to a local permanent electric field. Although this technique complements the predictions made by the electrochromic theory, it cannot really be used to calibrate the light-induced voltage jumps since they result from a different set of carotenoids.

1.4.6 Calibration of the flash-induced electric field:

Early estimates for the magnitude of the electric field set up across the thylakoid membrane, upon flash activation, were based on the following assumptions (Schliephake et al, 1968): a surface area of $2.2nm^2$ per chlorophyll, 600 chlorophylls per electron transport chain (i.e. PS2 + PS1 reaction centres) and an estimated specific capacitance of the thylakoid membrane of $0.5\ \mu F\ cm^{-2}$. This yielded a value of 48mV for a single turnover which is, in fact, quite close to the accepted measured values described below.

Schapendonk and Vredenberg (1977), taking care to avoid light scattering artefacts, attempted to calibrate the light induced electrochromic changes by comparison with the absorption changes induced by salt jumps in the presence of the ionophore valinomycin (analogous to the work of Jackson and Crofts, 1969, with chromatophores). A maximum voltage

of 58.5mV was initially calculated, but this was then reduced to 35mV, after taking into account the permeability ratio between K^+ and Cl^- in their experiments. The variation of the voltage among different samples was 15-35mV. A much higher estimate, however, for this single turnover voltage, has resulted from the use of the voltage-gated channel-forming antibiotic, alamethicin (Zickler et al, 1976). Comparing the observed extent of the electrochromic absorption change, when gating occurs, with the known gating voltage from studies with artificial membranes, a single turnover voltage of 105-135mV was proposed. Similarly high values have also resulted from measurements using the technique of delayed fluorescence (Jurinsic et al, 1978). In view of the indirect nature of all these estimates, it is difficult to favour one over the other. However, a figure ranging between 30mV and 50mV does seem probable.

In the case of chromatophores, two different calibration procedures for the electrochromic absorption changes have yielded similar values for the magnitude of the membrane potential generated by short flashes. The use of potassium diffusion potentials (after Jackson and Crofts, 1969) has yielded a value of 48mV. This results in a value of approximately 100mV for the transport of an electron through two electrogenic sites (see section 1.5). Calibration with alamethicin (after Zickler et al, 1976), however, has yielded the slightly lower values of 58-86mV, for the latter total transmembrane electron transport (Packham et al, 1978).

1.4.7 Limitations of the electrochromic method:

Analyses of the field-indicating absorption changes are mostly carried out at 515nm. However, measurements at this wavelength can

be confused with absorption and light scattering changes which are due to non-electrochromic events, with different kinetics. Possible complicating factors are :

(a) Fast changes at 515nm (rise time less than 20ns, decay 3μs) due to the formation of carotenoid triplets: these originate from a reaction that protects the antenna chlorophyll from photooxidation (Wolff and Witt, 1969; Cogdell et al, 1975).

(b) Slow optical changes (in thylakoids) at 515nm (in the range of seconds to minutes) due to light scattering changes, caused by the drastic structural changes induced by the electrochemical events. Double beam spectrophotometry does not entirely eliminate the problem: the difference spectrum of the apparent absorption changes due to light scattering, is rather similar to that of electrochromism (Thorne et al, 1975). Such scattering changes may have interfered in experiments with prolonged illumination (e.g. Larkum and Bonner, 1972), however, they are negligible during flash excitation of chloroplasts, where low repetition rates are used. Attempts to exclude such scattering artefacts in continuous illumination have, however, been successful in measurements with chlorella cells, by using careful calibration techniques (Gräber and Witt, 1974). Chromatophores, on the other hand, do not suffer from such light scattering interference, even during continuous illumination, since their vesicle diameter, approximately 360 Å (Packham et al, 1978), is much less than the wavelength of the measuring light.

(c) The location of the electrochromically-sensitive pigments in relation to the field-generating reaction centres, may also introduce artefacts. These, however, are pronounced in low temperature studies.

A transmembrane charge separation that occurs in a remote portion of the membrane, will only be sensed if the electric field is distributed evenly over the membrane: such a charge delocalization will only occur at temperatures where the electric conductivity of the aqueous phases is high enough (for low temperature effects, see Conjeaud et al, 1976; de Grooth and Amesz, 1977a).

1.5 Electrical events indicated by the flash-induced electrochromic absorption change: The fast phase.

In chloroplasts, the initial rise (phase a) of the electrochromic shift is very fast ($t_{\frac{1}{2}}$ < 20ns), and can be ascribed to the field created by the primary charge separation in the two photosystems (Witt, 1971; Junge, 1977). Since the polarity of this electric field is positive on the inner surface of the membrane (conclusively demonstrated by ion redistribution studies: Deamer and Packer, 1969; Schröder et al, 1971), charge separation occurs with an electron being transferred from the inner to the outer side of the membrane, from donor to acceptor, and fully crossing the dielectric core of the thylakoid membrane (Witt, 1979). Since the electric field generated at each photosystem contributes about equally to phase a (Schliephake et al, 1968; Malkin, 1978; Diner and Delosme, 1983), it is inferred that both P700 and P680, the primary electron donors of PS1 and PS2, respectively, are located towards the inner membrane surface, while the primary acceptors are located on the outer surface. Such a vectorial arrangement of components, within the thylakoid membrane, has since been supported by studies with inside-out vesicles (Andersson et al, 1981).

How the electron is rapidly channelled across the thylakoid membrane is not clear. Possibly, quantum mechanical tunnelling via overlapping

π-electron systems is involved (Mangel *et al*, 1975; Kuhn, 1979). Alternatively, the protein interior could act as an injection semiconductor (Tributsch, 1972). These hypotheses, however, remain speculative and have gained no experimental support.

In the case of bacterial chromatophores, the fast phase of the electrochromic absorption change comprises of two, kinetically distinct components (Jackson and Dutton, 1973): these are called phase I and phase II, and their contributions are approximately equal. In bacterial chromatophores, there is only one photosynthetic reaction centre, containing a specialized bacteriochlorophyll dimer, P870, and a quinone acceptor Q_A, and the light-driven electron transport reactions function as a closed cycle (Prince and Dutton, 1975; also see Fig. 1.10). The reaction centre serves to oxidize a *c*-type cytochrome and to reduce the ubiquinone pool, UQ. The cycling of the electron from UQ back to the *c*-type cytochrome then proceeds via the cytochrome *b*-c_1 complex, under optimal redox poise conditions, this cycling being complete within tens of milliseconds.

The very rapid rise kinetics of phase I ($t_{\frac{1}{2}} < 50$ns, Jackson and Crofts, 1971) thus associate it with the reaction $[BChl]_2 \rightarrow Q_A$; this has also been inferred from a correlation between the redox potential dependence (Jackson and Dutton, 1973) and the temperature dependence (de Grooth and Amesz, 1977a) of this reaction and phase I. Phase II, on the other hand, is generated within 100μs and has been associated with the reaction cyt $c_2 \rightarrow [BChl]_2^+$ (Dutton *et al*, 1975): phase II is found to be missing in mutants lacking cytochrome c_2 (Zannoni *et al*, 1980).

This two component reaction (corresponding to phases I and II), contained within the fast electrogenic phase, has been interpreted as indicating that the reaction centre bacteriochlorophyll is located towards

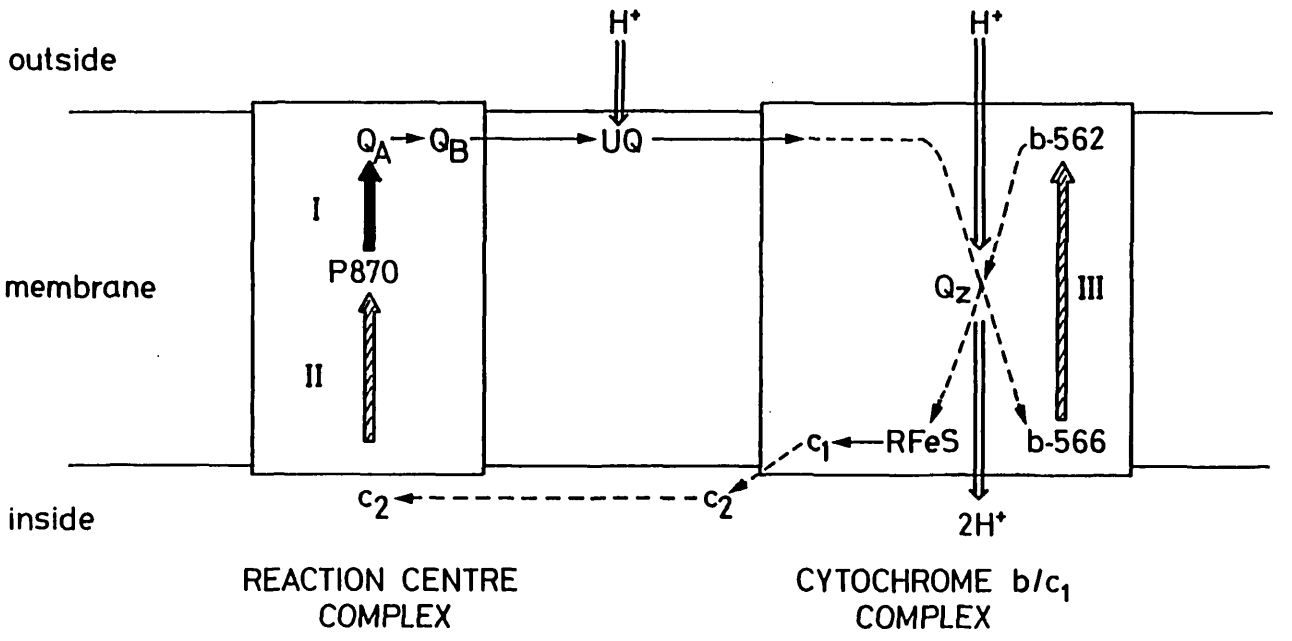


Fig. 1.10. Topology of electrogenic reactions and protolytic reactions in chromatophores. Electrogenic reactions are indicated by wide arrows (filled arrows for the most rapid photochemical steps; shaded arrows for slower electron transfer steps). P870, reaction centre BChl; Q_A, primary quinone; Q_B, secondary quinone; Q_Z, also a quinone; b-566, b-562, b-type cytochromes; c_1, c_2, c-type cytochromes.

the centre of the membrane dielectric (Takamiya and Dutton, 1977): this is very different to the situation in thylakoids. From this, and from the fact that the membrane potential, generated in light-activated chromatophores, is positive inside, it has been shown that the primary electron donor to the reaction centre, cytochrome c_2, is located on the inside of the chromatophore membrane (Prince et al, 1975), while the proton binding reaction accompanying the reduction of UQ, takes place on the outside of the membrane (Petty and Dutton, 1976b). Further evidence for such an organization of components (in Rp. sphaeroides and Rp. capsulata, at least) comes from diffusion potential studies (Jackson and Crofts, 1969), and reconstitution studies of purified reaction centres with artificial membranes (Crofts et al, 1977; Packham et al, 1980). In different species of photosynthetic bacteria, however, the organization of components may vary. For example, in Chromatium, the photochemical reaction centre appears to span a much smaller fraction of the dielectric because it contributes little, if any, to the carotenoid change (Case and Parson, 1973): the main electrogenic process appears to be the reduction of the oxidized reaction centre by a c-type cytochrome. Hence, it is suggested that the c-type cytochrome is located on the inside of the chromatophore membrane, while the reaction centre chlorophyll donor is located towards the outside.

1.6 Electrical events indicated by the flash-induced electrochromic absorption change: The slow phase.

1.6.1 Properties of the slow phase:

Initially, the slow phase of the electrochromic response was only observed to occur in algae (Joliot and Delosme, 1974; Bouges-Bocquet 1980b) and bacterial chromatophores (Jackson and Dutton, 1973).

However, more recently, it has also been observed in chloroplasts (Velthuys, 1978, 1979; Crowther et al, 1979; Slovacek et al, 1979). At present, evidence favours the concept that this slow absorption change represents an electrogenic step in the electron transport chain, outside the photochemical reaction centres: this would thus be in accordance with Mitchell's Q-cycle hypothesis (Mitchell, 1976; also see section 1.3.2). In chloroplasts, however, other interpretations for the origin of the slow phase have also been put forward (see section 1.6.3).

Under optimal conditions (see later), the slow phase has a rise time of approximately 2ms in bacterial chromatophores and 10ms in chloroplasts. Its amplitude is equal to that of the fast phase in bacterial chromatophores; in chloroplasts the amplitude of the slow phase is equal to that of the fast phase due to PSI alone (although this ratio can vary). In both systems the absorption spectrum of the slow phase matches that of the fast phase (Dutton et al, 1975; Crowther and Hind, 1980): this indicates that the slow phase does indeed reflect a transmembrane electric field, but subsequent to that generated at the photochemical reaction centres.

An effective inhibitor of the slow phase in bacterial chromatophores is antimycin (Jackson and Dutton, 1973). From the earlier discussion in section 1.3.3, this suggests that cytochrome b-563 is involved in the generation of the slow phase. On the other hand, in chloroplasts, DBMIB inhibits the slow phase (Crowther et al, 1979): this implicates the involvement of plastoquinone in its generation.

1.6.2 Conditions required for the generation of the slow phase:

In chloroplasts, it was initially thought that the slow phase, phase b, was solely driven by those reactions associated with PSI cyclic electron flow (Crowther et al, 1979). This was because phase b was only observed in chloroplasts that had been prepared with intact outer membranes, and which contained bound soluble ferredoxin, and other stromal cofactors necessary for the cyclic process to occur (Horvath et al, 1979; Shahak et al, 1980). Furthermore, the observation that addition of DCMU, after the reduction of the PQ pool, did not inhibit the generation of phase b or its amplitude (Crowther and Hind, 1980), inferred that phase b might be associated with the oxidation of plastoquinol by PS1.

Recently, the ambient redox poise, in the thylakoid membrane, has been found to be critical for the generation of phase b (Bouges-Bocquet, 1981b) more so than the presence of cyclic electron flow. It has been suggested that phase b can operate under conditions of non-cyclic electron flow, provided that a component U, probably a bound quinone, has been pre-reduced. The E_m of U has been calculated to be 40mV more positive than the bulk PQ pool i.e. the $E_{m,7}$ for U/UH_2 would be approximately +140mV (Bouges-Bocquet, 1981b).

Some of the observations that have led to the above proposal are given below. Reducing equivalents are required, in the presence of DCMU, to observe phase b (Crowther and Hind, 1980). Oxidizing conditions diminish the extent of phase b, although over-reduction of the system also causes a loss in its amplitude (Bouges-Bocquet, 1981b). Preillumination of broken chloroplasts with PS2 light, in the absence of DCMU, under aerobic conditions and without ferredoxin, generates

a condition in which phase b can be induced (Velthuys, 1978): such chloroplasts would be unable to sustain cyclic electron transport. Finally, the amplitude of phase b, in the absence of DCMU, exhibits a two-flash periodicity (Bouges-Bocquet, 1980b; Velthuys, 1980): although the change in amplitude is small, this effect is indicative of a component requiring electron flow through the secondary acceptor gating component, Q_B, described earlier.

A further condition required for phase b generation is that, when successive flashes are used, reduced U is allowed to be regenerated between flashes (Bouges-Bocquet, 1981b). It has been found that the slow phase is strongly inhibited after several closely spaced flashes (Bouges-Bocquet, 1977; 1981b) and that under these conditions, a lower ambient redox potential of -54mV is required to observe phase b (Crowther and Hind, 1980). However, a further possible contribution to the inhibition of phase b, using closely spaced flashes, is that a proton electrochemical potential builds up: this would also inhibit the formation of the slow phase (Bouges-Bocquet, 1981b).

In the case of bacterial chromatophores, the importance of ambient redox potential in the generation of the slow phase, called phase III here, has already been established (Jackson and Dutton, 1973; Prince and Dutton, 1977): typically an ambient redox poise of +100mV, pH 7.0, is required. Also postulated, is the involvement of a specialized ubiquinone, Q_Z (Bashford et al, 1979). In fact, the quinone U, predicted above in chloroplasts, has many of the properties of Q_Z.

1.6.3 Possible interpretations of the slow phase:

The site for the generation of the slow phase has been well established in the case of bacterial chromatophores, but is still a matter of controversy in the case of chloroplasts.

In bacterial chromatophores, phase III correlates with the reaction involving the rereduction of cytochrome c_2 by cytochrome b (Jackson and Dutton, 1973; see also Fig. 1.10). This reaction is specifically antimycin sensitive (Jackson and Dutton, 1973; van den Berg et al, 1979), suggesting that it is the oxidation of cytochrome b, in which one electron is transferred across the membrane dielectric, that generates the electrogenic phase III. From this, and other observations, a Q-cycle type mechanism has been inferred to operate in bacterial chromatophores (for example, see Crofts et al, 1983).

In the case of chloroplasts, however, experimental evidence concerning the origin of phase b has been less clear cut. The ineffectiveness of antimycin to completely inhibit phase b (Crowther et al, 1979) has hampered any correlations that would otherwise have been made with the analogous phase III in bacterial chromatophores. One possibility is that the generation of phase b, in chloroplasts, is closely linked with the electron transfer reactions either via the cyclic flow of electrons around PS1 (Crowther and Hind, 1980), or by some other mechanism which requires the pre-reduction of a bound form of quinone (Bouges-Bocquet, 1980a).

Alternative interpretations of the slow phase in chloroplasts, which indirectly correlate it with electron transport, have also been presented. Olsen and Barber (1981) have suggested that this slow component appears as a consequence of the neutralization of the fixed dipole on the reaction centre (as induced by the initial charge separation), due to the electron transport linked release of H^+ and OH^- into the aqueous phases. It was proposed that, initially, the field is localized (phase a) and that only a small absorption change will be observed if the distance

between the field generator (the reaction centre) and the field indicator (the P515 complex) is large. Upon neutralization of the fixed charge on the reaction centre, due to proton exchange, the electric field becomes fully delocalized and the P515 complex is exposed to an increased electric field which is manifested by the generation of the slow phase.

Zimanyi and Garab (1982), however, have interpreted the slow rise in terms of the actual translocation of light-induced charges from the dielectric membrane into the surrounding conductive phases. Their model calculations indicate that such an event induces an enhanced electrochromic response of the photosynthetic pigments. The slow rise is associated with the slow redox-chain-related charge transport processes, where the neutralization of the localized charge on cytochrome $\underline{f}^{+}$ is concomitant with the release of a proton. It is this proton translocation through the boundaries of the membrane, which is argued to induce an increase in the electric field and hence the generation of a slow phase.

Schapendonk *et al* (1979) have taken another different view on the origin of the slow phase. By correlating their flash-induced absorption changes with previous measurements of the transmembrane potential using microelectrodes (Vredenberg and Tonk, 1974), they have observed, instead, a much slower rise, of approximately 100-150ms, in the electrochromic absorption change. This very slow phase has been interpreted to reflect slow intra-membranal changes induced by field-dependent charge displacement in the vicinity of the P515 complex. Furthermore this slow phase has been shown to be activated by PS1 alone (Schapendonk and Vredenberg, 1979).

1.7 Objectives of this thesis:

The work presented in this thesis is primarily directed towards a clearer understanding of the underlying mechanism generating the slow phase (phase b) of the flash-induced 515nm electrochromic shift in chloroplasts. The approach taken in this study is similar to that taken in bacterial chromatophores, where the slow phase (phase III) is thought to be a manifestation of a secondary electrogenic event associated with electron transport. The results are thus analysed in terms of distinguishing between a Q-type cycle (which would include a Mitchellian Q-cycle and Wikströms b-cycle: see section 1.3.2) or a simple linear electron transport scheme (see section 5.6).

The dependence of phase b on ambient redox poise is initially characterized (chapter 4) and its occurrence under different electron transport conditions investigated, concomitant with a study of the flash-induced cytochrome redox reactions (chapter 5). The involvement of proton uptake and proton release is also investigated (chapter 6), with the final results section (chapter 7) concentrating on the effect of inhibitors. Redox titrations of the fast phase (phase a) of the 515nm electrochromic shift are also carried out (chapter 4). These are subsequently used (chapter 5) to monitor the ambient redox state under the particular conditions imposed to observe phase b. Together, these results suggest that phase b is a manifestation of the state of electron transport in a similar manner that phase a records the activity of the primary reaction centres. Alterations in the organization of the photosynthetic components within the thylakoid membrane, as induced by changes in cation concentrations, are also found to affect both phase a and phase b (chapters 4 and 5).

The alternative interpretations of the origin of phase b, presented in section 1.6.3, have been considered in the first results section (chapter 3) where the electrochromic nature of phase b is characterized. The validity of these interpretations are discussed both in this chapter and in chapter 8, where the results presented in this thesis are summarized and inter-related.

CHAPTER 2

Materials and Methods

2.1 Chloroplast preparation:

The chloroplast preparation used in this study yielded Class I type chloroplasts: these have their outer envelope intact and are able to maintain electron flow with CO_2 as the terminal electron acceptor. Such chloroplasts are suitable for studying the flash-induced absorbance changes of the electron transport reactions since they contain a full complement of soluble redox components (e.g. ferredoxin), and they possess thylakoid membranes with low ionic conductivity (i.e. not leaky) and which are stable over long periods of time after isolation. For experiments, these intact chloroplastwere subjected to osmotic shock. The chloroplast preparation described below is a modification of that used by Nakatani and Barber (1977).

Throughout this study, the leaves of 10-day old peas (Pisum sativum , variety: Feltham First) grown from micoldusted seeds in Vermiculite under supplementary lighting conditions (16 hour day), in a greenhouse, were used.

2.1.1 Preparation of Class I intact chloroplasts:

70g of freshly harvested pea leaves were macerated, using a Polytron (type PT 35 OD), in 200g ice-cold grinding medium consisting of 0.33M sorbitol, 0.2mM $MgCl_2$, 20mM MES, adjusted to pH 6.5 with Tris. The resulting homogenate was filtered through 10 layers of muslin cloth,

the first two layers being separated by a thin layer of cotton wool. The filtrate was collected on ice and then subjected to centrifugation at 2200 xg for 45 seconds at 4°C. The supernatant was removed, and the hard and soft pellets were resuspended carefully, using a paint-brush, in a medium containing low levels of cation (0.33M sorbitol, adjusted to pH 7.5 with Tris), before being subjected to centrifugation at 2200 xg for 20 seconds at 4°C. This time both the supernatant and soft pellet were removed carefully by aspiration, and the hard pellet was resuspended at high chlorophyll concentration in the low cation medium, 3mM $MgCl_2$ subsequently being added. These intact chloroplasts were then stored on ice.*

2.1.2 Determination of chlorophyll:

The amount of chlorophyll present in the chloroplast suspension, prepared as detailed above, was determined by the method of Arnon (1949), and was typically 2-3 mg/ml.

An aliquot of the chloroplast suspension, nominally 20 µl, was added to 80% acetone in a volumetric flask, such that the final total volume was 10ml: the chloroplast suspension was thus diluted by a factor of 500. This mixture was then shaken well and subsequently passed through a filter, into a test-tube, so as to remove any coagulated protein particles. The light absorption of the resultant supernatant was then measured in a Perkin-Elmer 554 spectrophctometer, against a blank (of 80% acetone), at 645, 663 and 750nm. The measurement at 750nm was used to determine the degree of light scattering in the sample. The chlorophyll concentration was then determined using the following formula, which also takes into account the chlorophyll dilution factor (see earlier):

---

* Footnote. Intactness estimated by comparing the ability of potassium ferricyanide to accept electrons before and after osmotic shock and was typically 50-60%.

$$\text{Total chlorophyll } (\mu g/ml) = \{ [8.02 \times \Delta A_{663}] + [20.2 \times \Delta A_{645}] \} \times 500$$

The absorption values, ΔA, at both 645nm and 663nm are corrected for scattering by subtracting the absorption value at 750nm.

2.2 Flash-induced absorption measurements:

The main theme of this study has been to probe electron transport related events, occurring in the millisecond time domain, induced by a short (10μs) pulse of saturating light. The events of interest have been electric field generation, cytochrome redox changes, P700 redox changes and proton uptake/release.

2.2.1 Apparatus:

Flash-induced absorption measurements were made with a single-beam flash apparatus constructed by Applied Photophysics Ltd.; a schematic diagram of the apparatus is given in Fig. 2.1. The measuring beam was provided by a 100W tungsten halogen lamp and passed through an M300 high radiance monochromator (slit widths 1.25mm). The intensity of the measuring beam was less than $0.2 Wm^{-2}$. After passing through a 10mm path length cuvette, containing the sample, the measuring beam fell directly onto the photomultiplier head, which had been placed right up to the side of the cuvette so as to minimize loss of light due to scattering from the sample. Saturating light pulses, of 10μs pulse duration (width at half height), were provided by a xenon flash tube placed at right angles to the measuring beam. For most absorption measurements, the actinic flash was filtered through a 2mm Schott RG665 filter and the photomultiplier was protected by a 4mm Corning

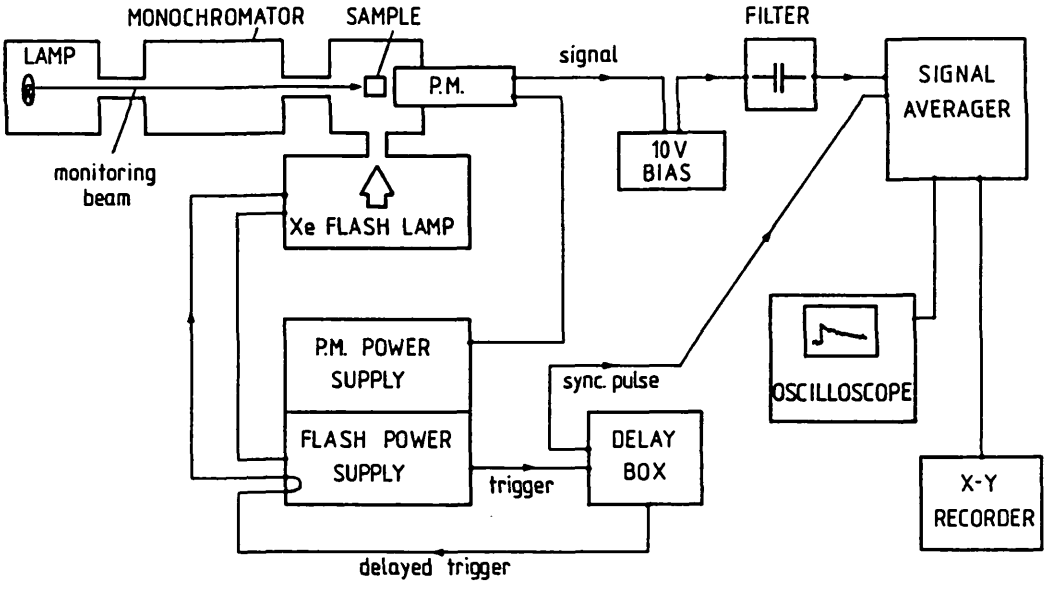


Fig. 2.1. Schematic diagram of the single-beam flash spectrophotometer, and the rapid recording devices, used in the measurement of flash-induced absorption changes.

4-96 filter. For the measurement of P700 absorption changes, however, the actinic flash was filtered through a 4mm Corning 4-96 filter and the photomultiplier was protected by a 2mm Schott RG665 filter. The signal from the photomultiplier was biased against a 10V direct current output and was thenfed into a signal averager (Nuclear Measurements, model 546C). The number of signals averaged (repetition rate 0.1Hz) depended on the absorption change being recorded (see later). The final signal could be viewed on an oscilloscope (Telequipment model S51B) and plotted on an X-Y recorder for further analysis. The time constant of the apparatus was normally 3ms and experiments were in general performed at 20°C.

2.2.2 Flash-induced 515nm electrochromic absorption changes:

The electrochromic shift was measured at 515nm by taking an average of 8 single sweeps (unless otherwise stated).

Intact chloroplasts, equivalent to 50μM chlorophyll in 2ml, were osmotically shocked in the cuvette, on ice, for 30 seconds, in 1.0ml distilled water containing either 10mM $MgCl_2$ (for stacked membranes) or 20mM KCl (for unstacked membranes) (see Barber, 1980). An equal volume of double strength buffer was then added to give a final concentration of 0.33M sorbitol, 10mM tricine/KOH (pH 8.3) and either 5mM Mg^{2+} or 10mM K^+. Also present in the sample was a fixed background level of 10mM K^+ from the buffer medium.

For experiments involving linear and cyclic electron flow through PS1, DCMU (25μM) was added together with a suitable reductant. The reductants used in this study were: sodium dithionite (1mM) made up in the above buffer medium; the couple ferredoxin (5μM) and NADPH (0.5mM),

in the presence of the oxygen trap glucose (5mM), glucose oxidase (0.1mg/ml) and catalase (0.2mg/ml); and duroquinol (0.5mM), prepared by the method of Izawa and Pan (1978). The reductants dithionite and duroquinol gave rise to pseudocyclic electron flow,* while the couple, ferredoxin** and NADPH maximized the endogenous cyclic electron flow. In addition to these reductants, the effect of the reducing couple ascorbate (0.5mM) and DCPIP (50mM) was also investigated.

Linear electron flow alone through PS1 was achieved by using the same conditions as above, i.e. + DCMU + reductant, but also in the presence of methyl viologen (50μM).

2.2.3 Flash-induced cytochrome and P700 absorption changes:

Cytochrome f and cytochrome b-563 were measured at 554nm minus 540nm and at 563nm minus 540nm, respectively, by averaging 16 sweeps at the measuring wavelength and subtracting the same number of sweeps at the reference wavelength. Similarly, P700 was measured at 703nm minus 730nm; an average of 16 sweeps was also recorded. For these measurements the samples were prepared as described in section 2.2.2 except that valinomycin (2μM) and nigericin (2μM) were also present: this ensured that any contribution from the relatively large electrochromic shift at 515nm was eliminated.

2.2.4 Redox titrations of the flash-induced 515nm absorption change:

Redox titrations of the flash-induced 515nm absorption change were carried out at 20°C using the standard criteria required for redox potentiometry (see Dutton, 1978). A similar cuvette to that described

* Footnote. Pseudocyclic electron flow is defined as the electron transport induced, in the presence of DCMU, by exogenous reductants.
** Footnote. Ferredoxin, purified from Spirulina maxima, was the kind gift of Dr.K.K.Rao, Kings College, London.

by Dutton (1978) was used. The potential of the medium was monitored by a combined platinum-calomel electrode (EIL, series no.1117 combination electrode) connected to a Philips PW9409 digital pH meter. The electrode was calibrated with respect to quinhydrone, $E_{m,7}$ = 296mV with a -60mV/pH unit dependency (Clark, 1960).

Intact chloroplasts, equivalent to 50μM chlorophyll in 3ml, were osmotically shocked in the cuvette on ice for 30 seconds in 1.5ml distilled water containing either 10mM $MgCl_2$ (for stacked membranes) or 20mM KCl (for unstacked membranes), as described previously. Again, an equal volume of double strength buffer was added, this time giving final concentrations of 0.33M sorbitol, 50mM HEPES/KOH (pH 7.5) and either 5mM Mg^{2+} or 10mM K^+. The solution was subsequently flushed for a few minutes with zero grade argon gas (less than 2ppm O_2); this was repeated again after the addition of similarly deoxygenated redox mediators. This suspension was stirred by a magnetic bar and argon gas was passed over the surface of the solution at all times.

Measurements were made by adjusting the potential to a desired value, allowing for equilibration, and then switching off the magnetic stirrer before flash-activating the sample. After a spectroscopic measurement, the stirring bar was again switched on. Each titration point represents the extent of the 515nm absorption change (ΔA_{515}) resulting from an average of 8 flashes at the indicated potential. Any further additions to the sample were made after a control measurement, in the absence of any additions, had been made at a potential of +200mV. Once the additions had been made, the measurement was repeated, again at the same potential. Both reductive and oxidative titrations were carried out. The reductive and oxidative titrants were solutions of 50mM sodium dithionite, freshly prepared before each

titration in 0.1M Tris-HCl(pH 9.0) and 50mM ferricyanide, respectively. A single titration took approximately 1-2 hours and care was taken to avoid misleading artefacts due to chloroplast degradation.

A list of the redox mediators employed is given below. They were all used at a concentration of 25μM except phenazine methosulphate which was used at 5μM. The number in parenthesis is the $E_{m,7}$ of the mediator: ferricyanide (+430mV), DAD (+220mV), 1,2-naphthoquinone (+143mV), phenazine methosulphate (+80mV), 1,4-naphthoquinone (+36mV), duroquinone (+5mV), 2,5-dihydroxybenzoquinone (-60mV), 2-hydroxy-1,4-naphthoquinone (-130mV), anthraquinone-2,6-disulphate (-185mV) and anthraquinone-2-sulphonate (-225mV). Control experiments with the omission of individual mediators or changes in mediator concentration demonstrated that there were no significant contributions of the mediators to the absorbance changes.

Redox titrations were also carried out at different ambient pH. The chloroplasts were suspended as described above but in the appropriate buffer media. The media (double strength) used were of the general form 0.66M sorbitol, 100mM buffer/KOH (pH x). The buffers were MES for pH 6.7 and HEPES for pH 7.0, 7.5 and 7.95.

The redox titration curves were fitted to the Nernst equation:

$$E_h = E_{m,x} + 2.303 \frac{RT}{nF} \log \frac{[ox]}{[red]} \quad \ldots\ldots\ldots\ldots\ldots\ldots \quad 2.1$$

where $E_{m,x}$ is the midpoint redox potential: $E_h = E_{m,x}$ at half reduction point i.e. when [ox] = [red]. x is the ambient pH of the

determination and n is the number of electrons transferred in the reaction. Also, 2.303RT/F is approximately 0.06 volts at 20°C. The Nernst relationship is shown in Fig. 2.2(a) for both an n = 1 and n = 2 redox reaction.

Such redox reactions often involve protons, a simplified example of which is given below, for an n = 1 redox reaction:

$$AH \rightleftharpoons A + e^- + H^+ \quad \ldots\ldots\ldots\ldots\ldots\ldots\ldots\ldots \quad 2.2$$

Using this in the above Nernst equation yields (for T = 20°C):

$$E_h = E_{m,x} + 0.06 \log \frac{[ox]}{[red\ H]} - 0.06\ pH \quad \ldots\ldots\ldots\ldots \quad 2.3$$

Eqn. 2.3 gives the pH dependence of the Nernst curve as a whole, and hence of its E_m: for every pH unit increase, there is a shift of -0.06V. A generalized form of Eqn. 2.3, including the n-value of the redox reaction is:

$$E_{m,x} = E_{m,y} - \frac{0.06}{n} (pH\,x - pH\,y) \quad \ldots\ldots\ldots\ldots\ldots\ldots \quad 2.4$$

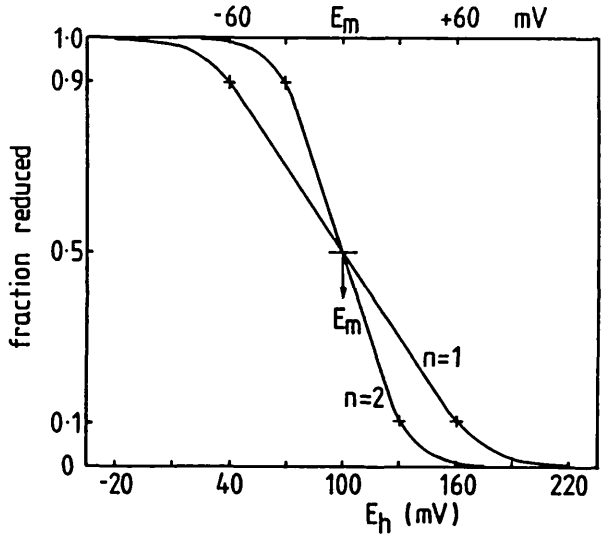
The titration curves of pH versus E_m values, determined experimentally in this study, were thus fitted to Eqn. 2.4.

To be noted, however, is that Eqn. 2.4 is only valid for redox reactions in which there is a net release and binding of a proton during oxidation-reduction. For most redox couples, this proton exchange is limited at high and low pH values by the pK of the reduced and oxidized form of the couple, respectively. From the Henderson-

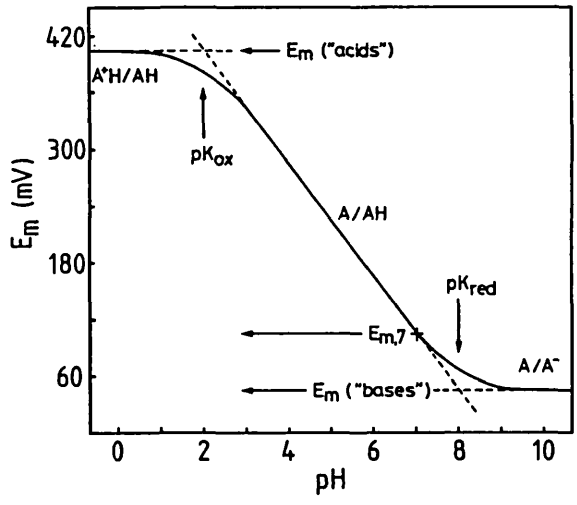
Fig. 2.2(a). The Nernst curves for one- and two-electron redox couples. Under conditions when the measured extent of reduction is 50% the redox couple is at its midpoint. In this example, the n=1 or 2 redox component is given at E_m of 100mV.

Fig. 2.2(b). The E_m/pH relationship. Three regions are shown: $pH < pK_{ox}$, where E_m approaches pH independence; $pK_{ox} < pH < pK_{red}$, where E_m varies approximately -60mV/pH unit; and $pH > pK_{red}$, where E_m again becomes pH independent. Dashed lines extrapolate to the respective pKs.

a.


-60
E_m
+60 mV
1·0
0·9
0·5
0·1
0
fraction reduced
E_m
n=1
n=2
-20
40
100
160
220
E_h (mV)

b.


420
300
180
60
E_m (mV)
E_m ("acids")
A⁺H/AH
pK_{ox}
A/AH
pK_{red}
$E_{m,7}$
A/A⁻
E_m ("bases")
0
2
4
6
8
10
pH

Hasselbalch expression, pH = pK + log { [base] / [acid] } , which is the proton analogue of the Nernst equation, the pK is defined as the pH when [base] = [acid]. The pKs of a redox couple can be revealed from a plot of E_m values versus pH values: above and below the pKs, the reaction in Eqn. 2.2 becomes simplified since there is no net proton exchange, the E_m value thus losing its dependency on the ambient pH, see Fig. 2.2(b).

There are therefore three distinct pH regions, to be kept in mind, where different redox reactions predominate:

(a) at pH values > pK_{red}, the redox reaction is:

$$A^- \rightleftarrows A + e^- \quad \text{..... 2.5}$$

(b) at pH values between pK_{ox} and pK_{red} the predominant reaction is as described in Eqn. 2.2

(c) at pH values < pK_{ox}, the redox reaction is:

$$AH \rightleftarrows A^+H + e^- \quad \text{..... 2.6}$$

2.2.5 Flash-induced proton uptake from the outer aqueous phase:

Flash-induced proton uptake was measured in an unbuffered suspension of chloroplasts by the absorption change of the pH-indicating dye cresol red at 574nm, pH 7.3(Junge and Ausländer, 1973). This indicator dye is thought to be located in the outer aqueous phase and not bound to the membrane (Petty and Dutton, 1976a). An average of 8 single sweeps was recorded: non-specific responses were virtually absent at 574nm as revealed by the zero signal after the addition

of 50mM tricine to the suspension, see Fig. 6.3(e). An alternative dye to cresol red is phenol red, which has an absorption maximum at 558nm, pH 7.3.

Intact chloroplasts, equivalent to 50mM chlorophyll in 2ml, were osmotically shocked in the cuvette on ice for 30 seconds in 1.0ml distilled water containing 10mM $MgCl_2$. An equal volume of double-strength buffer-free medium was then added to give a final concentration of 0.33M sorbitol, 50mM KCl and 10mM $MgCl_2$, pH 7.3. Cresol red (or phenol red) was subsequently added at a concentration of 40μM. The pH of the sample was checked and, when required, readjusted to pH 7.3 by the addition of small aliquots of HCl (1M) or KOH (1M).

The absorption changes of cresol red were calibrated into the number of protons bound or released, by measuring the steady state absorption change on the mixing of a known amount of acid into the suspension. Typically, 1μl of 1mM HCl was added to 2ml: this is equivalent to the addition of 1 nmole H^+. A rise in absorption at 574nm indicates alkalinazation of the outer aqueous phase.

pH titrations of the cresol red absorption change were carried out by altering the pH of the sample to the desired value by the direct addition of aliquots of HCl (1M) or KOH (1M).

2.2.6 Flash-induced proton release into the inner aqueous phase:

Flash-induced proton release was monitored by the absorption change of the dye neutral red at 540nm, pH 7.3 (Junge et al, 1979). An average of 8 single sweeps was recorded. Neutral red distributes itself over the inner and outer phases of the thylakoid membrane, and hence can indicate pH changes in both aqueous phases. The use of neutral red

as an indicator specific for pH changes in the internal phase can thus be achieved by selectively buffering the pH changes in the outer phase by a non-permeating buffer such as bovine serum albumin, BSA (Ausländer and Junge, 1975).

The chloroplast sample was prepared as described in section 2.2.5 , but BSA was also present in the double strength medium at a final concentration of 2mg/ml. Neutral red was then added at a concentration of 40μM. Also present was valinomycin (2μM) to eliminate the large contribution from the 515nm electrochromic absorption change. No further artefacts contributed to the neutral red absorption change as indicated by the null signal observed upon the addition of the permeating buffer imidazole (20mM), see Fig. 6.6(b). A rise in absorption at 540nm is indicative of acidification of the inner aqueous phase. A method used for the calibration of this signal will be discussed later.

2.3 Steady state chlorophyll fluorescence measurements:

Chlorophyll fluorescence was induced by broad band actinic light obtained from a tungsten-halogen light source passed through a combination of Schott BG18 (2mm) and Schott BG38 (2mm) cut-off filters: this resulted in a light intensity of $30Wm^{-2}$. The fluorescence was detected at right angles by an EMI 9558B S20 photomultiplier protected by a Balzar B-40 693 interference filter and a Schott RG695 cut-off filter. The output from the photomultiplier was displayed directly onto a pen chart recorder. All chlorophyll fluorescence yield measurements were carried out at room temperature.

The membranes were suspended as described in section 2.2.2, in either the stacked or unstacked condition, but giving a final total volume of 3ml; DCMU (20μM) was subsequently added. To observe salt-

induced chlorophyll fluorescence, $MgCl_2$(5mM) was added to a chloroplast suspension, initially prepared in the unstacked state, and rapidly mixed in.

CHAPTER 3

The electrochromic properties of the 515nm absorption change

The central feature of this thesis is the use of the intrinsic photosynthetic voltmeter, the 515nm electrochromic absorption change, ΔA_{515}, to monitor flash-induced electron transport processes. As stated in the introduction (sections 1.5 and 1.6), under certain conditions, the flash-induced ΔA_{515} is comprised of two kinetically distinct rise components: an initial fast phase (phase a) and a subsequent slow phase (phase b). The basic physical features of these two phases are presented in this chapter, and of fundamental importance, their electrochromic nature is emphasized. Also characterized is the nature of the underlying electric field (i.e. localized or delocalized) responsible for the rise and decay properties of phase a and phase b.

Except where stated, the experiments discussed here were carried out with stacked thylakoid membranes, under the condition of pseudocyclic electron flow (see section 2.2.2): high concentrations of DCMU were added so that electron input from PS2 was blocked, and reductant was supplied to obtain suitable redox poise for PS1 turnover.

3.1 Physical features of the 515nm absorption change:

Fig. 3.1(a) shows a typical flash-induced absorption change with biphasic rise kinetics. The addition of DBMIB, at a concentration which blocks plastoquinol oxidation, has little effect on the extent of the fast phase (phase a) but results in a loss of the slow phase (phase b), Fig. 3.1(b). From a comparison of the decay kinetics of Figs. 3.1(a) and (b) it is noted that DBMIB also introduces a slight

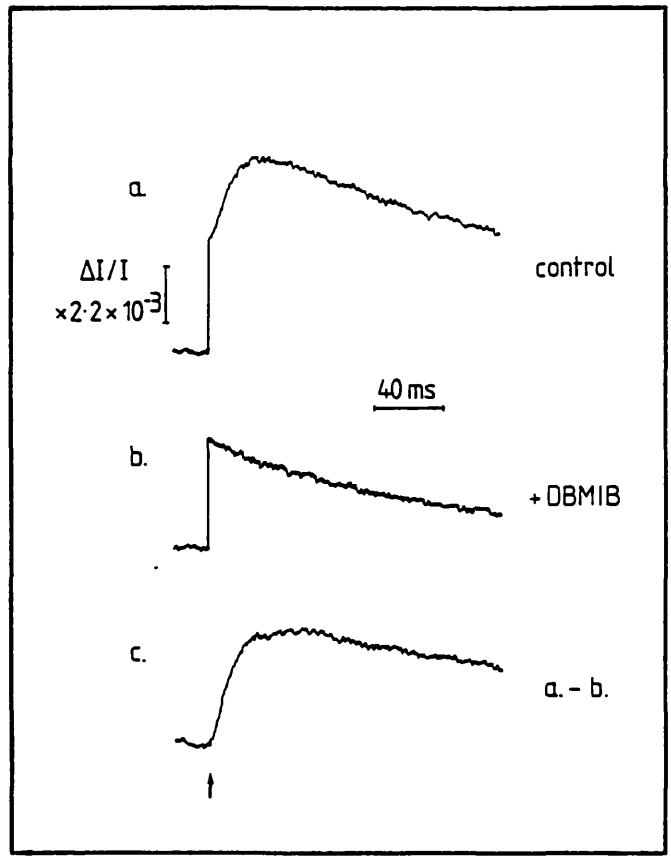


Fig. 3.1. Flash-induced ΔA_{515} for stacked thylakoid membranes. Conditions are as described in section 2.2.2 for pseudocyclic electron flow, with dithionite as reductant. (a) control, with no further additions; (b) as (a) + 15μM DBMIB: this reveals the extent and kinetics of phase a; (c) subtraction (a) - (b): this reveals the extent and kinetics of phase b.

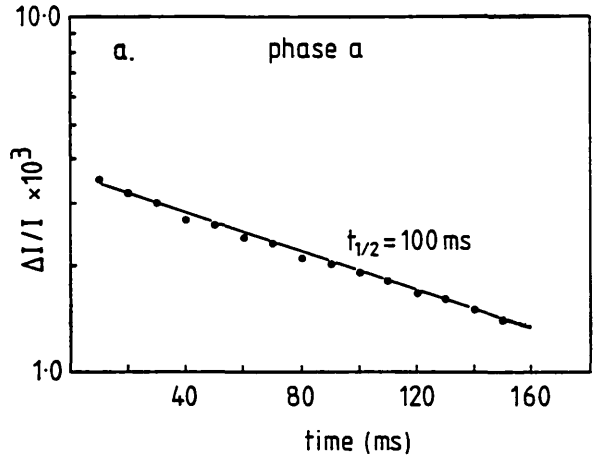
increase in the relaxation rate of the electric field. Since the contribution of phase b is revealed by the subtraction of the signals ± DBMIB, see Fig. 3.1(c), this latter effect may introduce an artefact in both the extent and the subsequent decay kinetics of phase b. The ratio of the extent of phase a to phase b, under these conditions of pseudocyclic electron flow, is, at maximum 1:1, but depending on the sample, this ratio can be lower.

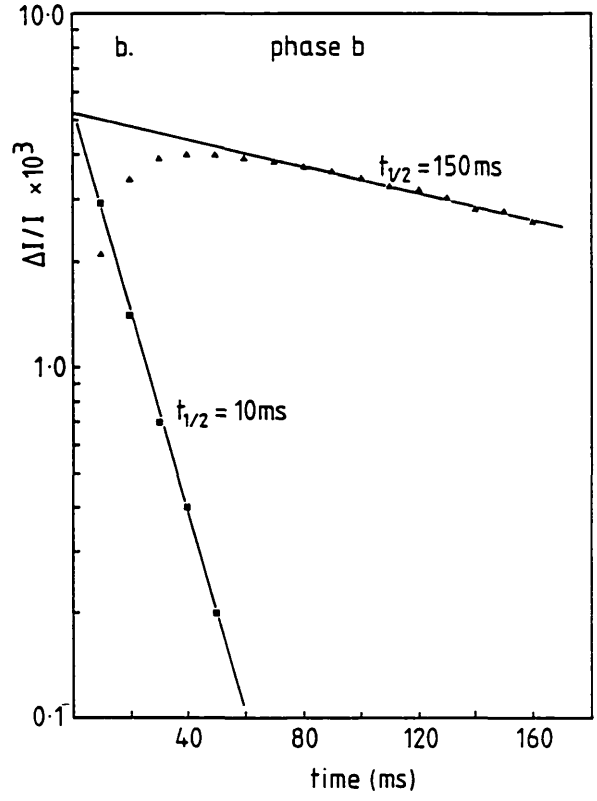
The rise of phase a is very rapid, occurring within the nanosecond timescale (see Wolff et al, 1969). The decay of phase a occurs with a half-time, $t_{\frac{1}{2}}$, of approximately 100ms and is exponential, as revealed by its semilogarithmic plot, Fig. 3.2(a); phase a is thus said to exhibit 1st order decay kinetics. Both the rise and decay of phase b are also 1st order reactions, Fig. 3.2(b), and have a $t_{\frac{1}{2}}$ of approximately 10ms and 150ms, respectively. Both the decay of phase a and that of phase b can be accelerated, in parallel, in the presence of ionophores (see later).

3.2 Evidence for the electrochromic nature of the ΔA_{515}:

The electrochromic nature of the fast phase a has been well characterized (Witt, 1975): it can be attributed to the electric field generated at the reaction centres upon flash activation. An analysis of phase a can thus provide some information concerning the state of electron transport. An example is given in Fig. 3.3. When no inhibitor or reductant is present, the magnitude of phase a is large, Fig. 3.3(a); presumably the electric field generated at both PS1 and PS2 contributes to its extent. Addition of DCMU, an inhibitor of electron transport, results in an almost complete disappearance of the flash-induced ΔA_{515}, Fig. 3.3(b). This effect of DCMU is, however,

Fig. 3.2. Semilogarithmic plots of the kinetics of the flash-induced ΔA_{515}. (a) The decay kinetics of phase a, as shown in Fig. 3.1(b): these fit a straight line, indicative of first order kinetics. (b) The kinetics of phase b, as shown in Fig. 3.1(c) (triangle symbols): both the decay and rise components exhibit first order kinetics. The rise component of phase b (square symbols) is resolved by the following procedure: the line for the decay kinetics is extrapolated to zero time, those points (at fast times) which do not lie on this line are subtracted from it and the difference is then replotted.


10·0
a.
phase a
ΔI/I ×10³
t1/2 = 100 ms
1·0
40
80
120
160
time (ms)


10·0
b.
phase b
ΔI/I ×10³
t1/2 = 150 ms
1·0
t1/2 = 10 ms
0·1
40
80
120
160
time (ms)

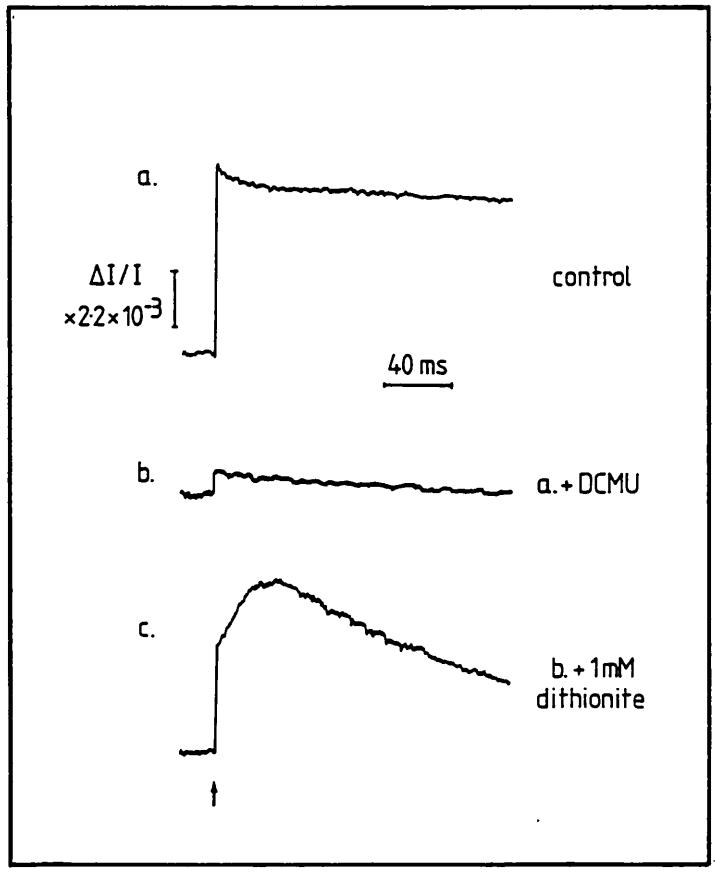


Fig. 3.3. Flash-induced ΔA_{515} for stacked thylakoid membranes. Conditions are as described in section 2.2.2 but with no added inhibitor or reductant. (a) control, with no further additions; (b) as (a) + 25μM DCMU; (c) as (b) + 1mM dithionite.

not immediate; several flashes are required to enable the removal of electrons from the inter-electron transport chain. Addition of reductant (dithionite) restores phase a to about 50% of its original amplitude, Fig. 3.3(c); also, phase b is now apparent. Dithionite is able to reactivate electron transport through PS1 by providing reducing equivalents for the plastoquinone pool, PS2 turnover being blocked by DCMU.

The flash-induced absorption spectrum of the dithionite-restored phase a is given in Fig. 3.4. It exhibits the characteristic electrochromic difference spectrum, see Witt (1975), with a maximum at 515nm and a minimum at 475nm. The spectrum of phase b, as monitored by the extent of the ΔA_{515} at 10ms, is also given in Fig. 3.4, and matches that of phase a very closely. This suggests that phase b also results from an electrochromic phenomenon. The fact that the extent of phase b is comparable with that of phase a indicates that phase b may be generated by a single charge moving across the membrane (per reaction centre). These observations are in agreement with previous work (Crowther and Hind, 1980; Olsen and Barber, 1981).

Further evidence concerning the electrochromic nature of phase a and phase b, comes from studies with the electrophoretic ionophore valinomycin (in the presence of K^+). The criterion behind such a study is as follows. The electric field generated across the thylakoid membrane is dissipated by the passive efflux of cations and influx of anions (see section 1.4.2). Valinomycin accelerates the passive efflux of K^+ and consequently the rate of dissipation of the electric field is increased. If phase a and phase b do reflect rises in membrane potential, then valinomycin should affect their decay rates similarly. The results are shown in Figs. 3.5(a) and (b): valinomycin is found

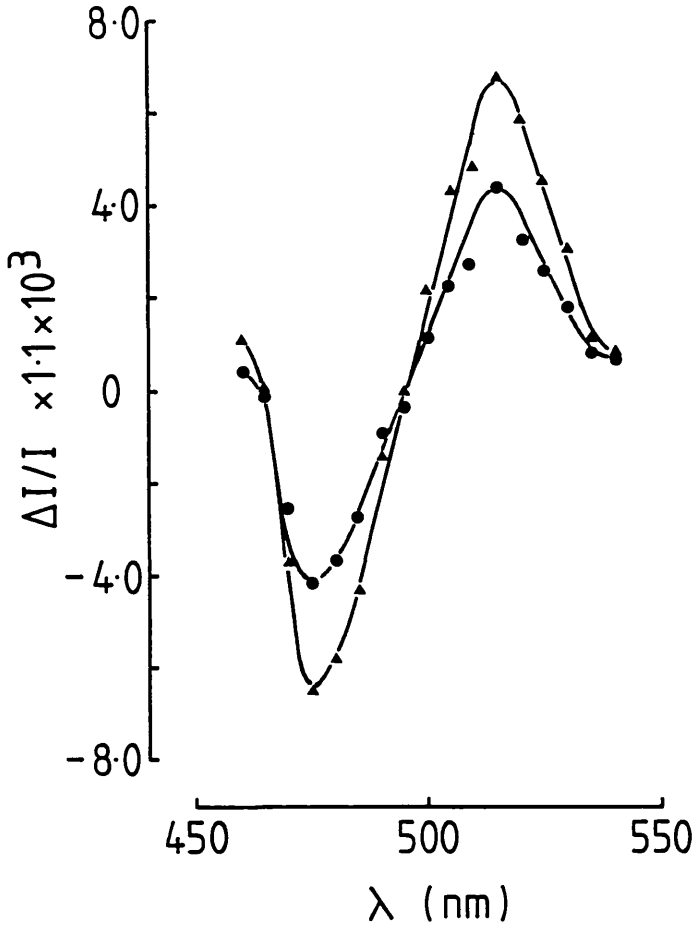
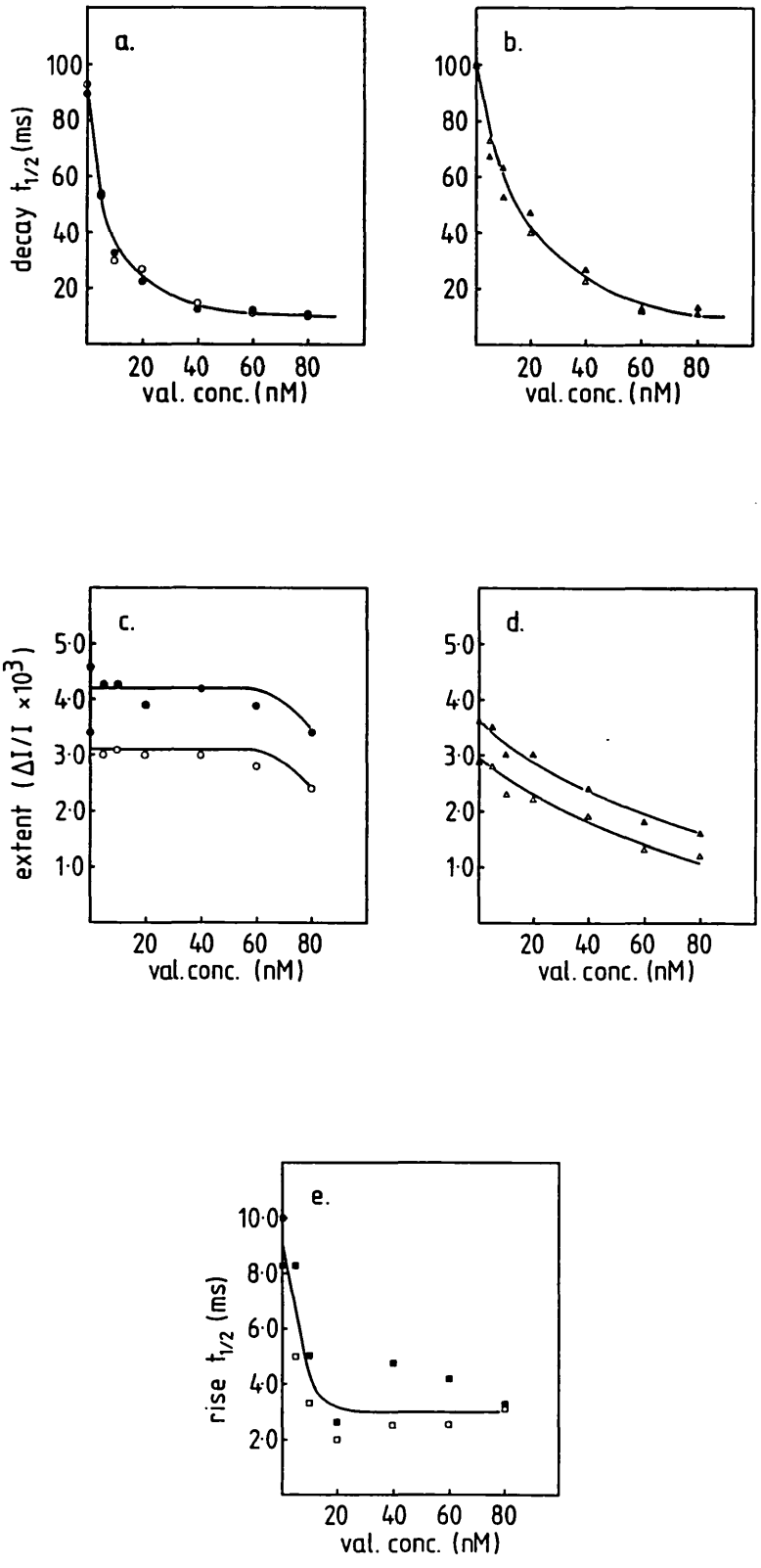


Fig. 3.4. Spectra of the extent of the flash-induced electrochromic shift detected at 3ms for phase a (circle symbols) and at 10ms for phase b (triangle symbols). Conditions are the same as those in Fig. 3.3(c).

Fig. 3.5. Titrations of the flash-induced ΔA_{515} with valinomycin (val.), and at different actinic light intensities. Conditions are those for stacked thylakoid membranes and of pseudocyclic electron transport (see section 2.2.2), with DQH_2 as reductant. The extent and kinetics of phase a and phase b are resolved by the procedure given in Fig. 3.1. Valinomycin titration of the $t_{\frac{1}{2}}$ for the decay of (a) phase a and (b) phase b. Valinomycin titration of the maximum extent of (c) phase a and (d) phase b. (e) Valinomycin titration of the $t_{\frac{1}{2}}$ for the rise of phase b. 100% actinic light intensity (closed symbols); 25% actinic light intensity (open symbols).


a.
b.
c.
d.
e.
decay $t_{1/2}$ (ms)
extent ($\Delta I/I \times 10^3$)
rise $t_{1/2}$ (ms)
val. conc. (nM)
val.conc. (nM)
100
80
60
40
20
5·0
4·0
3·0
2·0
1·0
10·0
8·0
6·0
4·0
2·0
20 40 60 80

to accelerate the decay rate of both phase a and phase b, and over the same concentration range. The consequence of the valinomycin concentration required to cause an acceleration of the field decay and that of the effect of lowering the actinic flash intensity will be discussed in the next section. To be noted here, though, is that the valinomycin titration curve for phase b does not drop quite as rapidly as that for phase a: this is most probably a result of the slight uncoupling effect of DBMIB discussed earlier. The difference is not significant enough to suggest that the electric fields of phase a and phase b are dissipated by different mechanisms.

3.3 Localized and delocalized electric fields:

The electric field generated across the thylakoid membrane, as a result of charge separation at the reaction centres (phase a), although initially localized, is thought to be rapidly delocalized. This subsequent delocalization is experimentally supported by the observation that less than one molecule of valinomycin is required per 10 electron transport chains to accelerate the rate of decay of phase a by a factor of 2, see Fig. 3.5(a). This calculation assumes that there are 600 chlorophyll molecules per electron transport chain; also assumed is that the movement of a valinomycin molecule, between electron transport chains, is slow. The above result is in agreement with similar studies that have been carried out with bacterial chromatophores (Jackson and Crofts, 1969), which conclude that the rapidly generated electric field is also subsequently delocalized. If the electric field responsible for phase a had remained completely localized for a very long time, e.g. tens of ms, a minimum requirement to observe an acceleration of its decay would have been one valinomycin molecule per electron transport chain.

The decay rate of phase b is affected by valinomycin over the same concentration range as in the case of phase a (compare Figs. 3.5(a) and (b)). This suggests that the electric field monitored by phase b, although generated on a slow timescale, is also subsequently delocalized.

Lowering the actinic light intensity does not affect the decay rate constant, i.e. $t_{\frac{1}{2}}$, of either phase a or phase b, in the absence of valinomycin; nor does it affect the valinomycin titration curves obtained in Figs.3.5(a) and (b), (note in each figure the curves are superimposable). This is interpreted as further evidence for the 1st order nature of the reactions involved in the dissipation of the electric fields generating phase a and phase b. Since such decay reactions are exponential, their $t_{\frac{1}{2}}$ values are independent of the magnitude of the electric field (see later for the effect of actinic light intensity), but are determined by the membrane permeability.

The effect of valinomycin on the amplitude of phase a is shown in Fig. 3.5(c). Valinomycin is observed to have no effect, except at high concentrations, when the field decay is very rapid (i.e. faster than the 3ms time response of the apparatus). Such a rapidly decaying field appears to cut into the amplitude of phase a, thus reducing its extent. This particular effect is in fact usefully employed in the study of flash-induced cytochrome redox changes (see later): these experiments are carried out in the presence of high concentrations of valinomycin (typically 1-2μM), to eliminate the contribution from the larger ΔA_{515}.

The extent of phase b is, however, reduced, even at low valinomycin concentrations, Fig. 3.5(d). Since the maximum extent of phase b occurs at 20ms and not promptly, as for phase a, the field decay effect on amplitude, discussed above, will be apparent at lower valinomycin concentrations. Moreover, this effect must occur, to a small extent, in the absence of any valinomycin, since the electric field generating phase b "grows", simultaneous to the electric field dissipation.

The effect of lowering the actinic light intensity on the amplitude of phase a and phase b is also shown in Figs. 3.5(c) and (d). It is assumed that such an effect will decrease the number of reaction centres that are activated per flash. Experimentally, this can be observed as a decrease in the amplitude of phase a. A similar decrease in amplitude is also observed for phase b, indicating that the electric field generating phase b is also dependent on the number of electron transport chains activated. This intensity effect on the amplitude of phase a and phase b, is independent of valinomycin concentration, as observed by the parallel titration curves for the different actinic light intensities, Figs. 3.5(c) and (d). A point to note in these light intensity experiments is that while the intensity was diminished by a factor of 75%, the amplitude of phase a was only reduced by 30%. This shows that the 100% actinic light intensity used in all subsequent experiments is saturating.

Finally, Fig. 3.5(e) shows the effect of valinomycin on the rise kinetics of phase b. Although the scatter of points is rather large, (note the faster timescale), the general trend is that valinomycin is effective over the same concentration range that it has an effect on the decay. From the above arguments, this is indicative of a delocalized electric field: although phase b might initially be a localized electric field, what is observed on a ms timescale is apparent-

ly a delocalized electric field.

3.4 Discussion:

The results presented in this chapter indicate that phase a and phase b, of the 515nm electrochromic absorption change, share analogous electrical properties. They exhibit similar absorption spectra, Fig. 3.4, the $t_{\frac{1}{2}}$ values of their decay are similarly accelerated by increasing valinomycin concentrations, Figs. 3.5(a) and (b), and their extents are similarly dependent on the number of activated reaction centres, Figs. 3.5(c) and (d). Concerning phase a, these results would agree with its already well established electrochromic nature. Phase a represents a rapidly formed localized electric field across the thylakoid membrane which is subsequently delocalized by the redistribution of ions: it is attributed to the primary charge separation occurring at the photochemical reaction centres upon light activation. Although the electrical properties of phase b appear to mimick those of phase a quite closely, it is observed that the generation of phase b represents a delocalized electric field created across the thylakoid membrane, Fig. 3.5(e). Phase b is also possibly associated with the electron transfer reactions, especially since its inhibition by DBMIB indicates the involvement of PQH_2 oxidation. Hence, the use of phase a and phase b, in subsequent chapters, as empirical indicators of transmembrane electrical events, seems justified.

The validity of the alternative interpretations for the generation of phase b, that were presented in section 1.6.3, are briefly discussed below. A fuller discussion will be given in chapter 8. The Olsen and Barber (1981) model would predict that the generation of phase b is due to the delocalization of the electric field, generated by the fixed dipole at PS1, by the release of the proton upon PQH_2 oxidation. In

the absence of further experimental data, at this stage, it is not possible to comment critically on this model. The Zimanyi and Garab (1982) model proposes that it is the actual translocation of the charged proton, upon PQH_2 oxidation, across the membrane boundaries, that generates phase b. This would seem to suggest that the rise of phase b would be highly dependent on the membrane permeability and hence strongly attenuated in the presence of low concentrations of valinomycin. Such a marked effect on either amplitude or rise kinetics of phase b is not observed in Figs. 3.5(d) and (e).

The slow phase observed by Schapendonk and Vredenberg (1979) has instead been suggested to result from field-dependent conformational changes. It must be noted here, though, that their analysis of the ΔA_{515} is very different to that presented in Fig. 3.1. Their slow phase, called reaction II, is obtained by subtracting the component due to the fast electric field, called reaction I, as recorded with microelectrodes, from that electric field registered by the P515 complex. In this way reaction II has been found to have rise kinetics which are an order of magnitude slower than those of phase b. Reaction II and phase b cannot thus be correlated directly. What is of interest here, though , is their interpretation of the effect of valinomycin. In the presence of valinomycin (200μM) they also observe an acceleration of the flash-induced ΔA_{515}. However, again on the basis of microelectrode studies, they assume that the decay of reaction I is unaltered under these conditions. The subsequent subtraction to yield reaction II indicates that its decay kinetics also remain unaltered, and that it is apparently the suppression of the magnitude of reaction II that is responsible for the acceleration of the total ΔA_{515}. They therefore propose that reaction II cannot be directly

related to a transmembrane potential. The assumptions made in the interpretation of their results and the conclusions they reach, concerning the nature of reaction II, are in complete contrast to those presented in this chapter regarding phase b. However, as stated above, the main reason for such a discrepancy, is in the analysis of the components of the ΔA_{515}: Schapendonk and Vredenberg (1979) do not consider the slow phase as defined in Fig. 3.1(c). A problem with their particular analysis in fact concerns the interpretation of the effect of DBMIB: their analysis would seem to suggest that reaction II still occurred in the presence of DBMIB. This is in contrast to the results presented here and also to the assumptions made in the alternative models discussed above.

The various models presented here, will be discussed more critically later (chapter 8), by taking into account the results to be presented in the following chapters. However, one particular feature that none of these alternative models can really account for, is the redox dependence, observed by different groups, for the generation of phase b (see section 1.6.2). This property is investigated more fully, in the next chapter, for both phase a and phase b.

CHAPTER 4

Redox potentiometric titrations of the 515nm absorption change

In this chapter the effect of salt on phase a and phase b of the flash-induced 515nm electrochromic absorption change is characterized. This property is further investigated in redox titrations of the ΔA_{515}. The purpose of these redox titrations is to define more clearly the reactions involved in the generation of phase a and phase b.

4.1 The salt dependence of the 515nm electrochromic shift:

Changes in salt concentration are known to bring about changes in the degree of stacking of the thylakoid membranes and in the distribution of intrinsic protein complexes (Barber, 1980). The electrostatic screening of the fixed negative charges on the thylakoid membrane, brought about by the addition of cations, induces changes in the chlorophyll fluorescence emitted by PS2, and changes in energy transfer from PS2 to PS1 which can be correlated with changes in membrane stacking and with alterations in the spatial separation between the two photosystems.

Fig. 4.1(a) shows the classical salt-induced fluorescence increase. In the presence of low levels of monovalent cations, approximately 10mM K^+, the chlorophyll fluorescence yield is low. Under these conditions the membranes are unstacked and energy transfer between PS2 and PS1 is good, little energy being lost as fluorescence. Addition of low concentrations of divalent cations, approximately 5mM $MgCl_2$, results in a large increase in chlorophyll fluorescence. Under these conditions the thylakoid membranes reorganize into stacked and unstacked lamellae:

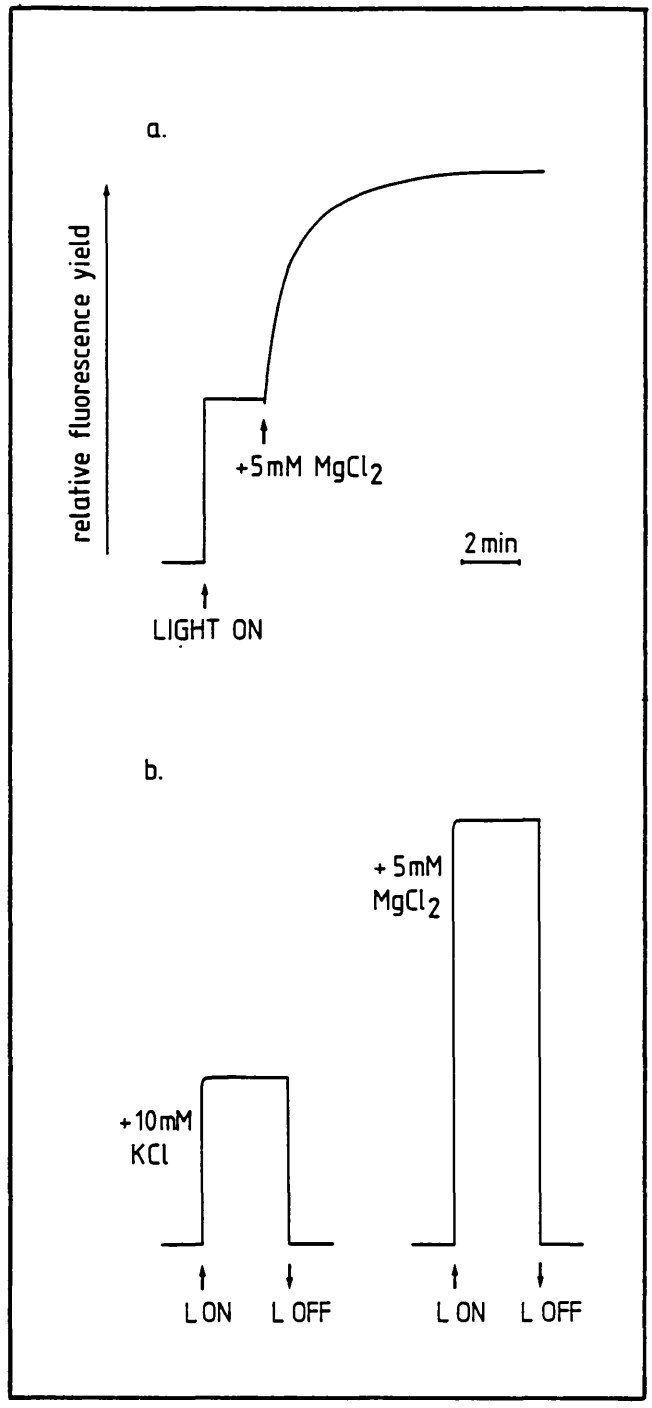


Fig. 4.1. Steady state fluorescence transients for samples prepared as described in section 2.3. (a) unstacked thylakoid membranes, subsequently subjected to the addition of 5mM $MgCl_2$; (b) thylakoids prepared either in the unstacked (+ 10mM KCl) or stacked (+ 5mM $MgCl_2$) state (also see text).

energy transfer between PS2 and PS1 is decreased and a larger amount of energy is lost in the form of fluorescence. A detailed analysis of this phenomenon (Barber, 1980; 1982) has indicated that the decrease in PS2 to PS1 energy transfer is due to the separation of the two photosystems into two discrete domains. These arguments, coupled with direct measurements on membrane fragments (Andersson and Anderson, 1980; Andersson and Haehnel, 1982) indicate that PS2 is located in the appressed regions of the thylakoid membranes, while PS1 is localized in the unstacked, exposed membranes (also see sections 1.2.2 and 1.2.3).

To obtain the stacked or unstacked condition directly, the chloroplasts are shocked in the presence of 10mM $MgCl_2$ (high salt) or 20mM KCl (low salt), respectively, giving final concentrations of 5mM Mg^{2+} or 10mM K^+, as described in section 2.2.2. Fig. 4.1(b) shows that this procedure does indeed induce the required stacking condition: the chlorophyll fluorescence promptly rises to either a high or low level, as determined in Fig. 4.1(a).

Such changes in salt concentrations, and hence the stacking condition, also induce changes in the flash-induced electrochromic shift. These are shown in Fig. 4.2, where pseudocyclic electron transport is operative, with dithionite as the reductant. Under low salt conditions phase a is approximately 20% larger than under high salt conditions, see Fig. 4.2(b). For phase b, however, this effect is reversed: its amplitude is larger in the presence of high salt than in the presence of low salt, see Fig. 4.2(c). To be noted, though, is that this effect of 5mM $MgCl_2$ on the amplitude of phase b is not the result of an artefact introduced by an increase in membrane conductivity under this salt condition: more pertinent is a slight increase in the decay rate of phase a in the presence of 10mM KCl, see Fig. 4.2(b).

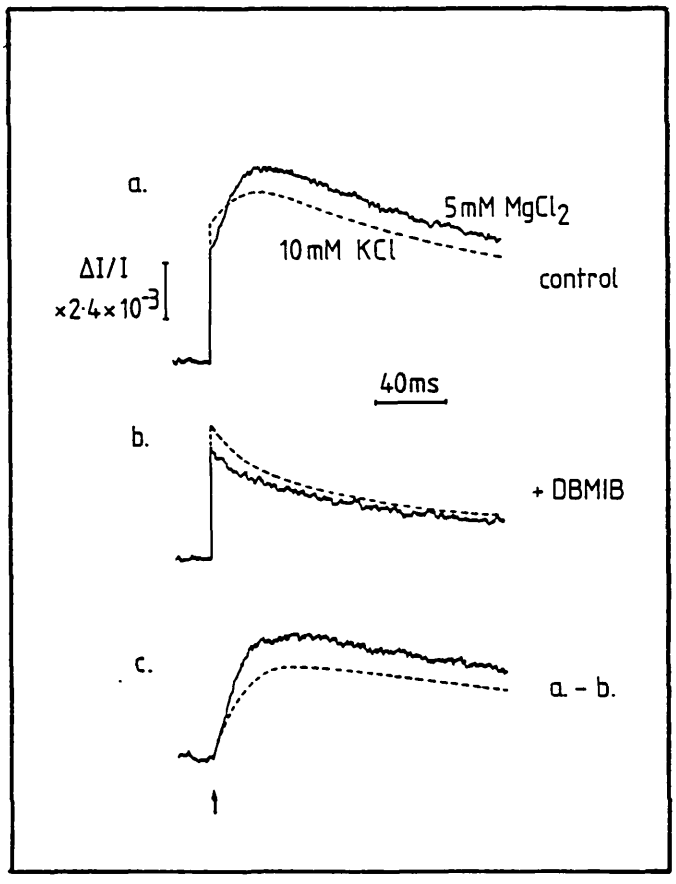


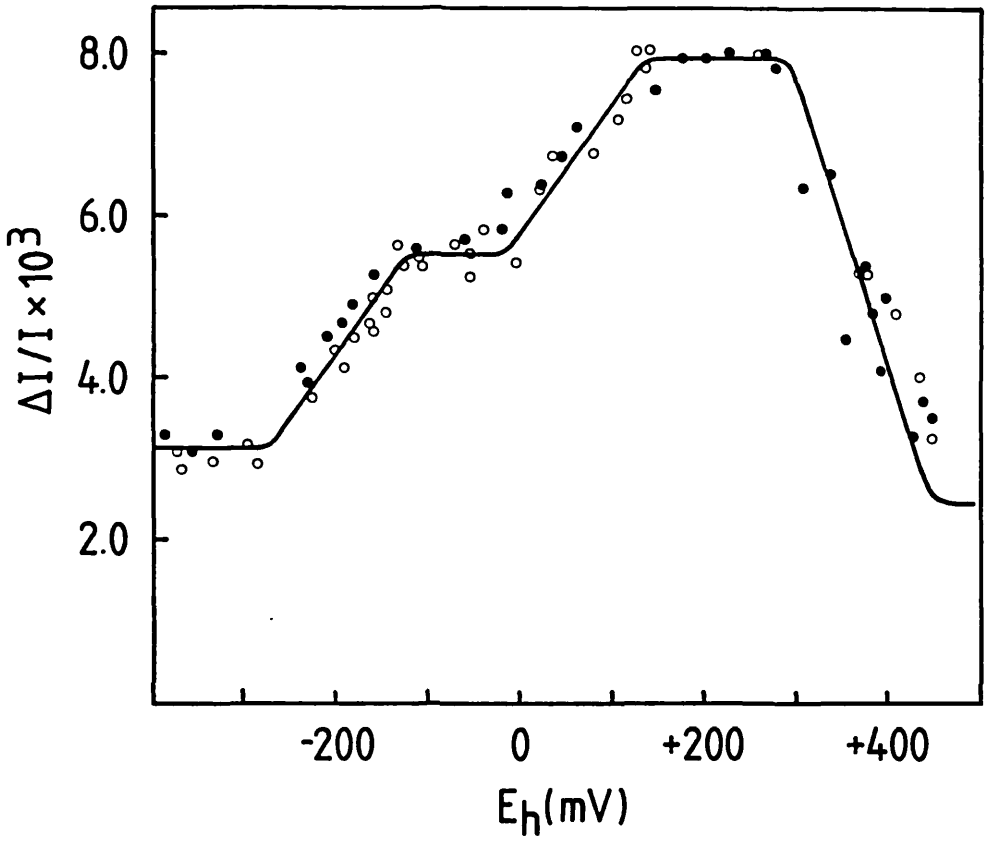
Fig. 4.2. Flash-induced ΔA_{515} for stacked (full line) and unstacked (broken line) thylakoid membranes. Conditions are as described in section 2.2.2 for pseudocyclic electron flow, with dithionite as reductant. (a) control, with no further additions; (b) as (a) + 15μM DBMIB; (c) subtraction (a) - (b).

Such an antagonistic behaviour of phase a and phase b to different levels of mono- and divalent cations has also been observed by Olsen and Barber (1981). Their interpretation of these results (see section 1.6.3) led them to propose a delocalization model for the generation of phase b. Alternative interpretations of the data are, however, possible. In fact, use of this salt effect in the redox titrations to follow and in the results presented in chapter 5 enables correlations to be made between phase a and phase b of the ΔA_{515} and electron transport related events.

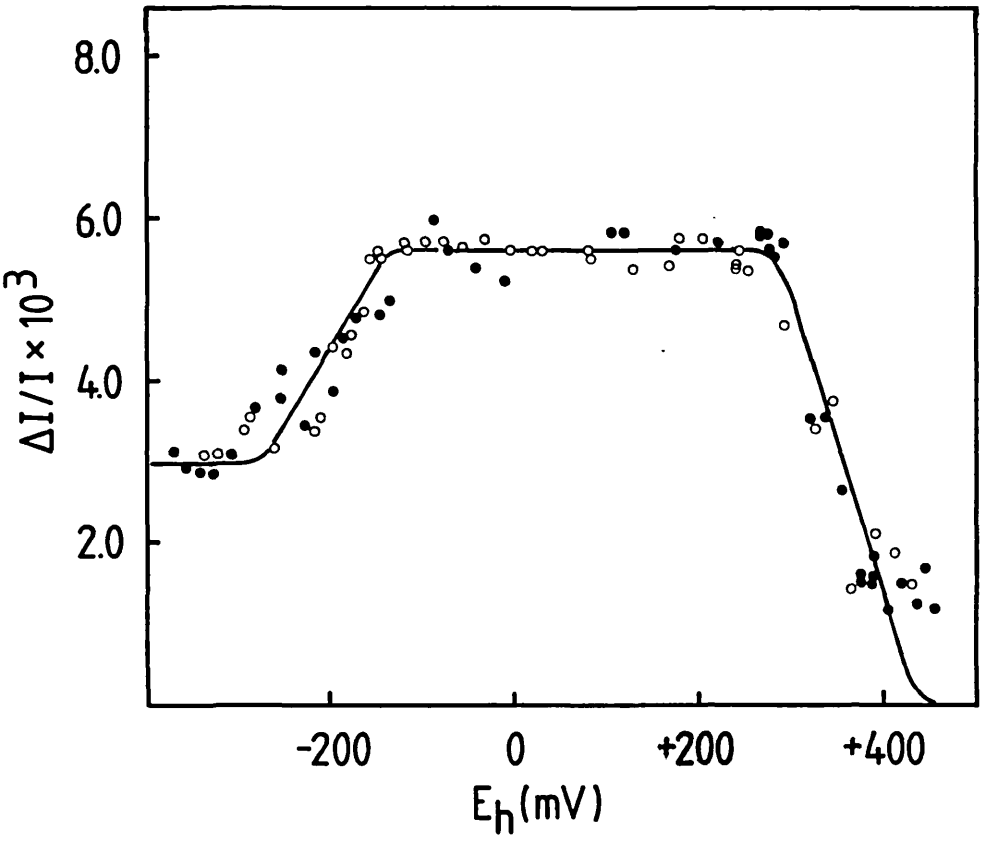
4.2 Redox potential titrations of phase a:

Redox potential titrations were carried out as described in section 2.2.4. Fig.4.3(a) shows the redox titration of the extent of phase a (detected at 3ms) under stacked conditions and in the absence of inhibitors. At low redox potentials (less than + 200mV) phase a exhibits a double wave in its titration. Each wave follows an n=1 Nernst curve (see section 2.2.4, Eqn. 2.1) and contributes a third to the total extent of the ΔA_{515}. The midpoint potentials ($E_{m,7.5}$) of each wave are +60mV and -195mV. The -195mV wave has a -60mV/pH unit dependency, as shown in Fig. 4.4. A residual 515nm absorption change exists at redox potentials < -400mV and presumably constitutes a third, non-titratable wave. Such a double wave titration curve, at low potentials, is similar to that observed by Malkin (1978) and to that very recently reported by Diner and Delosme (1983) for detection times greater than 3ms. Also observed in Fig. 4.3(a) is that at E_h values > + 300mV, the ΔA_{515} becomes smaller: presumably this is due to the chemical oxidation of the P700 electron donor of PS1. This component contributes more than one third to the total extent of the ΔA_{515}, and the data fits a single

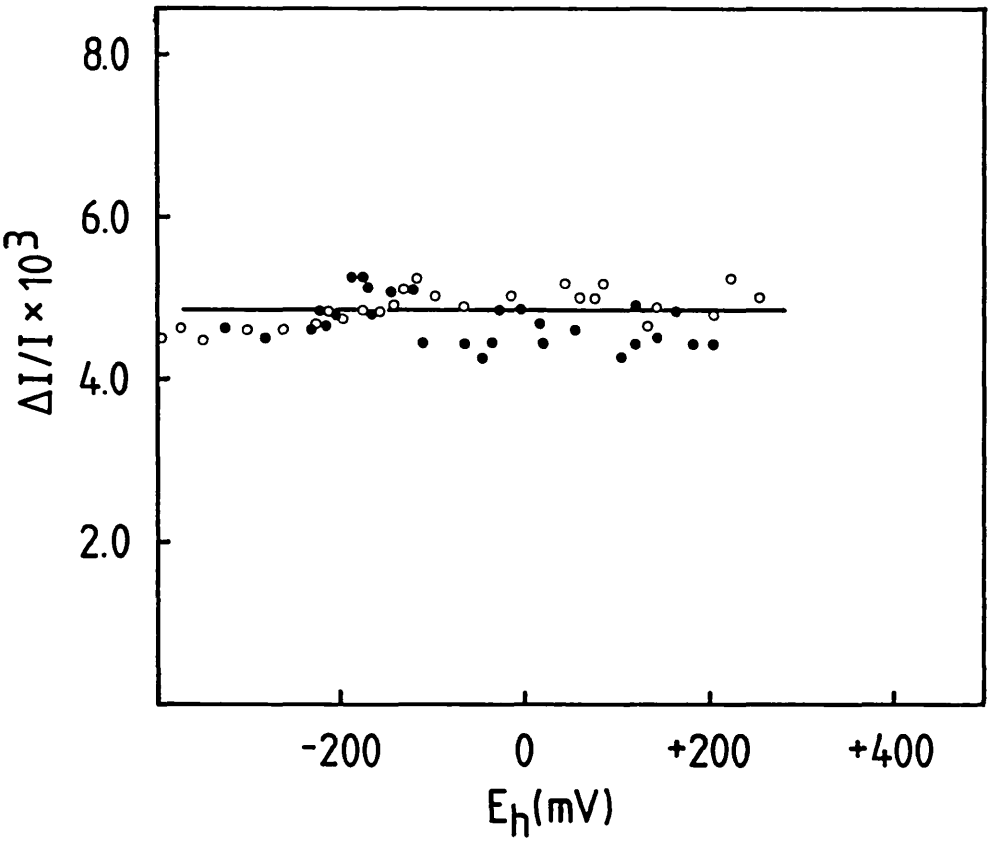
Fig. 4.3. Redox titrations of the flash-induced ΔA_{515}, detected at 3ms, for stacked thylakoid membranes suspended as described in section 2.2.4. (a) in the absence of any inhibitors; (b) + 25μM DCMU; (c) + 25μM DCMU + 50μM MV. Reductive titrations (open circles); oxidative titrations (closed circles).



(a) in the absence of any inhibitors



(b) + DCMU



(c) + DCMU + MV

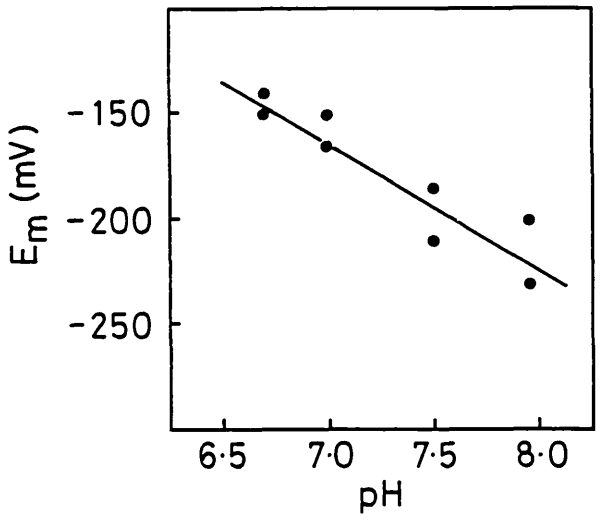


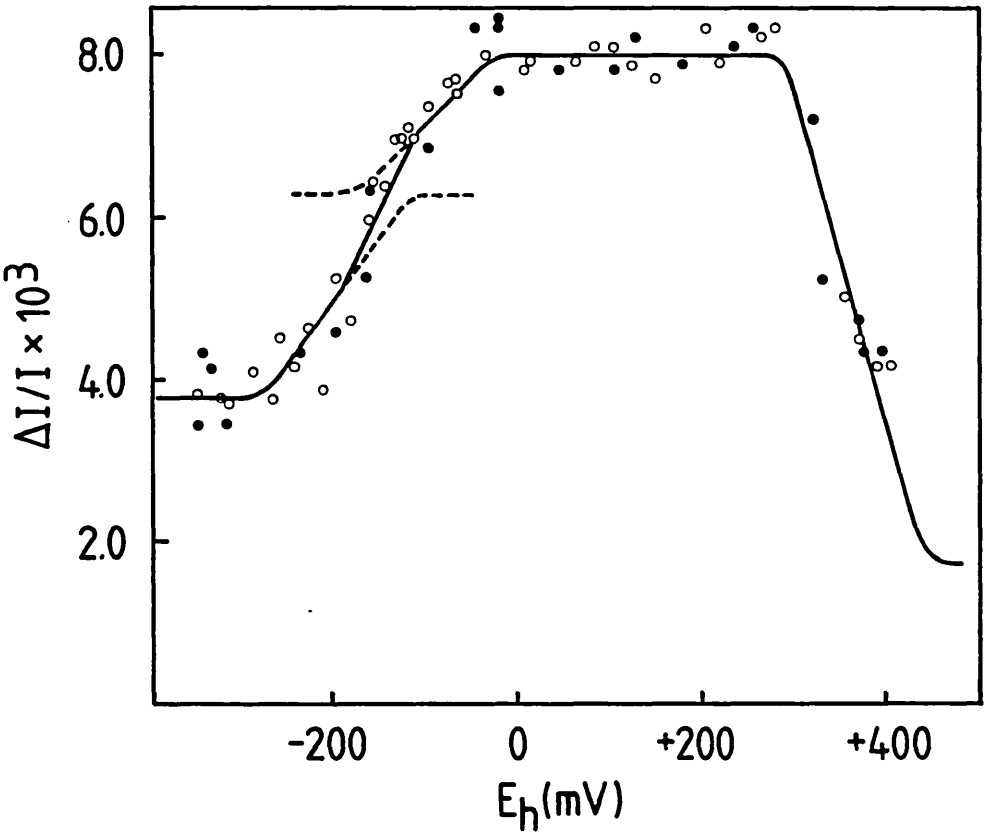
Fig. 4.4. pH dependence of the E_m for the low potential component of phase a ($E_{m,7.5}$ = -195mV), as determined under the conditions of Fig. 4.3(b). The required ambient pH was obtained by suspending the chloroplasts in the appropriate buffer medium, as described in section 2.2.4.

n = 1 Nernst curve with an $E_{m,7.5}$ = +370mV.

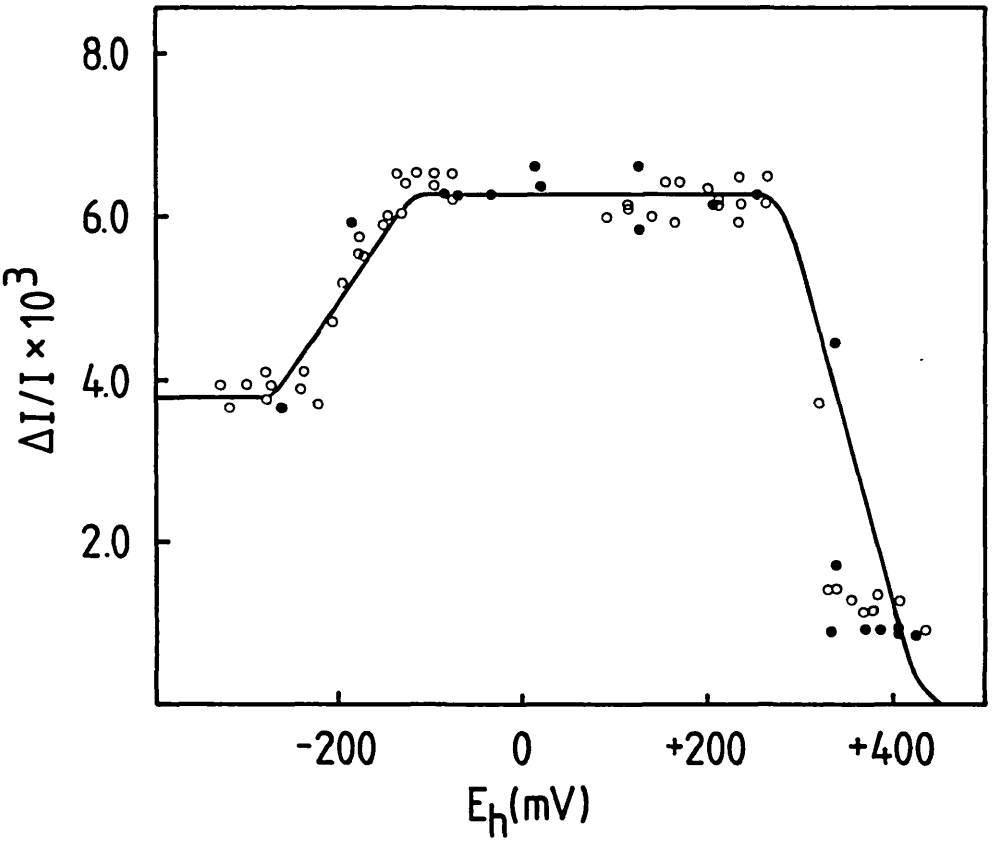
In the presence of DCMU, which is known to inhibit PS2 photochemical activity, only the +60mV component is completely inhibited, Fig. 4.3(b). This suggests that the +60mV component is responsible for the PS2 contribution to phase a. Both the -190mV and +370mV titration waves are still observed in the presence of DCMU and retain unaltered amplitudes. Also, the extent of the residual 515nm absorption change at redox potentials < -400mV is unchanged. This implicates these three components as manifestations of the PS1 contribution to phase a. Further evidence for this conclusion comes from a similar redox titration of phase a, but in the presence of DCMU and methyl viologen; methyl viologen is thought to accept electrons from PS1. Fig. 4.3(c) shows that, under these conditions, the -190mV wave is replaced by a non-titratable component, whose contribution at these low potentials is two-thirds of the total extent of the ΔA_{515} in Fig. 4.3(a). From the relative extents of the components titrated in Fig. 4.3, the PS1 contribution to phase a would thus seem to be twice that of PS2. Possible explanations for this observation will be discussed later.

Fig. 4.5 shows similar redox titrations of phase a, but carried out in the presence of low salt to ensure that the membranes are fully unstacked. In the absence of DCMU, Fig. 4.5(a), a double wave in the titration is still observed, but the relative contributions of each component are now altered. The -190mV component is present with an unaltered extent, suggesting that it does not result from an artefact due to the physical structure of the stacked membrane interfering with the equilibration of the redox mediators. The remaining contribution to phase a at very low potentials

Fig. 4.5. Redox titrations of the flash-induced ΔA_{515}, detected at 3ms, for unstacked thylakoid membranes suspended as described in section 2.2.4. (a) in the absence of any inhibitors; (b) + 25μM DCMU. Reductive titrations (open circles); oxidative titrations (closed circles).



(a) in the absence of any inhibitors



(b) + DCMU

is increased by approximately 12%. The most striking feature to note in Fig. 4.5(a), though, is the shift in potential of the +60mV component to -100mV and that its contribution has decreased by approximately 12%. Both the -190mV and -100mV titration waves can be fitted to n = 1 Nernst curves. The -100mV component is a manifestation of the PS2 contribution for unstacked membranes since the addition of DCMU results in its loss, Fig. 4.5(b). The remaining components in Fig. 4.5(b), are thus the PS1 contribution. Since the extent of the -190mV component remains unaltered in Fig. 4.5(b), it is the component with a midpoint redox potential < -400mV that is responsible for the increase in phase a observed in Fig. 4.2(b) under low salt conditions.

4.3 Redox potential titrations of phase b:

Fig. 4.6 shows the redox titration curve for phase b obtained with stacked membranes, by plotting the 10ms amplitude of the ΔA_{515} measured in the presence of DCMU. An increase in the amplitude of the ΔA_{515} is observed at potentials < + 150mV, correlating with the reduction of the plastoquinone pool. At lower redox potentials, the ΔA_{515} is attenuated with waves at -75mV and -195mV (pH 7.5). The titration wave with an $E_{m,7.5}$ = -75mV is presumably associated with the loss of phase b since it is not detected in the titration curve recorded at 3 ms, Fig. 4.3(b). Furthermore, it is absent from the 10ms titration curve in chloroplasts supplemented with DBMIB, Fig. 4.6. To be noted, however, is that at these lower redox potentials, the extent of phase b may be under-estimated due to an increased relaxation rate of the absorption change. With DBMIB present, a titration wave with an $E_{m,7.5}$ = +250mV is also observed, Fig. 4.6. The nature of this wave is uncertain, but may originate from the redox properties of DBMIB

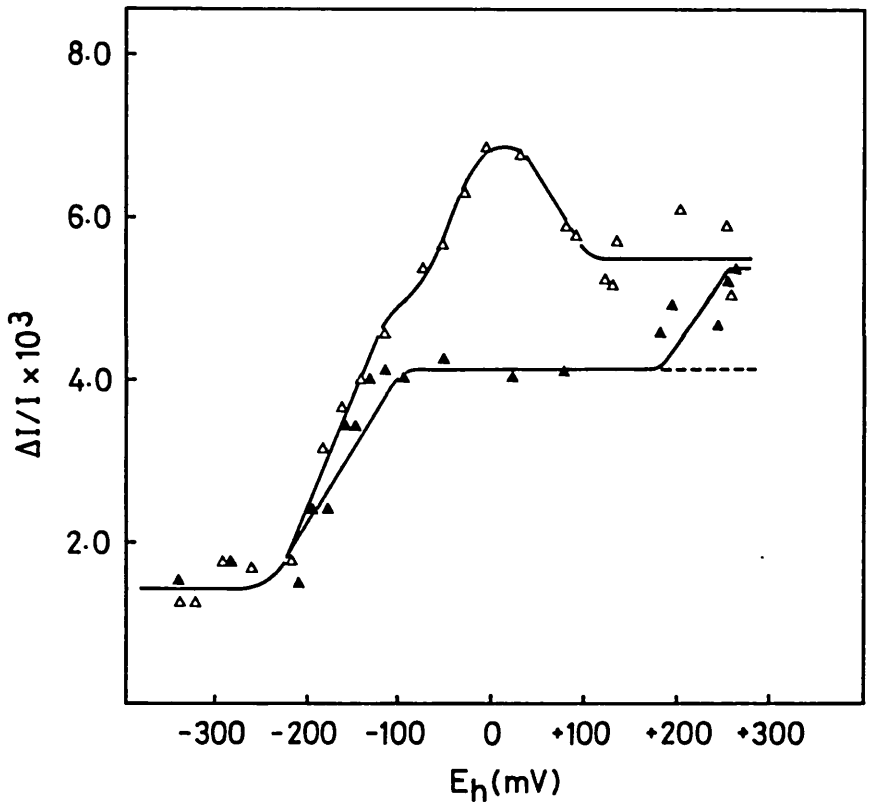


Fig. 4.6. Redox titration of the flash-induced ΔA_{515}, detected at 10ms, for stacked thylakoid membranes suspended as described in section 2.2.4. In the presence of 25μM DCMU (open triangles); in the presence of 25μM DCMU + 15μM DBMIB (closed triangles). Both redox titrations are reductive. The subtraction of these titrations yields the redox titration curve for phase b (see Fig. 4.7).

itself, and possibly indicates that the reduced form is an effective uncoupler of the thylakoid membrane.

Fig. 4.7(a) shows the phase b redox titration curve, obtained by the subtraction of the two curves of Fig. 4.6. Phase b is observed to appear with an $E_{m,7.5}$ = +100mV and to disappear with an $E_{m,7.5}$ = -75mV; both these waves can be fitted to an n = 1 Nernst curve and have a -60mV/pH unit dependency, as shown in Fig. 4.8. The +250mV wave due to DBMIB introduces a slight complication.

As shown in Fig. 4.7(b), the addition of methyl viologen does not inhibit the generation of phase b, indicating that cyclic electron flow around PS1 is not an essential requirement for its generation (see section 1.6.2): this is in agreement with the work of Selak and Whitmarsh (1982). Redox potential titrations of phase b in the absence of DCMU are complicated by the fact that the addition of DBMIB appears to have an added effect of behaving as an inhibitor of PS2 (Trebst et al, 1979), and hence these results have not been presented.

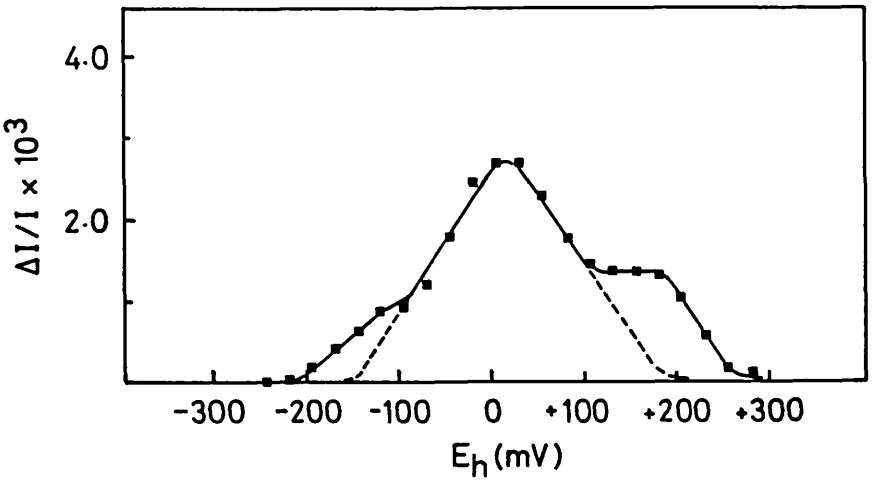
The redox titration for phase b in the presence of DCMU and under low salt conditions, Fig. 4.7(c), is very similar to that for the high salt condition, Fig. 4.7(a). The expected decrease in amplitude of phase b is not very large in comparison to that observed in Fig. 4.2(c): this could be due to an increased rate of decay of phase a, in the presence of the redox mediators and under the low salt conditions.

4.4 Discussion:

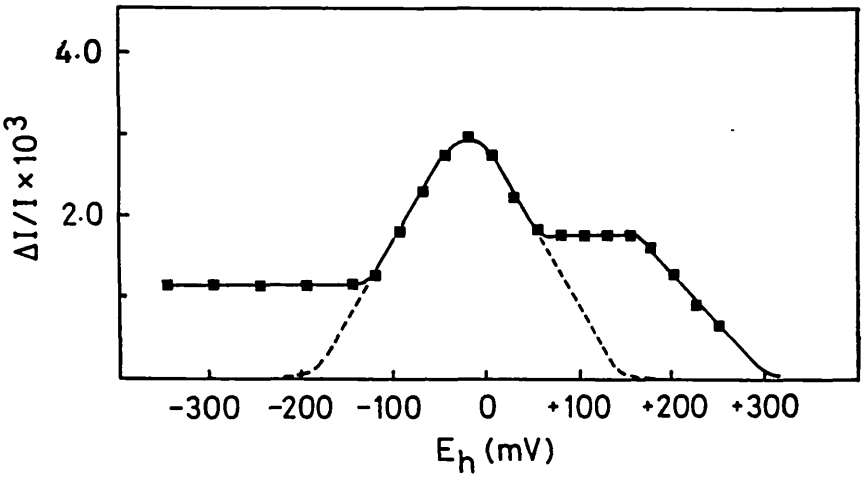
The redox titrations presented in this chapter characterize the components responsible for the generation of phase a and those res-

Fig. 4.7. Redox titrations of phase b, obtained as described in the legend of Fig. 4.6 (also see text). The samples were prepared as described in section 2.2.4 for (a) stacked thylakoid membranes, + 25μM DCMU; (b) stacked thylakoid membranes, + 25μM DCMU + 50μM MV; (c) unstacked thylakoid membranes, + 25μM DCMU.

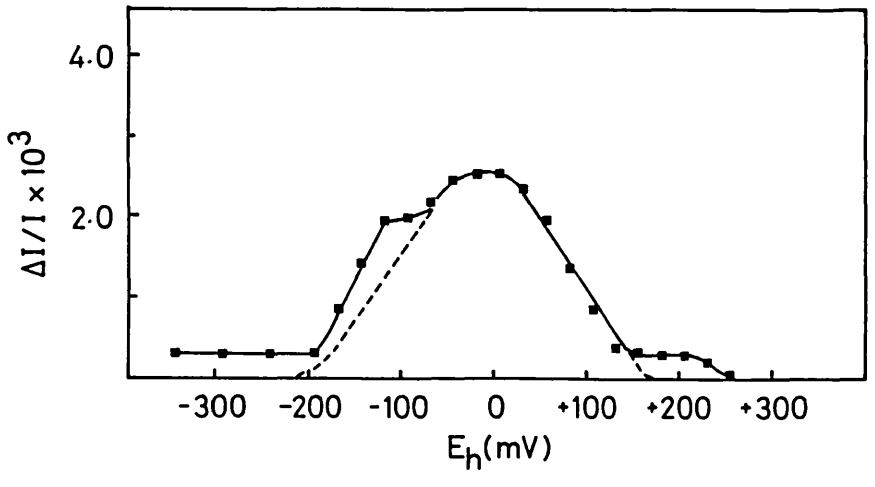
a.


4·0
2·0
ΔI/I × 10³
-300 -200 -100 0 +100 +200 +300
Eh (mV)

b.


4·0
2·0
ΔI/I × 10³
-300 -200 -100 0 +100 +200 +300
Eh (mV)

c.


4·0
2·0
ΔI/I × 10³
-300 -200 -100 0 +100 +200 +300
Eh (mV)

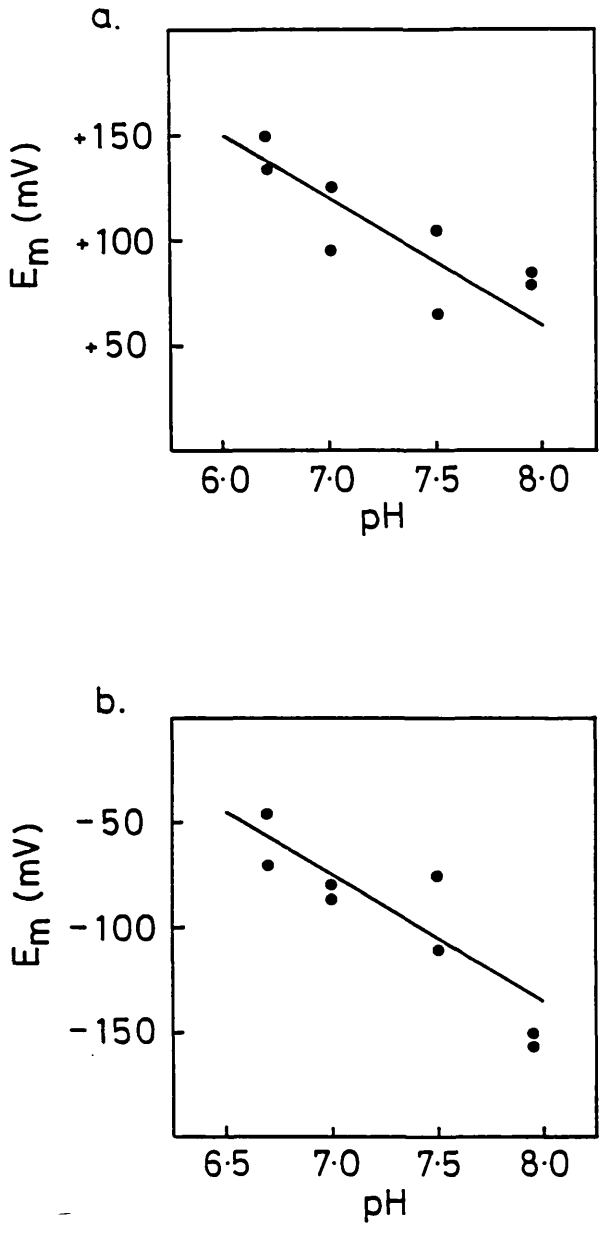


Fig. 4.8. pH dependence of the E_m for (a) the high potential component ($E_{m,7.5}$ = +100mV) and (b) the low potential component ($E_{m,7.5}$ = -75mV) of phase b, as determined under the conditions of Fig. 4.7(a). The required ambient pH was obtained by suspending the chloroplasts in the appropriate buffer medium, as described in section 2.2.4.

ponsible for phase b. The effect of salt is also found to have some interesting features.

The potentiometric titration of phase a, Fig. 4.3,indicates that it is the light-induced reduction of three low potential acceptor types that generate the full transmembrane electric field. These three acceptors have $E_{m,7.5}$ of +60mV, -195mV and < -400mV, respectively. Only the titration wave with an $E_{m,7.5}$ = +60mV is inhibited by the addition of DCMU. This species is probably the primary bound plastoquinone acceptor, designated Q_A, and is equivalent to the high redox potential quencher of chlorophyll fluorescence Q_H (Horton and Croze, 1979; Malkin and Barber, 1979). This same conclusion has been reached both by Malkin (1978) and by Diner and Delosme (1983).

The DCMU -insensitive titration waves, see Fig. 4.3(b), are presumably electron acceptors of PS1. Support for this conclusion comes from the observation that, in DCMU-treated chloroplasts, the whole absorption change is lost upon the chemical oxidation of the P700 donor, $E_{m,7.5}$ = +350mV. This thus implicates the -195mV wave as a manifestation of part of the PS1 contribution to the ΔA_{515}. Further evidence for this conclusion comes from the observation that, at redox potentials where the -195mV component is reduced, the inhibition of the ΔA_{515} can be overcome by the addition of methyl viologen, Fig. 4.3(c).

Malkin (1978), however, attributes a -235mV wave (pH 7.6)to the low potential PS2 fluorescence quencher, Q_L (Horton and Croze, 1979), due to its partial sensitivity to DCMU. Diner and Delosme (1983) also observe a low potential wave with $E_{m,7.5}$ = -240mV, but suggest that it does not arise from the primary electrogenic reaction as it is not observed at 50μs. They find, instead, that the full extent of this -240mV

wave, observed at 3ms, is still apparent upon excitation with far-red light, thus suggesting that it could be attributed to PS1. This latter finding is in agreement with the results presented here. However, limitation of the time resolution of the apparatus used in this present study (time resolution approximately 3ms) does not permit a more detailed analysis of the risetimes of phase a of the electrochromic shift, especially the -195mV component.

The identity of the two acceptor species of PS1 is uncertain. The species with an $E_{m,7.5} < -400mV$ is probably a bound iron-sulphur centre (ferredoxin?), although sufficiently low redox potentials have not been attained in these experiments to determine its actual midpoint. The origin of the ΔA_{515} due to the light-induced reduction of the -195mV species is even more difficult to determine. Its midpoint potential is difficult to reconcile with the "classic" views of low midpoint potential acceptors of PS1. Moreover, its involvement in the generation of phase a, which is surprising, leads to the suggestion that the PS1 contribution to the transmembrane electric field is twice that of PS2. There is as yet no direct experimental evidence in support of this. Indeed, most other types of studies favour a PS2: PS1 ratio of approximately 2:1 (Melis and Harvey, 1981).

A tentative model to account for the occurrence of the -195mV component in association with PS1 is that two acceptor types operate in parallel in two functionally distinct PS1 reaction centres: one would be involved in linear electron flow, resulting in the reduction of $NADP^+$, while the other could be associated with cyclic electron flow, a possible candidate for its primary acceptor being a b-type cytochrome. It is interesting to note that, from its midpoint redox potential, the -195mV component could be a b-type cytochrome, similar

to the low potential form detected by Hauska et al(1983). The implication of such a model, however, is that, apart from the expected ratio of 1:2 for PS2:PS1, the population of PS1 reaction centres would necessarily be heterogeneous: 50% being involved in linear electron flow and 50% being involved in cyclic electron flow. There is,however, no experimental evidence in support of this.

An alternative explanation for the unexpectedly large contribution of PS1 to the transmembrane electric field, is that, as a result of the (relatively long) duration of the actinic flash used in these experiments, double turnovers occur in the PS1 reaction centre. Delosme et al (1978) observed that, using xenon actinic flashes lasting a few microseconds, the fast rise of the electrochromic absorption change was followed by a "slow" rise in the time range of 4-100μs, and with a half-rise time of 15-20μs. This slower phase was found to be specifically activated by PS1 alone. However, no such slow rise was observed following a short actinic flash (of the order of ns), in agreement with the observations of Wolff et al (1969).

In the redox titrations carried out here, the actinic flash used had a duration of 10μs at half maximum amplitude. In view of the observations by Delosme et al (1978), this would be sufficient to induce double turnovers in PS1. One possible mechanism by which such double turnovers could be envisaged to generate an electric field at PS1, with two different acceptor species operative, is as follows. The first turnover would generate the expected electron transport pathway from P700 through to ferredoxin. The photooxidized P700 would then be rereduced by electron transfer from plastocyanin, with an approximate $t_{\frac{1}{2}}$ = 20μs (Delosme et al, 1978) and hence be able to turnover again. In a second turnover, if the reoxidation of ferredoxin is relatively slow, the electron cannot proceed via the same route as before. Perhaps under such conditions a cytochrome acceptor, possibly

the low potential cytochrome b-563, is favoured. This could explain why Diner and Delosme (1983) only detect the -240mV component at times greater than 3ms since this would thus be the half time required for the reduction of the low potential cytochrome b-563. To be noted, however, is that since the contribution of the -195mV component matches that of the < -400mV component, for high salt conditions, Fig. 4.3(b), all the flash-activated PSl reaction centres would need to turnover twice.

Turning now to the redox titrations of phase b, these indicate that phase b is apparent over a redox potential span between +100mV and -75mV, at pH 7.5 (see Fig. 4.7). The high potential value is probably set by the chemical reduction of the plastoquinone pool, $E_{m,7}$ = + 100mV (Goldbeck and Kok, 1979). A similar result has also recently been obtained by Girvin and Cramer (1983), and is consistent with the earlier work on the generation of the slow phase in bacterial chromatophore membranes (Prince and Dutton, 1977). In contrast, Crowther and Hind (1980) found that, in chloroplasts, the appearance of phase b required a much lower ambient potential, $E_{m,8.1}$ = - 55mV. They suggested that phase b is due to the reduction of an unknown low potential species, designated V, which is not correlated with the reduction of the plastoquinone pool.

The attenuation of phase b occurs with an $E_{m,7.5}$ = - 75mV, Fig. 4.7 (a). This potential corresponds to that of the high potential cytochrome b-563 located in the cytochrome b_6/f complex (Hauska et al, 1983). It is thus suggested that the chemical reduction of this cytochrome inhibits the generation of phase b. This observation is in contrast to that of Girvin and Cramer (1983): they observe that phase b can still be detected at redox potentials significantly lower than -75mV (pH7.5) and hence suggest that it cannot be related to cytochrome b-563

oxidation or to Q-cycle activity. In this context it should be noted that, in the case of bacterial chromatophores, both the slow and fast phases of the electrochromic absorption change titrate out with the inhibition of photochemical activity, $E_{m,7}$ = 0mV, and not with the chemical reduction of the high potential cytochrome b-562, $E_{m,7}$ = + 50mV (O'Keefe and Dutton, 1981). In these membranes, the equilibrium midpoint potential of the reaction centre Q_A/Q_AH couple is higher than that of the cytochrome b-566 with its $E_{m,7}$ = -90mV.

The redox potential titration curves for phases a and b in the unstacked condition are similar to those obtained in the presence of divalent cations, except for two main differences:

- a shift in the $E_{m,7.5}$ of the DCMU-sensitive phase a component is observed, from +60mV in stacked to -100mV in unstacked thylakoid membranes;

- the contribution of PS2 to the 3ms extent of the electrochromic shift is decreased, whereas that due to PS1 is increased, when unstacked membranes are compared to stacked.

The shift in the equilibrium E_m of the quinone acceptor of PS2 may indicate that the Q_A/Q_AH redox couple is susceptible to changes in surface potential. Such a shift may be mediated by a decrease in the pK of the Q_A/Q_AH redox couple, (see section 2.2.4).

Concerning the observed amplitude changes, there are a number of possible contributing factors. One is that changes in the salt level could induce changes in the surface charge density. Such an effect might interfere with the delocalization of the electric field, generated

by each reaction centre, along the surface of the membrane. In addition to this there are the known changes in the spatial separation between PS2, PS1 and the cytochrome $\underline{b}_6/\underline{f}$ complex (see section 1.2.2). Furthermore, the conductance properties of the membrane might also be altered: changes in salt concentrations are accompanied by changes in the relative amount of stacked and unstacked regions and hence in the amount of exposed regions. An alternative possibility that such salt-induced amplitude changes in the ΔA_{515} reflect changes in the redistribution of energy between the photosystems can be discounted, since these experiments were performed using saturating light flashes.

CHAPTER 5

The electrochromic absorption change related to electron transport

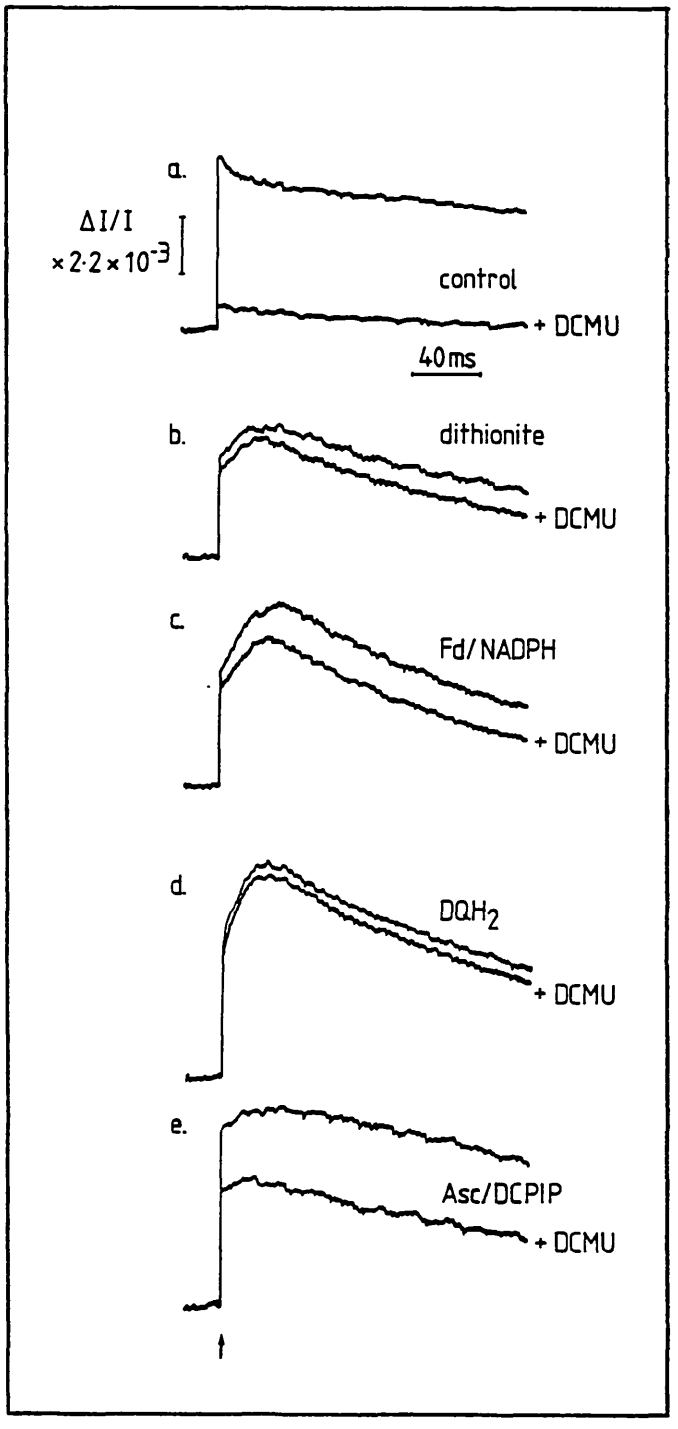
The effectiveness of different reductants to generate phase a and phase b of the flash-induced 515nm electrochromic absorption change is characterized. The related flash-induced cytochrome redox reactions are studied and the effect of salt levels on these signals investigated. Furthermore, an attempt is made to correlate the generation of phase b with specific electron transport reactions.

5.1 A comparative study of the ΔA_{515} with different reductants:

In this study a number of different reductants (see section 2.2.2) are used to poise the electron transport system. Redox mediators have, however, been omitted since their presence may alter the cytochrome absorption changes examined later. On the other hand, in their absence, equilibrium E_h may not be attained with the various reductants used; this will be especially true for "artificial" reductants e.g. dithionite. Fig. 5.1 shows that, according to the particular reductant used, the extents of phase a and phase b of the ΔA_{515} can vary. Such changes in the ΔA_{515} can be compared with the changes observed in the redox titrations of the ΔA_{515}, Figs. 4.3 and 4.7.

Fig. 5.1(a) shows the control ΔA_{515}, in the absence of added inhibitor or reductant. As discussed earlier (section 3.2), both PS1 and PS2 are presumably operative under these conditions and hence phase a of the ΔA_{515} is large. Addition of DCMU inhibits electron transport and subsequently inhibits charge separation in the reaction centres: this thus leads to the inhibition of the generation of phase a.

Fig. 5.1. Flash-induced ΔA_{515} for stacked thylakoid membranes. Conditions are as described in section 2.2.2 but with no added inhibitor or reductant. (a) control, with no added reductant; (b) as (a) + 1mM dithionite; (c) as (a) + 5μM Fd + 0.5mM NADPH + O_2 trap (see section 2.2.2); (d) as (a) + 0.5mM DQH_2; (e) as (a) + 0.5mM Asc + 50mM DCPIP. The traces obtained in the presence of these various reductants + 25μM DCMU are labelled.


a.
ΔI/I
×2·2×10⁻³
control
+ DCMU
40ms
b.
dithionite
+ DCMU
c.
Fd/NADPH
+ DCMU
d.
DQH2
+ DCMU
e.
Asc/DCPIP
+ DCMU

In the presence of dithionite, Fig. 5.1(b), and in the absence of DCMU, the extent of phase a is inhibited by approximately 40%. The addition of DCMU results in a further small decrease in the extent of phase a. In view of the redox titrations presented in Fig. 4.3, the results in Fig. 5.1(b) suggest that, in the absence of DCMU, dithionite acts partially on PS1, as well as on PS2, PS2 being fully inhibited on the subsequent addition of DCMU. A possible explanation for this is that, in the absence of redox mediators, equilibrium is not fully attained in the presence of dithionite. Since dithionite is apparently able to reduce chemically part of the -195mV component, then from Fig. 4.7(a), phase b would be expected to be inhibited at such low redox potentials. There is, however, a discrepancy since phase b is observed. A possible explanation for this contradiction is that the control in Fig. 5.1(a) is an overestimation of the true contribution from PS1 and PS2. Alternatively, the redox titration of phase b shown in Fig. 4.7(a) is underestimated at these low redox potentials. To be noted is that the extent of phase b is unaltered by the addition of DCMU.

In the presence of the Fd/NADPH couple, Fig. 5.1(c), and in the absence of DCMU, the extent of phase a is again inhibited, but only by approximately 30%. This immediately suggests that the redox poise set up by the Fd/NADPH couple is more positive than that in the presence of dithionite. The Fd/NADPH couple is thus only able to reduce part of the +60mV component, Fig. 4.3(a): this is subsequently totally inhibited in the presence of DCMU, the remaining contribution to phase a being due to PS1. The extent of phase b generated by the Fd/NADPH couple is larger than that observed in the presence of dithionite. This is in accordance with the redox titration of phase b, Fig. 4.7(a):

as the redox potential becomes more positive, the extent of phase b increases. Again, the extent of phase b is unaltered by the addition of DCMU.

The addition of duroquinol (DQH_2), Fig. 5.1(d), in the absence of DCMU, results in an approximate 25% inhibition of phase a. Only by the addition of DCMU is the extent of phase a further decreased to reveal the PS1 contribution alone. By comparison with the redox titrations in Figs. 4.3(a) and (b), this suggests that DQH_2 is a milder reductant than the Fd/NADPH couple. Also, the large extent of phase b, which is unaltered by the addition of DCMU, is in accordance with this.

The Asc/DCPIP couple is the mildest reductant investigated here. In the absence of DCMU, approximately 90% of the control phase a is still apparent, see Fig. 5.1(e). The addition of DCMU decreases this extent to approximately 60% of the control, as is observed with DQH_2, see Fig. 5.1(d). A rather small phase b is now generated, which is still apparent upon the addition of DCMU. From the redox titration of phase b, Fig. 4.7(a), it can be observed that, at redox potentials above 0mV, the extent of phase b starts to decrease. The small extent of phase b observed in Fig. 5.1(e) is an indication that the Asc/DCPIP couple is unable to reduce the PQ pool.

By correlating the extent of phase a with the redox titration curve for the ΔA_{515} in Fig. 4.3(a), as described above, the following ambient redox potentials are estimated for the particular reductant present: dithionite, -200mV; Fd/NADPH, -100mV; DQH_2, 0mV; and Asc/DCPIP, +100mV. In the remaining part of this chapter, these different reductants are used in an attempt to correlate the gener-

ation of phase b with the light-induced redox reactions of cytochromes.

5.2 Dithionite induced electron transport:

The use of dithionite to reactivate phase a and phase b of the ΔA_{515}, in the presence of DCMU, has already been discussed in section 3.2: also see Fig. 3.3. As expected from the data of Figs. 4.7(a) and 4.3(a), high concentrations of dithionite inhibit phase b, and subsequently inhibit phase a, Fig. 5.2.

In the presence of methyl viologen (MV), a competitive inhibitor for cyclic electron flow, the extent of phase a is expected to be large, Fig. 4.3(c), and the generation of phase b apparent, Fig. 4.7(b). The ΔA_{515} observed, however, is very different to that expected and is found to depend on the concentration of MV present, Fig. 5.3. At low concentrations of MV, typically 3-5μM, the extent of phase a is decreased by approximately 40%, compare Fig. 5.3(b) with Fig. 5.3(a), and a "delayed" slow phase is observed; at high concentrations, typically 30-50μM, phase a is again decreased by a further 10%, compare Fig. 5.3(c) with Fig. 5.3(b), and now no phase b or "delayed" slow phase is observed. To be noted is that cyclic electron flow is only inhibited at the high MV concentrations.

The properties of the delayed slow phase are very similar to those of phase b. Its spectrum matches that of phase a, Fig. 5.4, indicating that it also results from an electrochromic event. It is inhibited by DBMIB, Fig. 5.5(b). The subtraction of the absorption changes ± DBMIB reveals that the rise and decay kinetics of this delayed slow

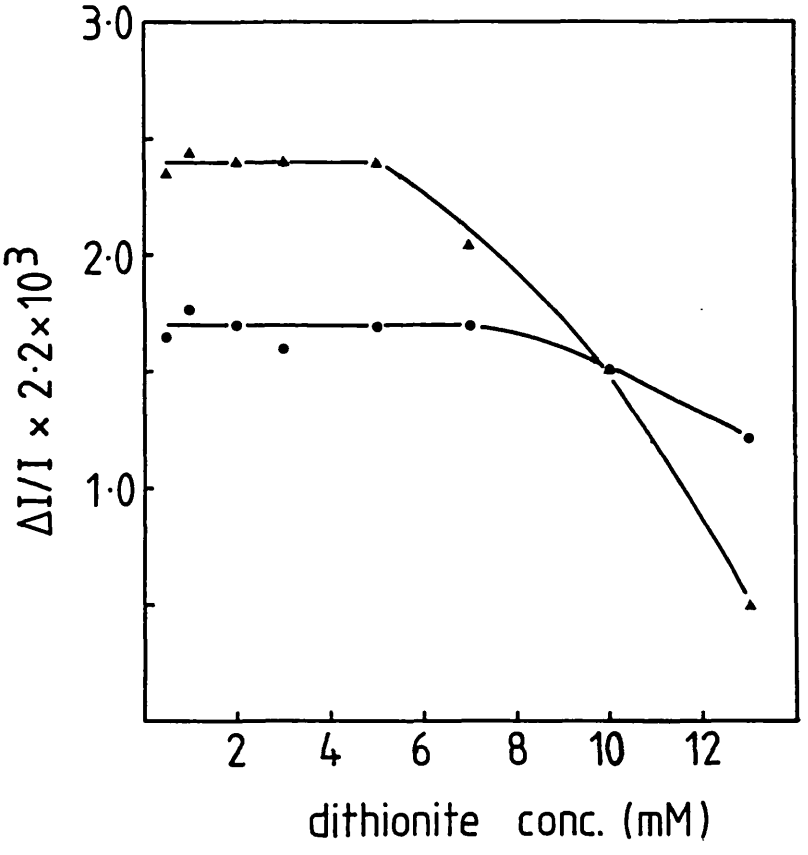


Fig. 5.2. Titration of the extent of the flash-induced ΔA_{515}, detected at 3ms for phase a (circle symbols) and at 10ms for phase b (triangle symbols), with dithionite. Conditions are as described in section 2.2.2 for stacked thylakoid membranes and for pseudocyclic electron flow, where the concentration of dithionite is varied.

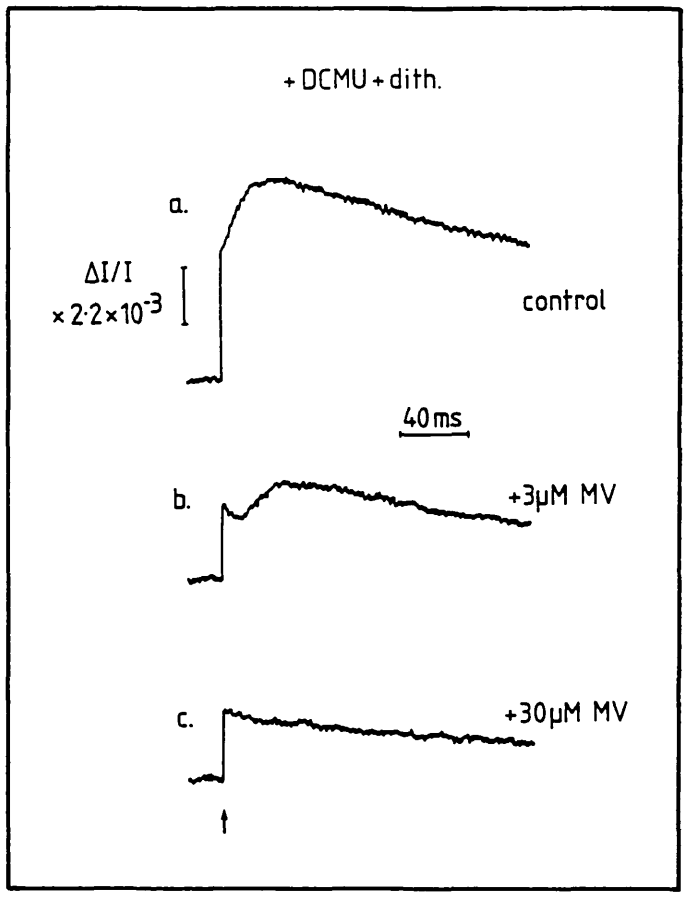


Fig. 5.3. Flash-induced ΔA_{515} for stacked thylakoid membranes. Conditions are as described in section 2.2.2 for pseudocyclic electron flow, with dithionite (dith.) as reductant. (a) control, with no further additions; (b) as (a) + 3μM MV; (c) as (a) + 30μM MV.

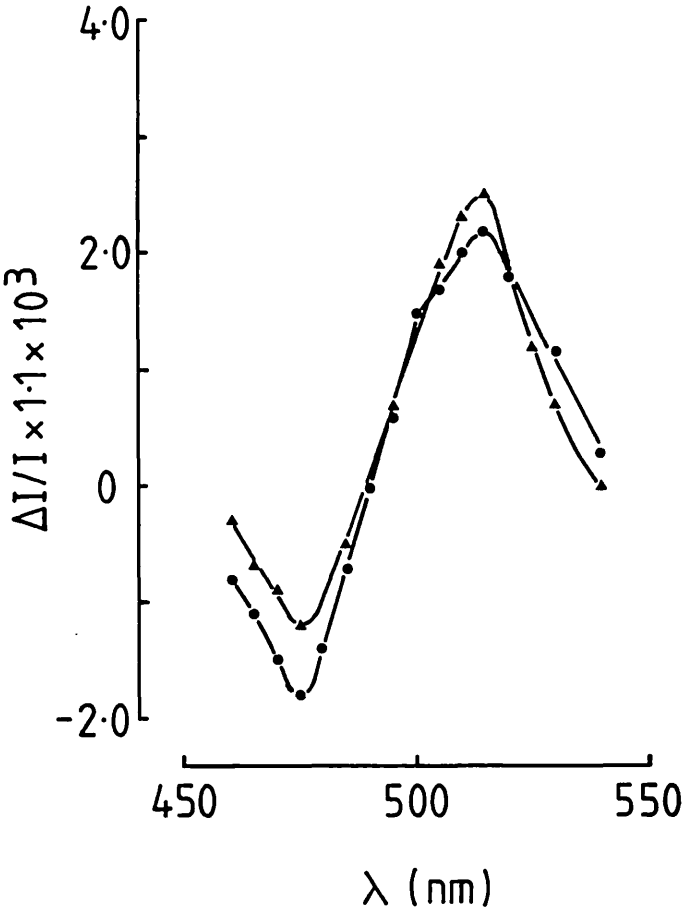


Fig. 5.4. Spectra of the extent of the flash-induced electrochromic shift detected at 3ms for phase a (circle symbols) and at 20ms for the delayed slow rise (triangle symbols). Conditions are as for Fig. 5.3(b).

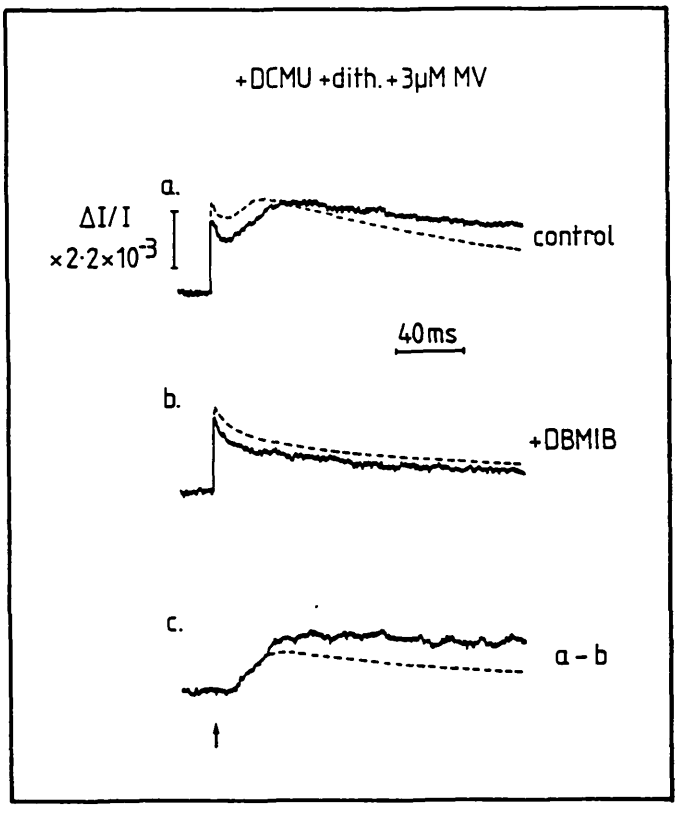


Fig. 5.5. Flash-induced ΔA_{515} for stacked (full line) and unstacked (broken line) thylakoid membranes. Other conditions are as for Fig. 5.3(b). (a) control, with no further additions; (b) as (a) + 15μM DBMIB; (c) subtraction (a) - (b).

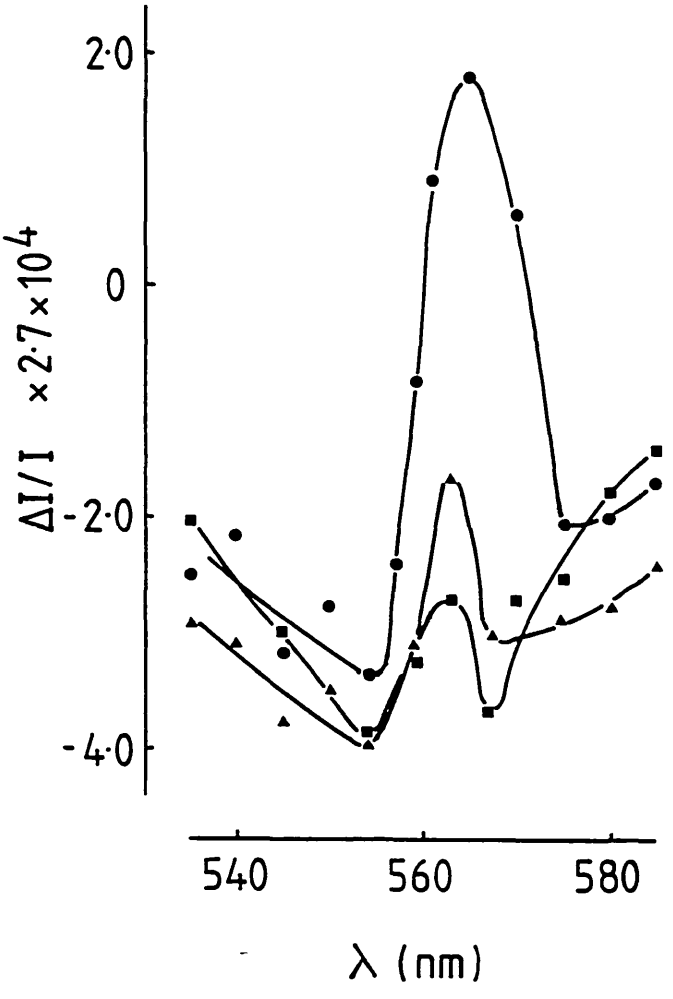
phase are very similar to those of phase b, compare Fig. 5.5(c) with Fig. 3.1(c), except that the rise occurs 10 ms after flash activation. The magnitude of the delayed slow phase is altered by different salt conditions, Fig. 5.5(c), in a manner comparable to the salt effect on the extent of phase b, Fig. 4.2. In the discussion to follow, this delayed slow phase is assumed to be the manifestation of phase b, the generation of which has been delayed. The nature of this delay is discussed later.

Time resolved spectra, under the different conditions depicted in Fig. 5.3, were carried out in the cytochrome absorption region, i.e. between 540nm and 590nm. These are shown in Fig. 5.6. The figures were obtained by measuring at discrete wavelengths the extent of the absorbance transients relative to the initial dark level at selected time intervals following the flash; the extents of the transients were then plotted against the wavelength of the measurement.

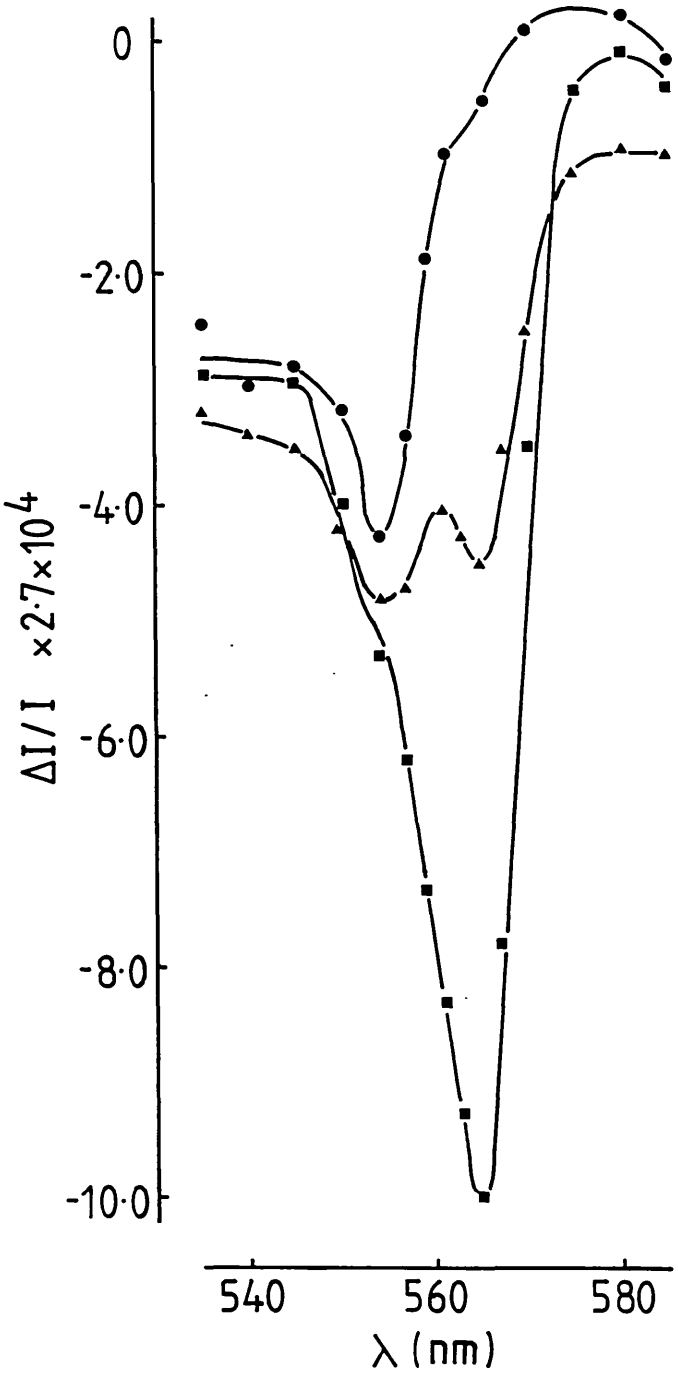
From these spectra, it can be observed that the dominant spectral species in this time range are the transients due to the oxidation and reduction of cytochrome f (λ_{max} = 554nm) and cytochrome b-563 (λ_{max} = 563nm). From the sequence of electron carriers shown in Fig. 1.2 (also see Haehnel, 1977; Bouges-Bocquet and Delosme, 1978), absorption changes due to plastocyanin might be expected in these spectra. Such changes, however, would only appear as small displacements through this spectral region since the spectrum of plastocyanin (Katoh et al, 1962) is relatively featureless and of low extinction coefficient (5×10^3 M^{-1} cm^{-1}, oxidized minus reduced).

When dithionite and DCMU alone are present, Fig. 5.6(a), the main features of the spectrum 3ms after flash activation, are the reduction of cytochrome b-563 and the concomitant oxidation of cytochrome f.

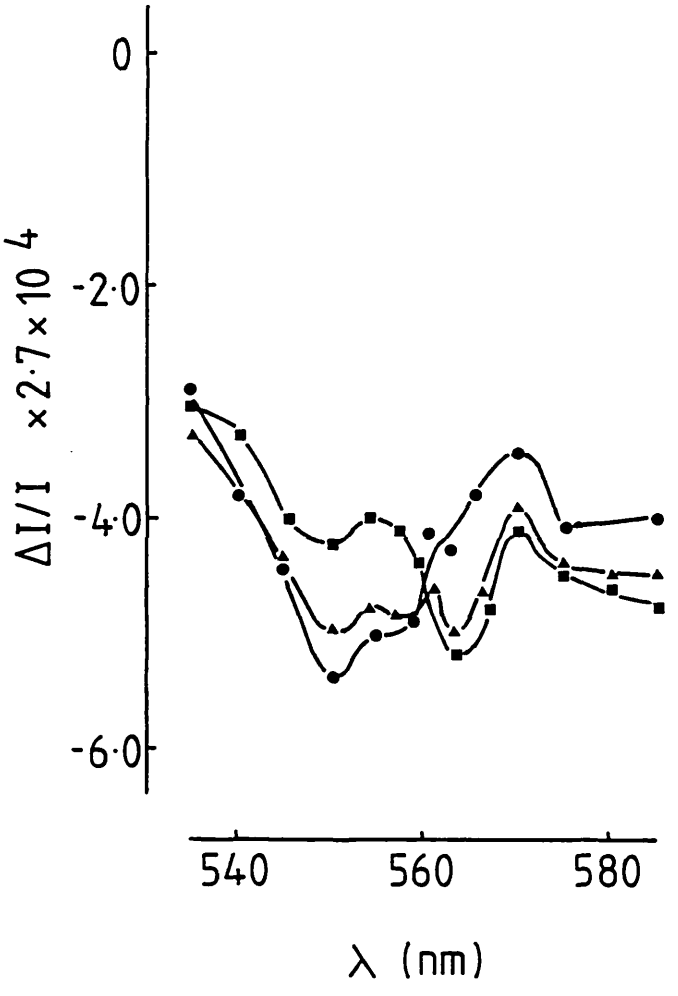
Fig. 5.6. Flash-induced spectra through the cytochrome α-band region. Kinetic traces at the indicated wavelengths were obtained for stacked thylakoid membranes under conditions of pseudocyclic electron transport (see section 2.2.2), with dithionite as reductant. Valinomycin (2μM) and nigericin (2μM) were also present (see section 2.2.3). An average of 32 traces was taken. The extents of the change relative to the initial dark level were measured at the following times after a flash: 5ms (circle symbols); 20ms (triangle symbols); 60ms (square symbols). (a) control, with no further additions; (b) as (a) + 3μM MV; (c) as (a) + 30μM MV.



(a) control



(b) + 3μM MV



(c) + 30μM MV

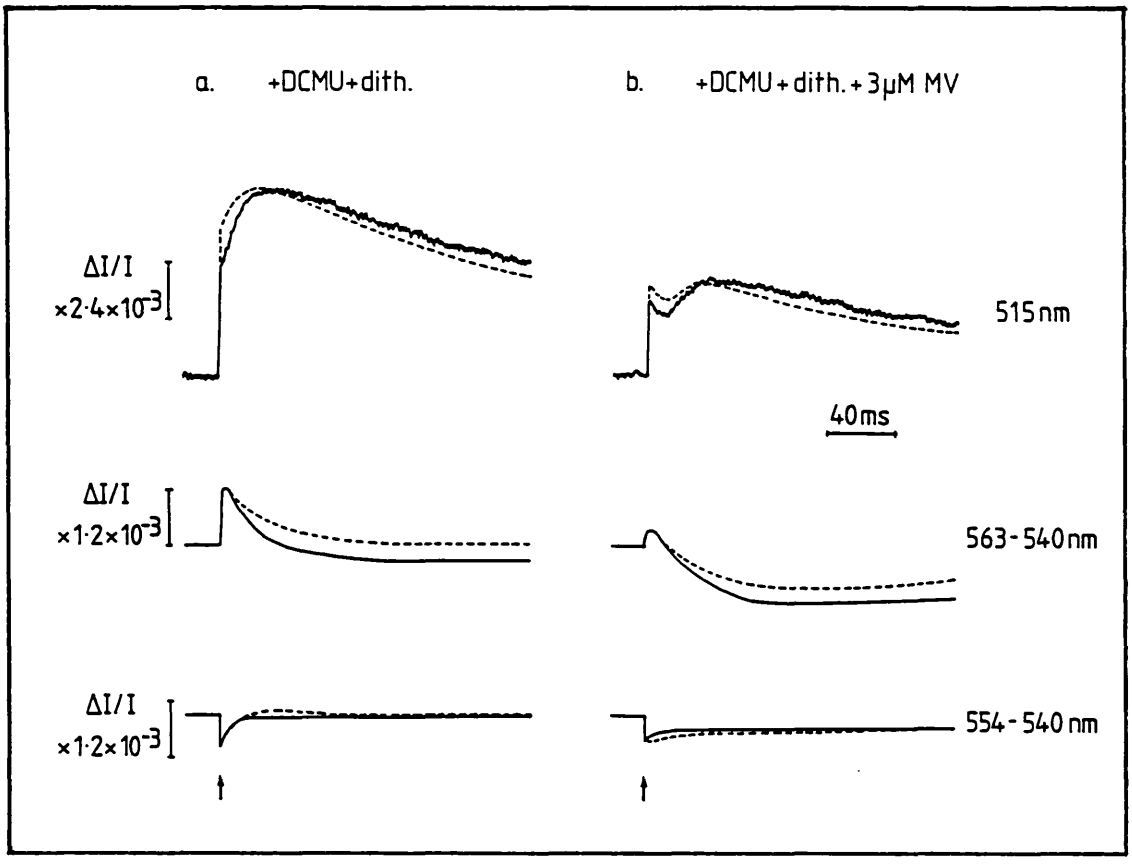
Their subsequent, respective, dark reoxidation and dark rereduction occurs within 100ms. Subtracting any non-redox linked absorption changes at 540nm and using $\Delta\varepsilon_{563-575} = 2 \times 10^{+4}\ M^{-1}\ cm^{-1}$ (Stuart and Wasserman, 1973), cytochrome b-563 is reduced equivalent to an extent of 24nM, i.e. 1 molecule/2000 chlorophylls. Similarly, using $\Delta\varepsilon_{554-540} = 2.2 \times 10^{+4}\ M^{-1}\ cm^{-1}$ (Forti et al, 1965), cytochrome f is oxidized equivalent to an extent of 11nM i.e.1 molecule/4000 chlorophylls. This indicates an approximate 2:1 turnover of cytochromes b-563 and f, although later, stoichiometries closer to 1:1 are also observed.

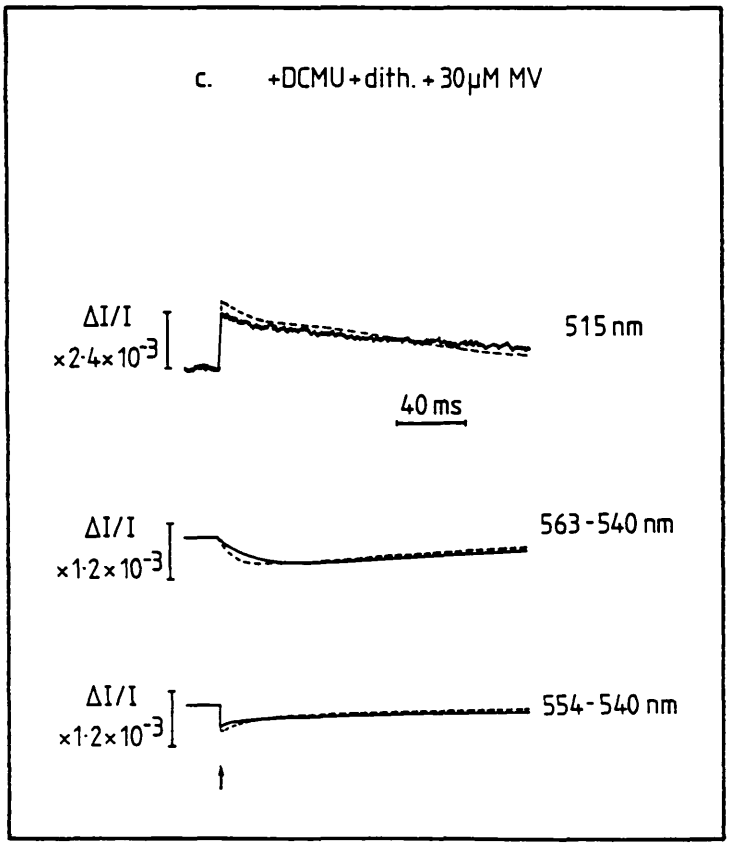
In the presence of dithionite, DCMU and 3μM MV, Fig. 5.6(b), although there is little flash-induced reduction of cytochrome b-563, it is followed by a large dark reoxidation (equivalent to approximately 50nM oxidized cytochrome b-563) which occurs maximally at 60ms. Cytochrome f, on the other hand, still undergoes a flash-induced oxidation, of approximately the same magnitude as in the absence of MV, but its dark rereduction is now slow.

In the presence of dithionite, DCMU and 30μM MV, Fig. 5.6(c), the absorbance changes of both cytochromes b-563 and f are small, the prominent features observed in Fig. 5.6(a) being partially suppressed. This suggests that, under these conditions, electron transport has been partially inhibited. Also observed is that around 540nm there are now relatively large scattering changes.

The flash-induced kinetics of cytochromes b-563 and f are shown in Fig. 5.7, together with the ΔA_{515}, again under the different conditions depicted in Fig. 5.3. The effect of salt is also shown. In Fig. 5.7(a),

Fig. 5.7. Flash-induced electrochromic and cytochrome absorption changes for stacked (full line) and unstacked (broken line) thylakoid membranes. Conditions are as described in section 2.2.2 for pseudocyclic electron flow, with dithionite as reductant. For the cytochrome ΔA, valinomycin (2μM) and nigericin (2μM) were also present (see section 2.2.3). (To be noted, for the cytochrome ΔA, the ΔA at the reference λ was subtracted manually from that at the measuring λ). (a) no further additions; (b) as (a) + 3μM MV; (c) as (a) + 30μM MV.


a. +DCMU+dith.
b. +DCMU+dith.+3μM MV
ΔI/I
×2·4×10⁻³
515nm
40ms
ΔI/I
×1·2×10⁻³
563-540nm
ΔI/I
×1·2×10⁻³
554-540nm


c. +DCMU+dith.+30μM MV
ΔI/I
×2·4×10⁻³
515nm
40ms
ΔI/I
×1·2×10⁻³
563-540nm
ΔI/I
×1·2×10⁻³
554-540nm

the cytochrome absorption changes for pseudocyclic conditions, with dithionite as reductant, are shown. Considering the high salt condition, the flash-induced reduction of cytochrome b-563 occurs within a few ms, and its dark reoxidation occurs with an approximate $t_{\frac{1}{2}}$ = 10ms. In the case of cytochrome f, its flash-induced oxidation is too rapid to be resolved by the apparatus used, but its dark rereduction occurs with an approximate $t_{\frac{1}{2}}$ = 5ms. These results are in accordance with the time-resolved spectra depicted in Fig. 5.6(a) and agree with the observations of Crowther and Hind (1980) and Olsen et al (1980).

The interesting feature, though, in Fig. 5.7(a) is the effect of salt. As discussed earlier, the salt level alters the extent of both phase b (and phase a): low salt (≡ 10mM K^+) results in a small phase b (and a large phase a), while high salt (≡ 5mM Mg^{2+}) results in a large phase b (and a small phase a), see Fig. 4.2. In the case of cytochrome b-563, although the extent of its flash-induced reduction remains unaltered when the salt level is lowered, the extent of its dark reoxidation is decreased. The amount by which the extent of this oxidation is decreased (approximately 20%), matches the amount by which the extent of phase b is decreased under similar conditions, compare Fig. 5.7(a) with Fig. 4.2(c). Coupled to the decrease in extent, there is also observed a deceleration in the rate of oxidation of cytochrome b-563: compare $t_{\frac{1}{2}}$ = 15ms for the oxidation of cytochrome b-563 in the low salt condition, to $t_{\frac{1}{2}}$ = 10ms in the high salt condition. This again mimicks a similar effect observed in the rise kinetics of phase b, Fig. 4.2(c): compare $t_{\frac{1}{2}}$ = 10ms in the low salt condition with a $t_{\frac{1}{2}}$ = 7ms in the high salt condition. No such salt effects are apparent in the absorption kinetics of cytochrome f. From these salt effects, the oxidation of cytochrome b-563 might be implicated in association

with the generation of phase b, as predicted by a Q-cycle type mechanism (see section 1.3.2). However, on a kinetic basis, cytochrome b-563 oxidation is apparently slower than the rise of phase b.

In Fig. 5.7(b), the cytochrome absorption changes in the presence of dithionite, DCMU and 3μM MV, are shown. Under these conditions, for which a delayed phase b is observed, the redox poise of the system is, apparently, such that cytochrome b-563 is in a reduced state prior to flash activation. After a single flash, a small transient reduction is observed, but the prominent feature of the absorption change is the net oxidation of cytochrome b-563. Under the high salt condition, the actual extent of this absorption change matches that observed for the oxidation of cytochrome b-563 in Fig. 5.7(a), although the rate of reoxidation is slightly slower. In the case of cytochrome f, however, although its flash-induced oxidation is still fast, and its extent is unaltered, when compared with Fig. 5.7(a), its rate of dark rereduction is decelerated. Again, only the extent of cytochrome b-563 oxidation is affected by salt, Fig. 5.7(b), such as would suggest that it correlated with the generation of the delayed phase b, see Fig. 5.5(c).

In the presence of dithionite, DCMU and high concentrations of MV, such that inhibit phase b, Fig. 5.7(c), only a flash-induced oxidation of cytochrome b-563 is observed: the extent of this oxidation is approximately half that observed in Figs. 5.7(a) and (b). The cytochrome f kinetics are very similar to those observed in Fig. 5.7(b). These absorption changes suggest that, under these conditions, turnover of photosynthetic electron transport has slowed considerably.

5.3 Ferredoxin/NADPH induced electron transport:

From Fig. 5.1, the Fd/NADPH couple was concluded to be almost as strong a reductant as dithionite. The use of Fd/NADPH to reactivate electron transport, and hence regenerate the ΔA_{515}, in the presence of DCMU, requires the presence of an oxygen trap; otherwise ferredoxin is rapidly oxidized in the presence of oxygen. Also, several pre-flashes are required to observe a maximal phase b: in these particular experiments it was found that 16 pre-flashes were sufficient to attain optimal reducing conditions, as manifested by the large extent of phase b.

Fig. 5.8(a) shows the effect of salt on the extents of phase a and phase b of the ΔA_{515}, in the presence of DCMU and Fd/NADPH. In the high salt condition, the ΔA_{515} observed is similar to that in Fig. 5.1(c) where phase b is large. In the low salt condition, however, the expected increase in phase a is only very small, while the decrease in the extent of phase b is rather large. These results suggest that, apart from the expected effect of salt on the ΔA_{515}, there is a further effect of salt on the reducing ability of the Fd/NADPH couple: under the low salt condition this reducing couple is apparently less effective. In agreement with this, Shahak et al (1980) found that divalent cations, especially Mg^{2+}, were required to bind ferredoxin to the membrane and hence increase its effectiveness, in the presence of NADPH, as a reductant.

In the presence of Fd/NADPH, DCMU and 50μM MV, Fig. 5.8(b), the extent of phase a in the low salt condition is now significantly larger than that in the high salt condition, as would be expected following Fig. 4.2. A possible explanation for the now apparent salt effect

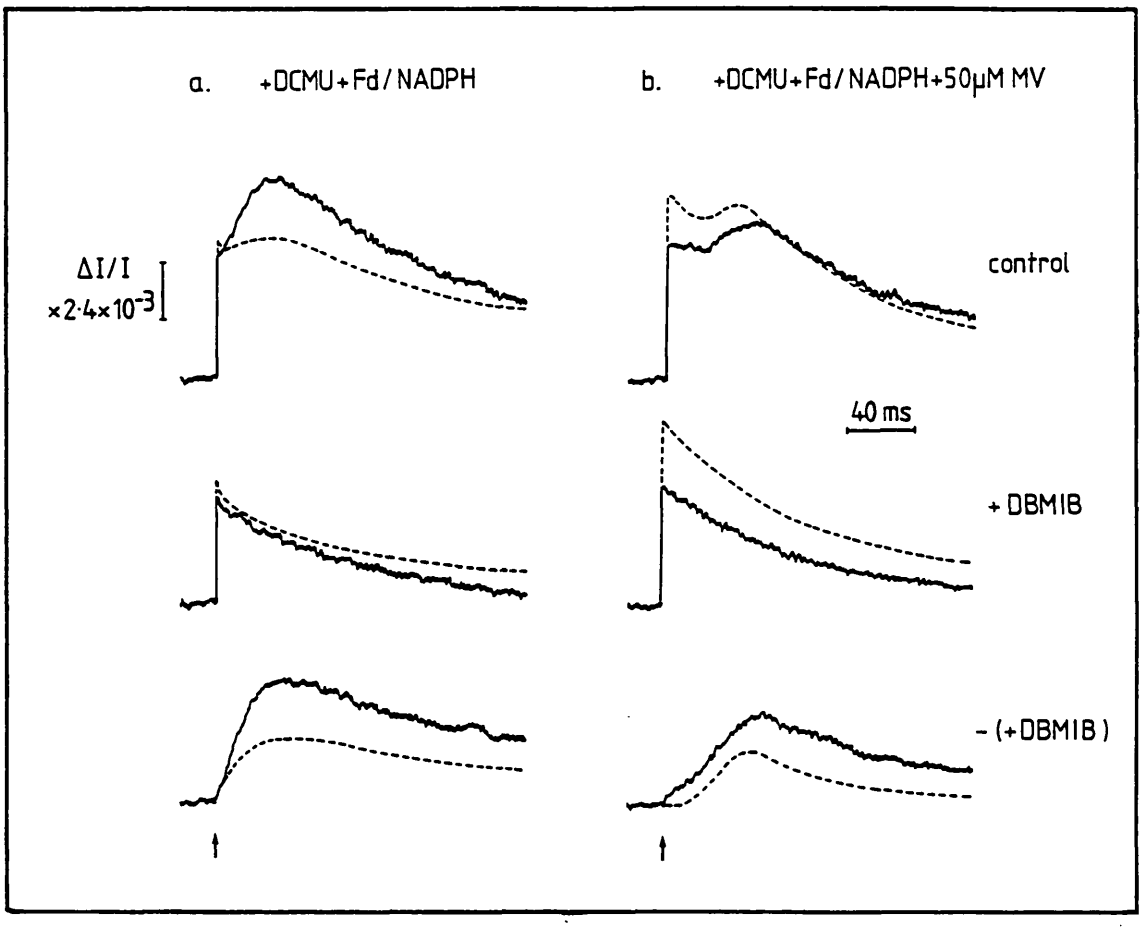


Fig. 5.8. Flash-induced ΔA_{515} for stacked (full line) and unstacked (broken line) thylakoid membranes. Conditions are as described in section 2.2.2 for pseudocyclic electron flow, with Fd/NADPH as reductant (in the presence of an O_2 trap). (a) no further additions; (b) as (a) + 50μM MV. The true extent and kinetics of phase a and phase b are obtained by the same procedure as that given in Fig. 3.1.

is the actual presence of MV. Under the low salt condition the concentration of ferredoxin bound to the membrane will be diminished. The effect of this is, conceivably, two-fold: (1) the concentration of the endogenous PS1 acceptors may be reduced and (2) the redox poise of the system may become more positive. The additional MV will act as electron acceptor for all PS1 reaction centres, regardless of whether their own endogenous acceptors are present or not, thus increasing the extent of phase a. This increase in the extent of phase a can also be observed in the high salt condition, but it is not so prominent.

A delayed slow rise is also observed, Fig. 5.8(b), although the conditions are slightly different to those described earlier, Fig. 5.3(b): in the presence of Fd/NADPH, high concentrations of MV are required to observe this particular effect. The delayed slow rise in Fig. 5.8(b) is electrochromic, it is inhibited by DBMIB and it is affected by salt in a manner similar to that shown in Fig. 5.5. The extent of the delay is approximately 10-15ms and it is apparently unaffected by salt.

The flash-induced cytochrome redox changes associated with the use of Fd/NADPH as reductant, are shown in Fig. 5.9. In the absence of MV, Fig. 5.9(a), the cytochrome b-563 absorption changes are similar to those obtained in the presence of dithionite, Fig. 5.7(a). Again under the low salt condition, the extent of cytochrome b-563 oxidation is smaller than under the high salt condition, thus correlating with the smaller extent of phase b, Fig. 5.8(a). The rereduction kinetics of cytochrome f are now much faster, approximate $t_{\frac{1}{2}}$ = 3ms, and again exhibit no salt dependence.

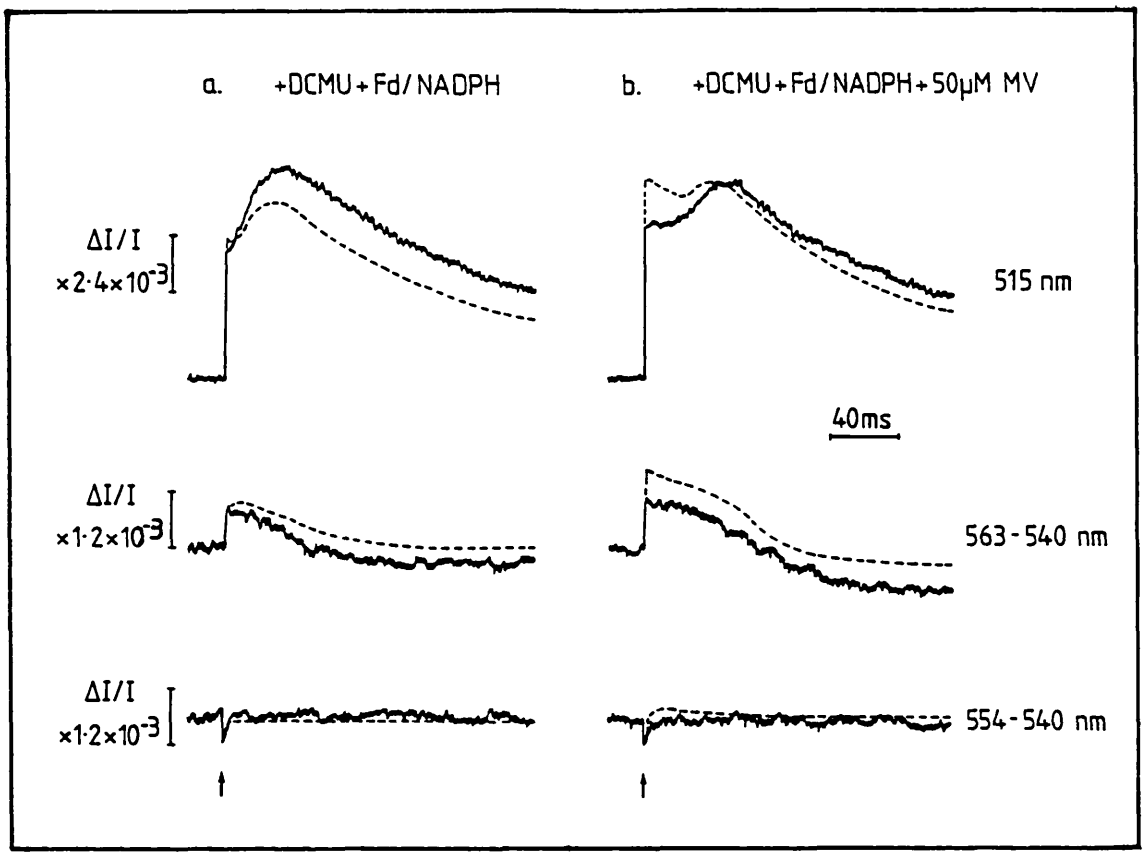
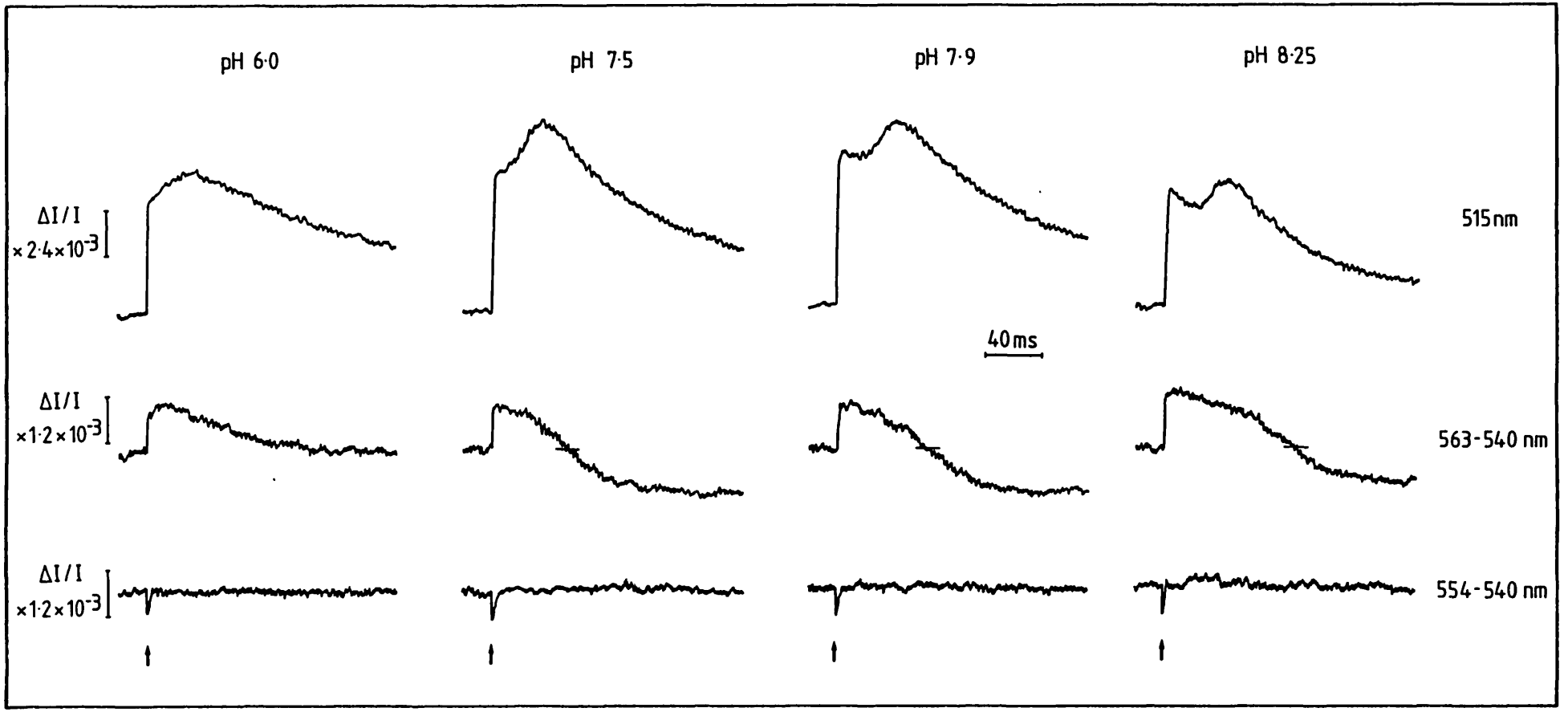


Fig. 5.9. Flash-induced electrochromic and cytochrome absorption changes for stacked (full line) and unstacked (broken line) thylakoid membranes. Conditions are as described in section 2.2.2 for pseudocyclic electron flow, with Fd/NADPH as reductant (in the presence of an O_2 trap). For the cytochrome ΔA, valinomycin (2μM) and nigericin (2μM) were also present (see section 2.2.3). (a) no further additions; (b) as (a) + 50μM MV.

In the presence of Fd/NADPH and 50μM MV, Fig. 5.9(b), the ambient redox poise remains, apparently, unaltered. However, although the flash-induced reduction of cytochrome b-563 is still observed, the rate of its reoxidation has become slower, with an approximate $t_{\frac{1}{2}}$ = 60ms, and its total amplitude has increased. Also, while the extent of the delayed phase b is reduced under the low salt condition, Fig. 5.8(b), no such change in the extent of the oxidation of cytochrome b-563 is observed, as would be expected in view of previous results; instead, the extent of the flash-induced reduction of cytochrome b-563 is increased. The rereduction kinetics of cytochrome f are still fast, as in the absence of MV, and again no salt effect is observed.

The role of protons in the deceleration of cytochrome b-563 oxidation in the presence of Fd/NADPH and 50μM MV is shown in Fig. 5.10: the effect of pH on the extent of the delay of the delayed phase b, under these conditions, is shown together with its effect on the redox kinetics of cytochromes b-563 and f. At low pH, no delayed phase b is observed, and the kinetics of cytochrome b-563 oxidation are similar to those in Fig. 5.9(a), where no MV is present. As the pH is increased, the length of the delay in the ΔA_{515} increases and the kinetics of cytochrome b-563 oxidation are slowed down. The cytochrome f kinetics are, evidently, unaffected by pH. These pH effects are not artefacts due to the changing redox properties of MV: its E_m is pH independent (Prince et al, 1981). Although the underlying mechanism of this effect is unclear (a possible suggestion is discussed later), its actual observation again points to a correlation between the oxidation of cytochrome b-563 and the generation of phase b.

Fig. 5.10. The effect of pH on the flash-induced electrochromic and cytochrome absorption changes, for stacked thylakoid membranes under the conditions of Fig. 5.9(b). For the cytochrome ΔA, valinomycin (2μM) and nigericin (2μM) were also present (see section 2.2.3). The required ambient pH was obtained by suspending the chloroplasts in the appropriate buffer medium, see section 2.2.4.


pH 6·0
pH 7·5
pH 7·9
pH 8·25
ΔI/I
×2·4×10⁻³
515nm
40ms
ΔI/I
×1·2×10⁻³
563-540 nm
ΔI/I
×1·2×10⁻³
554-540 nm

5.4 Duroquinol induced electron transport:

Duroquinol, like dithionite, is able to reduce the PQ pool, although it is not as strong a reductant as dithionite, see section 5.1. Fig. 5.11(a) shows the effect of salt on the ΔA_{515} induced by the addition of DQH_2, in the presence of DCMU. The changes induced in the extents of phase a and phase b are now not so large: compare an approximate 10-15% change in Fig. 5.11(a) to an approximate 20-25% change observed previously, see Figs. 4.2, 5.5 and 5.8(b). Furthermore, the extent of phase b, under these particular reducing conditions, is slightly larger than that induced by dithionite, compare Figs. 5.11(a) and 4.2(c).

The addition of 50μM MV has no effect on either the extent of phase a or that of phase b, the ΔA_{515} traces being superimposable in the presence or absence of MV; similarly, the effect of salt is not altered upon the addition of MV. Hence, it suffices that the results presented in Fig. 5.11, (a) and (b), hold for both ± MV. The unaltered extent of phase a in the presence of MV is further evidence for the positive ambient redox poise set by DQH_2: from Fig. 4.3(c), MV causes an increase in the extent of phase a only at low redox potentials. The unaltered extent of phase b is that predicted by the redox titration in Fig. 4.7(c).

Fig. 5.12(a) shows the flash-induced cytochrome redox changes when DQH_2 is present as the reductant. In the presence or absence of MV the cytochrome absorption changes are very similar to those obtained in the presence of dithionite alone, Fig. 5.7(a). To be noted is that, although the extent of phase b induced by DQH_2 is larger than that in-

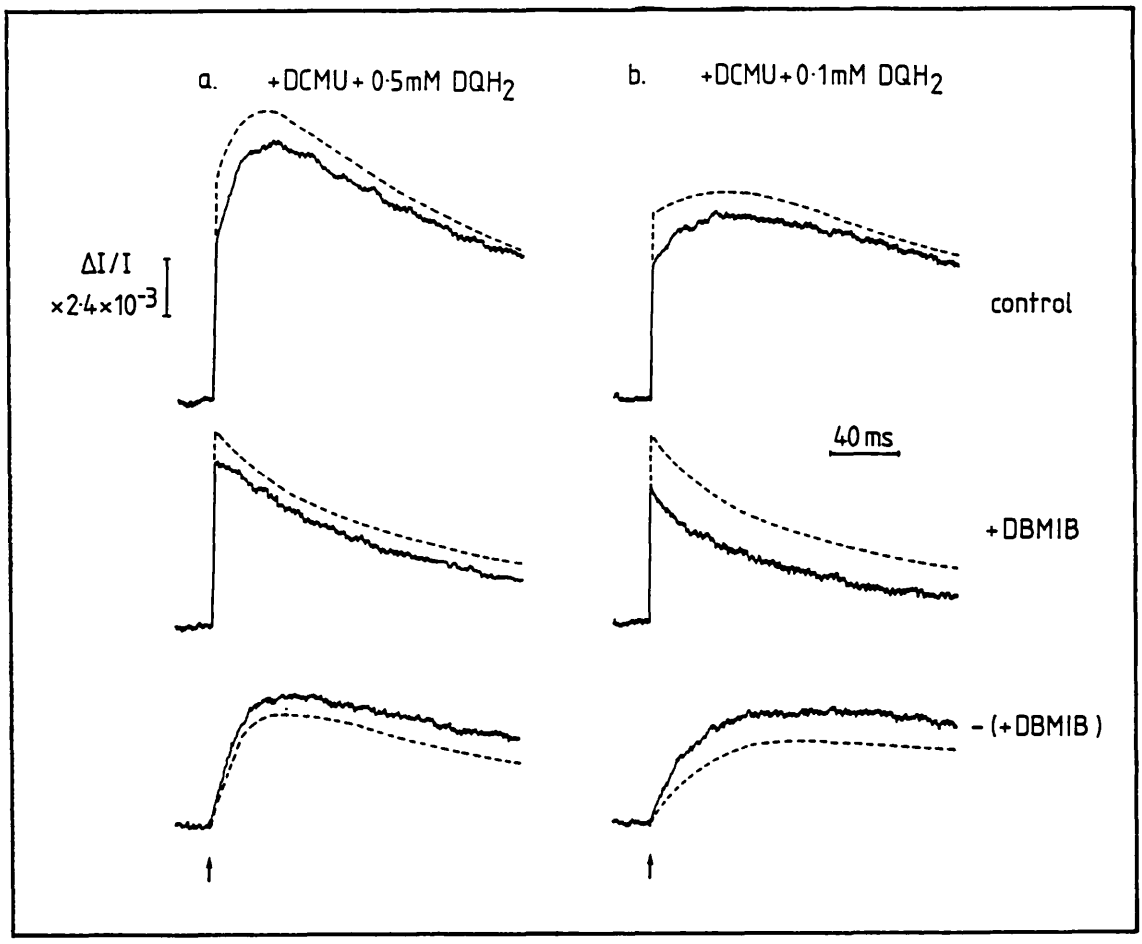


Fig. 5.11. Flash-induced ΔA_{515} for stacked (full line) and unstacked (broken line) thylakoid membranes. Conditions are as described in section 2.2.2 for pseudocyclic electron flow, with DQH_2 as reductant. (a) in the presence of 0.5mM DQH_2; (b) in the presence of 0.1mM DQH_2. The true kinetics and extent of phase a and phase b are obtained by the same procedure as that given in Fig. 3.1. The addition of 50μM MV does not alter these traces.

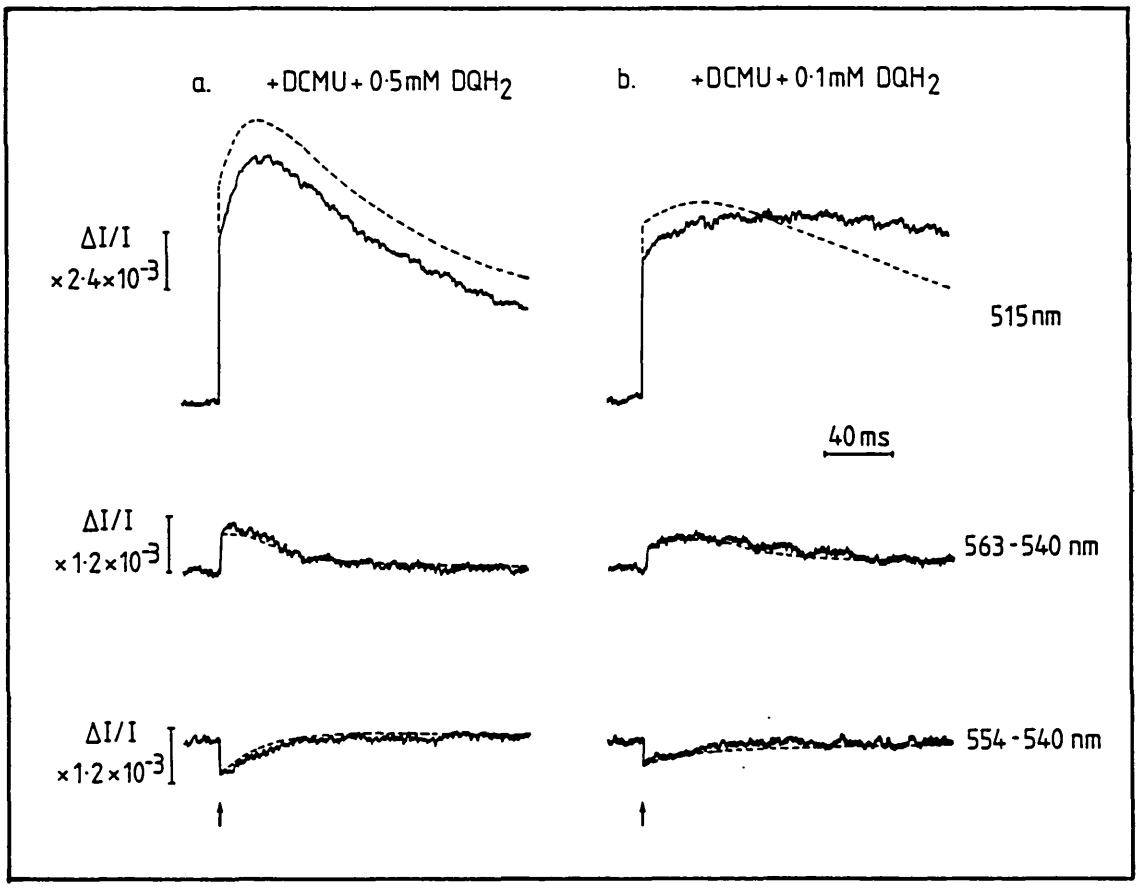


Fig. 5.12. Flash-induced electrochromic and cytochrome absorption changes for stacked (full line) and unstacked (broken line) thylakoid membranes. Conditions are as described in section 2.2.2 for pseudocyclic electron flow, with DQH_2 as reductant. For the cytochrome ΔA, valinomycin (2μM) and nigericin (2μM) were also present (see section 2.2.3). (a) in the presence of 0.5mM DQH_2; (b) in the presence of 0.1mM DQH_2. The addition of 50μM MV does not alter these traces.

duced by dithionite, the extent of cytochrome b-563 oxidation is not very different in either case, compare Fig. 5.12(a) with Fig. 5.7(a). The effect of salt on the extent of oxidation of cytochrome b-563 is small, Fig. 5.12(a), but it is comparable with the small salt-induced change on the extent of phase b, Fig. 5.11(a).

Fig. 5.11(b) shows the effect of lowering the DQH_2 concentration. Again, these results hold for both ± MV. Although the full extent of phase a is observed, the generation of phase b is now slow, its extent being comparable to that observed under optimal DQH_2 concentrations, Fig. 5.11(a). Fig. 5.12(b) shows that both the dark reoxidation of cytochrome b-563 and the dark rereduction of cytochrome f have also been slowed down. These results suggest that, overall, the rate of electron transport is slow under these limiting reducing conditions. Again, the effect of salt on the extents of phase a and phase b and on the cytochrome absorption changes, is as in Figs. 5.11(a) and 5.12(a), respectively.

5.5 Ascorbate/DCPIP induced electron transport:

A brief investigation of the effect of the Asc/DCPIP reducing couple was also carried out. As indicated in section 5.1, this couple is a very mild reductant: although a large phase a is generated upon the addition of Asc/DCPIP, in the presence of DCMU, only a small phase b is observed, Fig. 5.13(a). The addition of DBMIB inhibits phase b; however it also causes an unexpected increase in the extent of phase a, thus making it difficult to resolve out the phase b contribution. This increase in the extent of phase a suggests that the Asc/DCPIP and DBMIB combination (in the presence of DCMU) is able to reactivate some of the PS2 reaction centres.

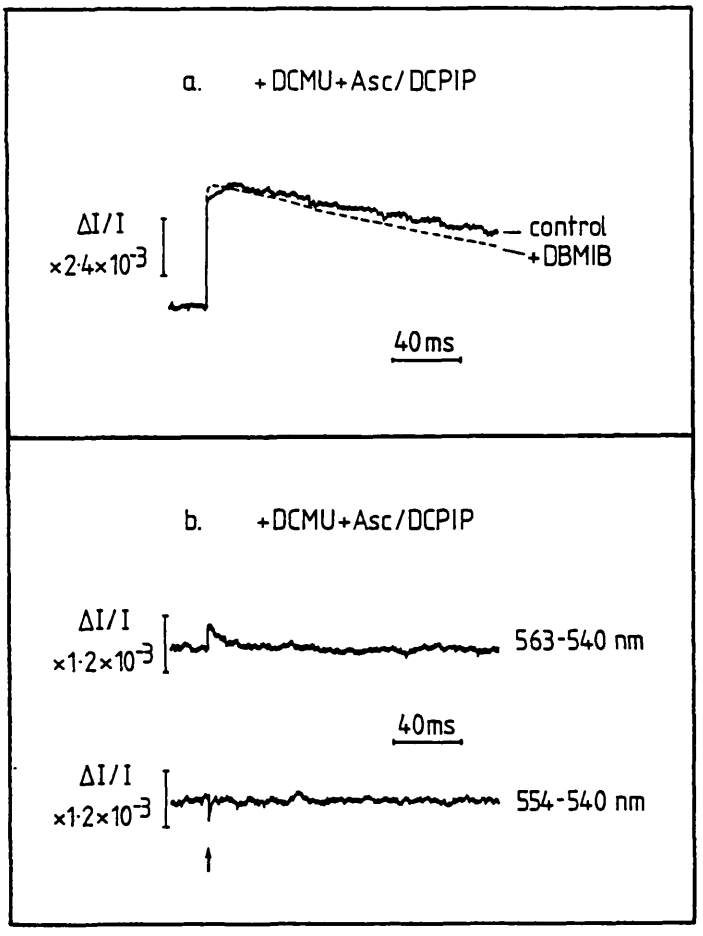


Fig. 5.13. (a) Flash-induced ΔA_{515} for stacked thylakoid membranes. Conditions are as described in section 2.2.2 for pseudocyclic electron flow, with Asc/DCPIP as reductant. Control, with no further additions (full line); control + 15μM DBMIB (broken line). (b) Flash-induced cytochrome absorption changes under the "control" conditions of (a), and in the presence of valinomycin (2μM) and nigericin (2μM), see section 2.2.3.

The cytochrome absorption changes in the presence of Asc/DCPIP are shown in Fig. 5.13(b): these are unaltered by the addition of DCMU. Cytochrome b-563 undergoes a rapid flash-induced reduction, whose magnitude is comparable to that observed in the presence of either dithionite, Fd/NADPH or DQH_2. Its dark reoxidation, however, is more rapid and occurs rather promptly. Both the flash-induced oxidation and dark rereduction of cytochrome f are rapid: Asc/DCPIP is thought to donate electrons after the Rieske FeS centre.

An interesting effect of Asc/DCPIP is shown in Fig. 5.14. The addition of Asc/DCPIP in the presence of DCMU and DQH_2 results in the partial loss of phase b, although there is an increase in the decay rate of the ΔA_{515}. This is accompanied by an inhibition of cytochrome b-563 dark reoxidation and an acceleration in the rate of cytochrome f dark rereduction, compare Fig. 5.14 with Fig. 5.12(a).The addition of Asc/DCPIP, in the presence of an alternative reductant, possibly acts as a competitive electron donor to cytochrome f: in this way the reoxidation of cytochrome b-563 is inhibited. This effect, again emphasizes a correlation between cytochrome b-563 oxidation and the generation of phase b, thus invoking the involvement of a Q-cycle type mechanism.

5.6 Discussion:

In this chapter, the use of different reductants, in the presence of DCMU, is found to generate phase a and phase b of the flash-induced 515nm electrochromic absorption change with differing extents. The effect of MV on both the ΔA_{515} and the cytochrome redox changes is also found to depend on the reductant present. This latter effect has interesting consequences in terms of electron transport operation. Also, it leads to the suggestion that the generation of phase b can

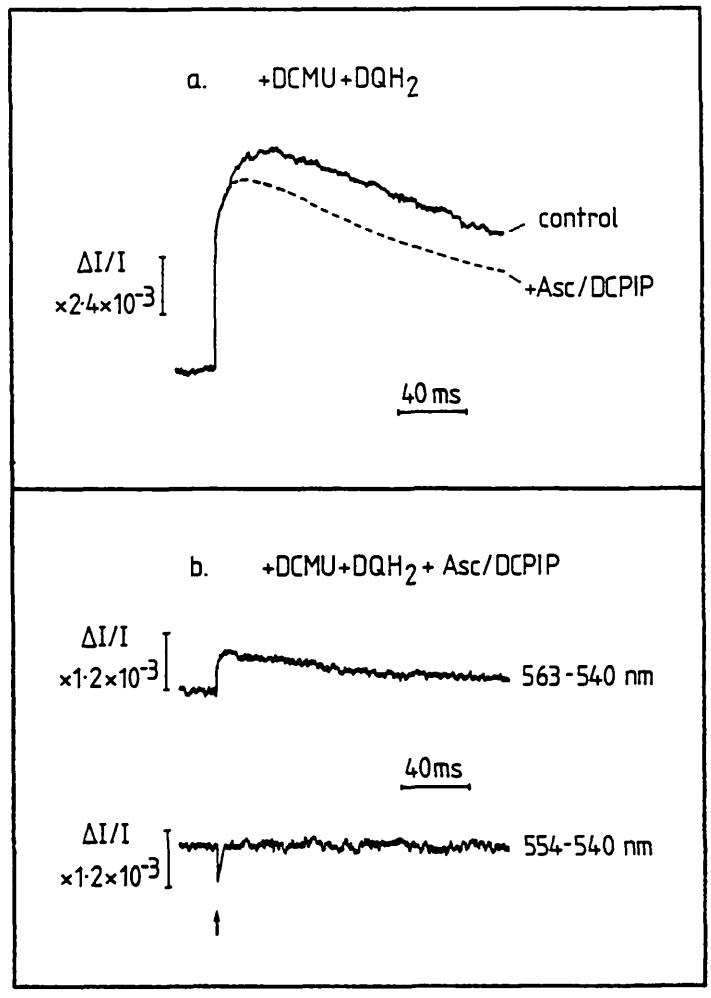


Fig. 5.14. (a) Flash-induced ΔA_{515} for stacked thylakoid membranes. Conditions are as described in section 2.2.2 for pseudocyclic electron flow, with DQH_2 (0.5mM) as reductant. Control, with no further additions (full line); control + 0.5mM Asc + 50mM DCPIP (broken line). (b) Flash-induced cytochrome absorption changes under the "control + Asc/ DCPIP" condition of (a), and in the presence of valinomycin (2μM) and nigericin (2μM), see section 2.2.3.

be correlated to electron transport in which a Q-cycle type mechanism is operative.

The reducing strengths of the reductants used in this study are well characterized in section 5.1. The extents of phase a and phase b, obtained in the presence of the different reductants, are compared with the redox titrations in Figs. 4.3 and 4.7. On this basis, the reductants can be placed in order of their reducing ability: dithionite > Fd/NADPH > DQH_2 > Asc/DCPIP. In the discussion to follow only those results which have been obtained in the presence of dithionite, Fd/NADPH and DQH_2 will be included; the effect of Asc/DCPIP will only be briefly mentioned.

In the presence of the above reductants, and in the absence of any further additions, cytochrome b-563 is oxidized in the dark while the high potential PS1 donor pool, which includes the FeS centre, cytochrome f and plastocyanin, is reduced. A single turnover flash oxidizes P700. An electron from the high potential donor pool rapidly reduces P700, leaving the FeS centre mostly oxidized and cytochrome f partially oxidized. It is this light-induced oxidation of the FeS centre that instigates the reduction of cytochrome b-563. The kinetics of these events following an actinic flash are: (1) cytochrome f oxidation ($t_{\frac{1}{2}} < 1$ ms); (2) cytochrome b-563 reduction($t_{\frac{1}{2}} \sim 1$ms);(3) cytochrome f rereduction($t_{\frac{1}{2}} \sim 5$ms);and (4) cytochrome b-563 reoxidation ($t_{\frac{1}{2}} \sim 10$ms).From these kinetics, however, it is difficult to determine whether cytochrome b-563 is involved in a Q-cycle type mechanism (see Fig. 1.6) or in a simple linear electron transport scheme (see below):

$$PQH_2 \rightarrow \text{cyt } \underline{b}\text{-563} \rightarrow RFeS \rightarrow \text{cyt } \underline{f} \rightarrow PC \rightarrow PS1$$

In a Q-cycle type scheme, the flash-induced reduction of cytochrome b-563 would be expected to match the dark rereduction of cytochrome f. In a linear type scheme, however, it is the dark reoxidation of cytochrome b-563 that would be expectedto match the dark rereduction of cytochrome f. No such correlations in favour of either model can be made from the results presented in Figs. 5.7(a) and 5.12(a). A possible distinction is, however, discussed later, in view of the results obtained in the presence of MV.

To be noted is that in the presence of Fd/NADPH, the dark rereduction kinetics of cytochrome f are very rapid, Fig. 5.9(a); as such, these kinetics would match the kinetics of the flash-induced reduction of cytochrome b-563, in accordance with a Q-cycle type mechanism. However, why such kinetics should become apparent under these particular conditions is unclear. The possibility that Fd/NADPH is able to reduce cytochrome f directly, can be discounted since PQH_2 oxidation would be expected to be slow and hence cytochrome b-563 reduction would also be slow: this, however is not observed.

There is no apparent salt effect on the extent of the flash-induced cytochrome b-563 reduction or on the cytochrome f absorption change. Changes in the ionic strength,however, do appear to affect the extent of cytochrome b-563 dark reoxidation, see Figs. 5.7(a), 5.9(a) and 5.12(a), in a similar manner to that observed regarding the extent of phase b. This effect of salt on the extent of phase b and that of cytochrome b-563 oxidation is possibly dependent on ambient redox poise. When comparing the salt induced effect in the

presence of DQH_2 with that in the presence of dithionite, it is found not to be so large in the case of phase b, compare Figs. 5.11(a) and 4.2(c), and even less apparent for the oxidation of cytochrome b-563, compare Figs. 5.12(a) and 5.7(a).

The addition of MV, a competitive PS1 electron acceptor, in the presence of certain reductants apparently alters the sequence of electron transport events. This thus gives further insight into the possible mechanism of electron transport. In the presence of dithionite, high concentrations of MV are found to have an inhibitory effect on both the extent of phase a and that of phase b, Fig. 5.3(c). As discussed previously, this observation is contrary to that expected in view of the redox titrations presented in Figs. 4.3(b) and 4.7(c). It does however suggest that an unusually low ambient redox potential has been attained. A possible explanation for this is as follows. The ability of MV to inhibit cyclic electron flow relies on the fact that it can donate the electrons it accepts from PS1, to oxygen. In this way the oxidized form of MV is regenerated, from the reduced form, provided there is an indefinite supply of oxygen present. Dithionite, on the other hand, is an efficient oxygen trap (hence its effectiveness as a reductant). In the presence of dithionite, therefore, the system will be relatively anaerobic. The oxidized form of MV will thus not be regenerated by molecular oxygen, but MV itself may possibly become an efficient reductant, thus inhibiting phase b and also part of phase a (in Fig. 5.3(c) it is part of the PS1 contribution to phase a that is inhibited). The partial inhibition of electron transport, by this particular combination of dithionite and MV, is also indicated by the flash-induced cytochrome absorption changes, Fig. 5.7(c). Further evidence for the presence of the reduced form of MV (which is blue in colour), under these conditions, is the relatively large scattering changes observed in the spectra of Fig. 5.6(c).

The appearance of a delayed phase b in the presence of dithionite and low concentrations of MV, Fig. 5.3(b), must also result from the altered properties of MV induced by the anaerobic conditions in the presence of dithionite. A possible explanation for the occurrence of this delayed slow phase comes from an analysis of the flash-induced cytochrome absorption changes observed under these conditions, Fig. 5.7(b): these cytochrome redox changes would be in favour of a Q-cycle type mechanism. Cytochrome b-563 is apparently fully reduced, prior to flash activation, under these particular conditions: in view of the earlier discussion concerning the operation of MV in the presence of dithionite, low redox potentials are to be expected. The particular redox potential achieved in this case will not be inhibiting, as in the presence of high MV concentrations. In accordance with this, and considering a Q-cycle type mechanism to be operative, it can be envisaged that both b_h and b_l in Fig. 1.6 will be pre-reduced. For PQH_2 oxidation to occur, b_l, and hence b_h, need to be oxidized. b_h oxidation will occur when bound Q_o is available; subsequently, the oxidation of b_l and PQH_2 will also occur, but on a time-scale that is comparable with b_h oxidation. The rereduction of cytochrome f would thus be expected to be slow (for an operational Q-cycle): this is indeed observed, Fig. 5.7(b). If a linear electron transport scheme were operative, and cytochrome b-563 pre-reduced, as is indicated by these particular conditions, then both the reoxidation of cytochrome b-563 and the rereduction of cytochrome f would be expected to be very rapid: this, however, is not observed.

The above argument can thus be extended to explain the occurrence of a delayed phase b. If phase b occurs as the result of b_h oxidation (the redox titration in Fig. 4.7(a) seems to suggest that the chemical reduction of a high potential b-type cytochrome is respon-

sible for the inhibition of phase b) then the observed delay would be a measure of the Q_o binding time constant, which in some way has been modified by the state of reduction of the system. If, on the other hand, phase b occurs as the result of $\underline{b}_l$ oxidation, then the delay will be a measure of the time required for $\underline{b}_h$ oxidation to occur (which will also include the Q_o binding time constant).

In the case of Fd/NADPH and high concentrations of MV, similar arguments to those above can be used to explain the occurrence of a delayed slow phase and the concomitant slow cytochrome $\underline{b}$-563 oxidation, Fig. 5.9(b). To be noted, though, is that the ambient redox poise in this particular case is very different to that in the presence of dithionite and low concentrations of MV. In the presence of Fd/NADPH and MV, reducing conditions prior to flash activation are similar to those in the absence of MV, in that cytochrome $\underline{b}$-563 is only partially reduced. The results presented in Fig. 5.9(b), however, would still favour the Q-cycle type mechanism. Since cytochrome $\underline{b}$-563 is only partially reduced, PQH_2 oxidation can still occur and hence the rereduction kinetics of cytochrome $\underline{f}$ will be unaffected, compare Figs. 5.9(b) and 5.9(a). It is the subsequent reoxidation of cytochrome $\underline{b}$-563 that is temporarily inhibited. This is manifested in the ΔA_{515} as a delayed phase b, and, as discussed above, possibly reflects a slowness in Q_o binding as a consequence of the unusual mode of action of MV under anaerobic conditions.

The results presented in Fig. 5.10 would suggest that the partial inhibition of cytochrome $\underline{b}$-563 oxidation, and the resultant delayed slow phase in the ΔA_{515}, is associated with a restricted supply of protons. Conceivably, if protons are not available, the reduction of Q_o, by the oxidation of $\underline{b}_h$, will be limited.

In the presence of DQH_2, neither the ΔA_{515} nor the cytochrome redox changes are altered in the presence of MV. Such observations are in agreement with those predicted by the redox titrations in Figs. 4.3(c) and 4.7(b). The role of MV as an inhibitor of cyclic electron transport is apparently unaffected by this particular reductant: there is now a continuous supply of oxygen.

The effect of salt in the presence of MV and a reductant is very similar to that discussed earlier where MV was absent. An exception to this, however, is in the case of Fd/NADPH and MV, Fig. 5.9(b). In the presence of low salt, no decrease in the extent of cytochrome b-563 oxidation is observed; instead the extent of its flash-induced reduction is increased. This could merely reflect the salt-dependent binding properties of ferredoxin, as discussed earlier, which in turn alter its effectiveness as a reductant (in the presence of NADPH).

In conclusion, two main features are apparent from these results. Firstly, a correlation between the generation of phase b and the oxidation of cytochrome b-563 appears to be favoured, where cytochrome b-563 is involved in a Q-cycle type mechanism. The inhibitory effect of Asc/DCPIP on the extent of phase b , generated in the presence of DCMU and DQH_2, and the concomitant inhibition of cytochrome b-563 oxidation, Fig. 5.14, is further evidence for this conclusion. Secondly, the sensitivity of electron transport, as monitored by cytochrome b-563 and cytochrome f redox reactions, to changes in ambient redox poise, is emphasized by the results obtained in the presence of MV. Such a sensitivity to redox potential poise has also been observed for electron transfer in bacterial chromatophores (O'Keefe et al, 1981).

CHAPTER 6

The electrochromic absorption change related to proton uptake/release

The effect of pH on the 515nm electrochromic absorption change and on the cytochrome absorption changes is investigated. A study of the flash-induced proton uptake and proton release, which both occur as the result of electron transport, is also carried out. An attempt is made to determine the associated H^+/e^- ratio.

6.1 The effect of pH on the ΔA_{515} and cytochrome absorption changes:

Fig. 6.1 shows the pH titration curve for the extent of phase a and that of phase b. The conditions are those forpseudocyclic electron flow, where the reductant is dithionite. The extent of phase a is observed to be pH independent. This is to be expected since the charge separation within the reaction centres is known not to involve the uptake or release of protons. The extent of phase b is, however, pH dependent: its pH titration curve follows a classical Henderson-Hasselbalch equation (see section 2.2.4) with a pK of 8.7.

Fig. 6.2(a) shows the ΔA_{515} at high and low pH values and under the same electron transport conditions as in Fig. 6.1. Although the decay rate of the ΔA_{515} at pH8.6 is faster than that at pH 7.4, the actual extent of phase b is markedly decreased. The related cytochrome absorption changes are shown in Figs. 6.2(b) and (c). Both the extent of the flash-induced reduction of cytochrome b-563, and that of its dark reoxidation, are decreased when the pH is increased, Fig. 6.2(b). On the other hand, the rate of cytochrome b-563 dark reoxidation remains unaltered by these changes in pH.

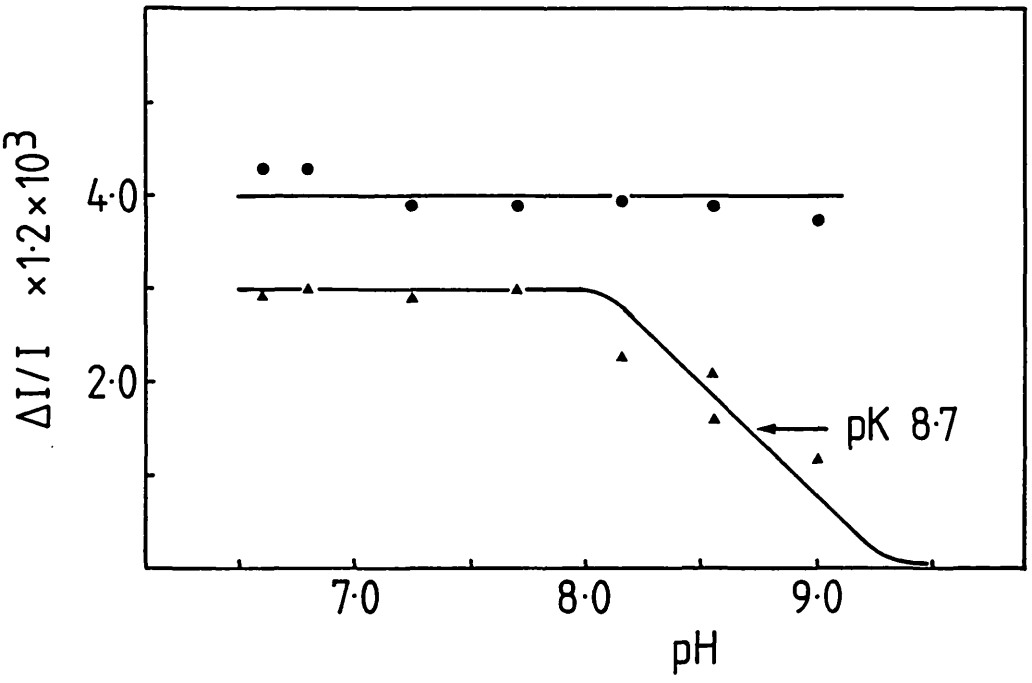


Fig. 6.1. pH dependence of the flash-induced ΔA_{515} for stacked thylakoid membranes. Conditions are as described in section 2.2.2 for pseudocyclic electron flow, with dithionite as reductant. The extents of phase a (circle symbols) and of phase b (triangle symbols) were resolved by the procedure given in Fig. 3.1. The required ambient pH was obtained by suspending the chloroplasts in the appropriate buffer medium, see section 2.2.4.

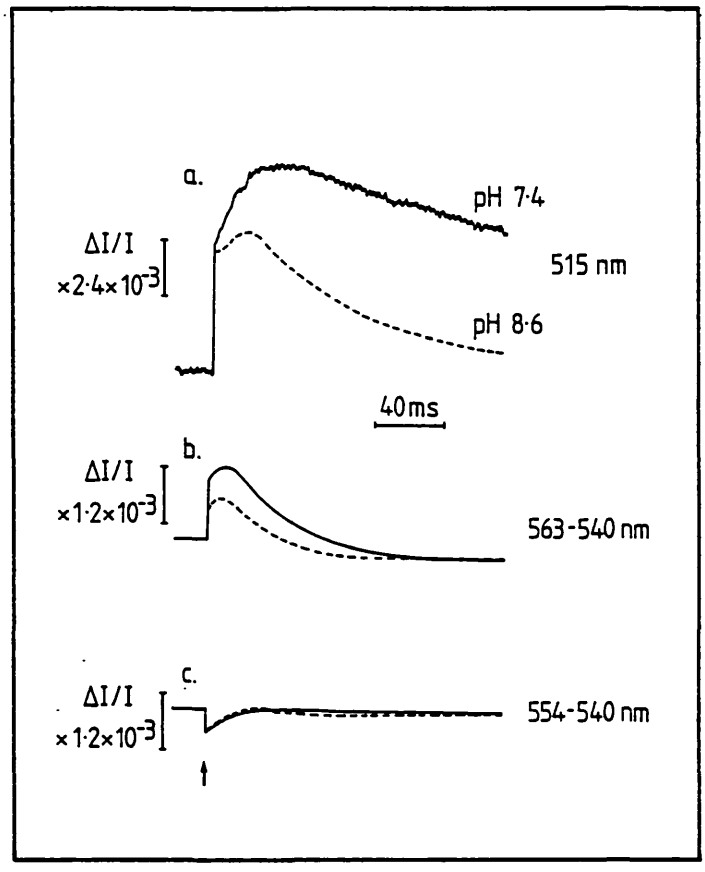


Fig. 6.2. The effect of pH on the flash-induced electrochromic and cytochrome absorption changes. The conditions are as in Fig. 6.1. For the cytochrome ΔA, valinomycin (2μM) and nigericin (2μM) were also present (see section 2.2.3). (To be noted, for the cytochrome ΔA, the ΔA at the reference λ was subtracted manually from that at the measuring λ). pH 7.4 (full line); pH 8.6 (broken line).

In the case of cytochrome f, however, no such pH changes are observed in either the extent or in the kinetics of its redox absorption changes, Fig. 6.2(c). These results would again favour the involvement of cytochrome b-563 in the generation of phase b.

6.2 Flash-induced proton uptake:

Fig. 6.3 shows the kinetics of flash-induced proton uptake, measured at 574nm using cresol red. The traces (a)-(d) display an increase in absorption, indicating that the outer aqueous phase has become more alkaline due to the uptake of protons by the thylakoid membrane. In the absence of any reductant or inhibitor, Fig. 6.3(a), proton uptake is slow, occurring with an approximate $t_{\frac{1}{2}}$ of 40ms. This indicates that, under these conditions, the rate of electron transport is not optimal. The extent of the absorption change in Fig. 6.3(a) represents the uptake of approximately 160 pmoles of protons, as determined by the calibration method described in section 2.2.5. Later, this particular concentration of protons will be related to the concentration of P700 present, and hence a H^+/e^- ratio determined.

The addition of DCMU results in the complete inhibition of the ΔA_{574}, Fig. 6.3(b). This corresponds to the condition depicted by the ΔA_{515} in Fig. 3.3(b): electron transport is inhibited and consequently neither the reduction of PQ nor the uptake (or release) of protons will take place.

The subsequent addition of a reductant, in this case DQH_2, restores the ΔA_{574}, Fig. 6.3(c), concomitant with the reappearance of the ΔA_{515} in Fig. 3.3(c). The ΔA_{574} now exhibits an initial

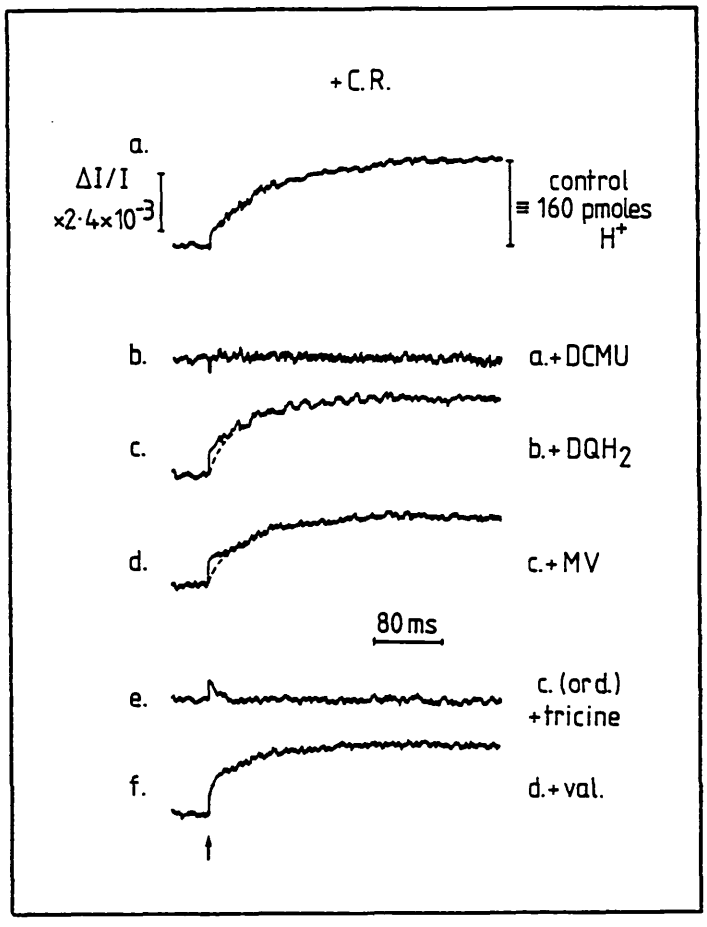


Fig. 6.3. Flash-induced proton uptake absorption changes recorded with the dye cresol red (C.R.) at 574nm (pH 7.3). The sample was prepared as described in section 2.2.5, with stacked thylakoid membranes, the control condition in (a) being with no further additions. Subsequent additions are as stated in the figure, the concentrations of which are: DCMU (25μM), DQH_2 (0.5mM), MV (50μM), tricine (50mM) and valinomycin (2mM). The dotted lines in traces (c) and (d) are the result of subtracting the buffered (+50mM tricine) signal, as shown in (e). For the calibration of these ΔA, see section 2.2.5 and text.

small rapid increase, followed by a larger slow increase. The initial rapid increase is due to non-specific absorption changes at 574nm: it can still be observed in the presence of 50mM tricine, Fig. 6.3(e). Cresol red records pH absorption changes in the outer unbuffered aqueous phase; any buffer subsequently added will thus eliminate such pH changes. In accordance with this, since the slow increase of the ΔA_{574}, Fig. 6.3(c), is totally inhibited by the addition of tricine, this suggests that it represents proton uptake. Subtraction of the buffered signal, Fig. 6.3(e), from the unbuffered signal, Fig. 6.3(c), reveals the true kinetics of proton uptake, as manifested by the dotted line shown in Fig. 6.3(c), the maximum extent of proton uptake remaining unaltered. Thus, in the presence of DCMU and DQH_2, proton uptake occurs with an approximate $t_{\frac{1}{2}}$ of 20ms: this is comparable with the rise kinetics of phase b, Fig. 5.11(a), and the kinetics of cytochrome b-563 dark reoxidation, Fig. 5.12(a). Calibration of the extent of the ΔA_{574} in Fig. 6.3(c) also yields a value of approximately 160 pmoles of protons taken up from theouter aqueous phase. To be noted is that similar results to those in Fig. 6.3(c) are obtained in the presence of DQH_2 alone. The addition of MV, in the presence of DCMU and DQH_2, does not alter the kinetics or the calibrated extent of the ΔA_{574}, compare Figs. 6.3(d) and (c). Similarly, most of the absorption change is eliminated by the addition of tricine, except for the initial rapid increase.

A point to note is that there is the possibility that cresol red does not monitor total proton uptake due to the build up of an electrical gradient, across the thylakoid membrane, that cannot be dissipated in-between flashes. This, however, is not the case since the addition of valinomycin, in the presence of K^+, which would dissipate any electrical gradients present, does not enhance the total extent of the ΔA_{574}, Fig. 6.3(f). Furthermore, it is noted that the decay rate of the ΔA_{574}

is slow. This indicates that the extrusion of protons into the outer phase, via the ATPase complex,is slow compared with the time-scale required for electron transport.

Use of the dye phenol red, instead of cresol red, to monitor proton uptake,yields similar results to those presented in Fig. 6.3. Furthermore, the series of experiments carried out in Fig. 6.3, were also attempted using the reductants dithionite and Fd/NADPH. However, the combination of anaerobic conditions, as imposed by these reductants, and the absence of any buffering capacity in the sample, in order to measure proton uptake, resulted in a rather unstable sample. This thus made reliable measurements difficult.

Fig. 6.4 shows the pH titration for the calibrated extent of the cresol red absorption changes; the conditions are as in Fig. 6.3(d). As to be expected, a similar pH titration curve is obtained in the absence of any added reductant or inhibitor, in the presence of 50μM MV alone and using the dye phenol red in the presence of DCMU + DQH_2^+ MV. The data in Fig. 6.4 can be fitted to a classical Henderson-Hasselbalch equation with a pK of 7.5.

The axis on the right hand side of Fig. 6.4 indicates the approximate number of protons taken up per P700, and hence per electron transported along the electron transport chain. The concentration of P700 present in the sample was calculated from the extent of the flash-induced P700 oxidation, obtained in the absence of reductant or inhibitor, see Fig. 6.5(a). The extent of P700 oxidation is unaltered in the presence of DBMIB, but its dark rereduction is inhibited, Fig. 6.5(b). Furthermore, the total P700 absorption is inhibited in the presence of DCMU, Fig. 6.5(c). Using $\Delta\varepsilon_{703-725} = 6.4 \times 10^{+4}\ M^{-1}\ cm^{-1}$ (Hiyama

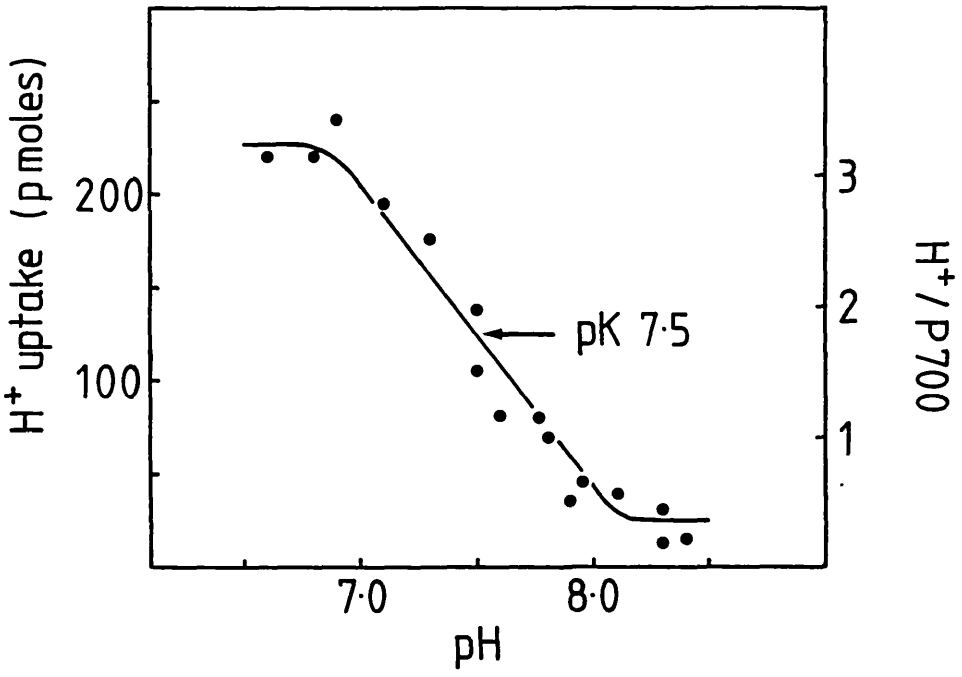


Fig. 6.4. pH dependence of the calibrated extent (left-hand axis) of the flash-induced proton uptake absorption change, ΔA_{574}, under the conditions of Fig. 6.3(d). For calibration procedure, see section 2.2.5. Also shown (on the right-hand axis) is the H^+/P700 ratio: for calculation of the concentration of P700 present in the sample, see text. The required ambient pH was obtained as described in section 2.2.5.

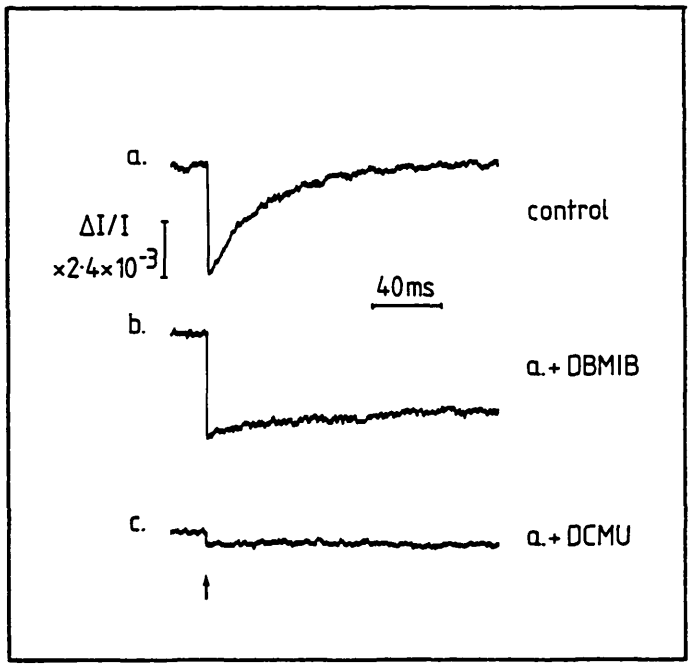


Fig. 6.5. Flash-induced P700 absorption change, recorded at 703-725nm (see section 2.2.3), for stacked thylakoid membranes. The sample was prepared as described in section 2.2.3, with no added inhibitor or reductant. (a) control, with no further additions; (b) as (a) + 15μM DBMIB; (c) as (a) + 25μM DCMU.

and Ke, 1972), P700 is oxidized to an extent of 35nM: in a 2ml sample this is equivalent to 70 pmoles of P700. Hence, under the conditions of Fig. 6.3(d), namely at pH 7.3, the approximate H^+/e^- ratio is 2. To be noted, however, is that the above experimentally calculated concentration of P700 corresponds to 1 P700 per 1200 chlorophylls; this is rather smaller than the expected 1 P700 per 600 chlorophylls.

Concomitant with the pH titration carried out in Fig. 6.4, a pH titration of the extent of phase b was also carried out: this yields the same curve as that depicted in Fig. 6.1.

6.3 Flash-induced proton release:

Fig. 6.6 shows the kinetics of the flash-induced proton release measured at 540nm using the dye neutral red. In the absence of any added reductant or inhibitor, Fig. 6.6(a), an increase in absorption is observed. This indicates that the inner aqueous phase has become more acidic due to the release of protons from the thylakoid membrane. The proton release detected in Fig. 6.6(a) is slow, occurring with an approximate $t_{\frac{1}{2}}$ of 60ms, and no rapid phase is observed. This absorption change is totally inhibited in the presence of the permeable buffer imidazole, Fig. 6.6(b), and in the presence of nigericin, Fig. 6.6(c): nigericin dissipates any proton gradient that builds up across the thylakoid membrane. Both these results suggest that the total extent of the neutral red response in Fig. 6.6(a) is due to proton release. To be noted is that the decay rate of the ΔA_{540} is slow. This is in accordance with the earlier observation of a slow decay rate for the ΔA_{574}, Fig. 6.3.

Fig. 6.7 shows the ΔA_{540} in the presence of the reducing couple Fd/NADPH. An attempt was also made to record similar absorption

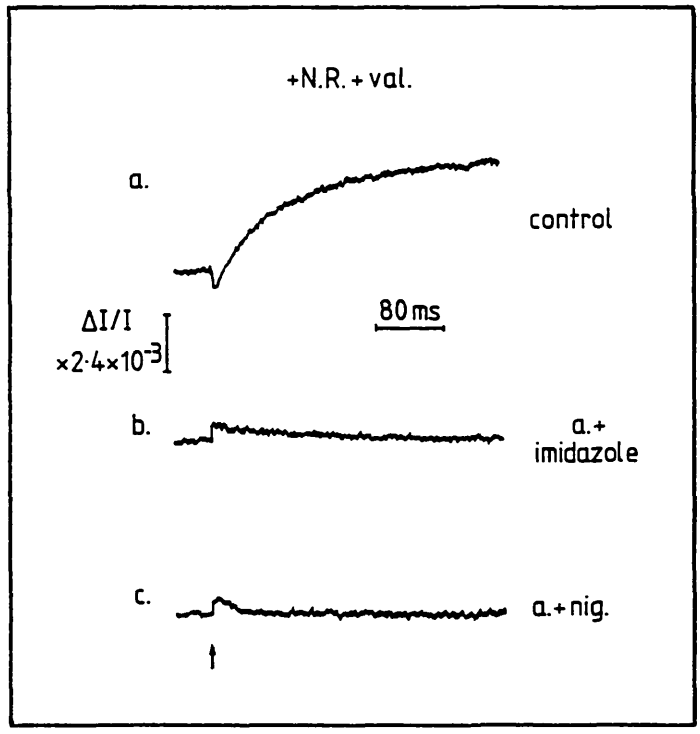
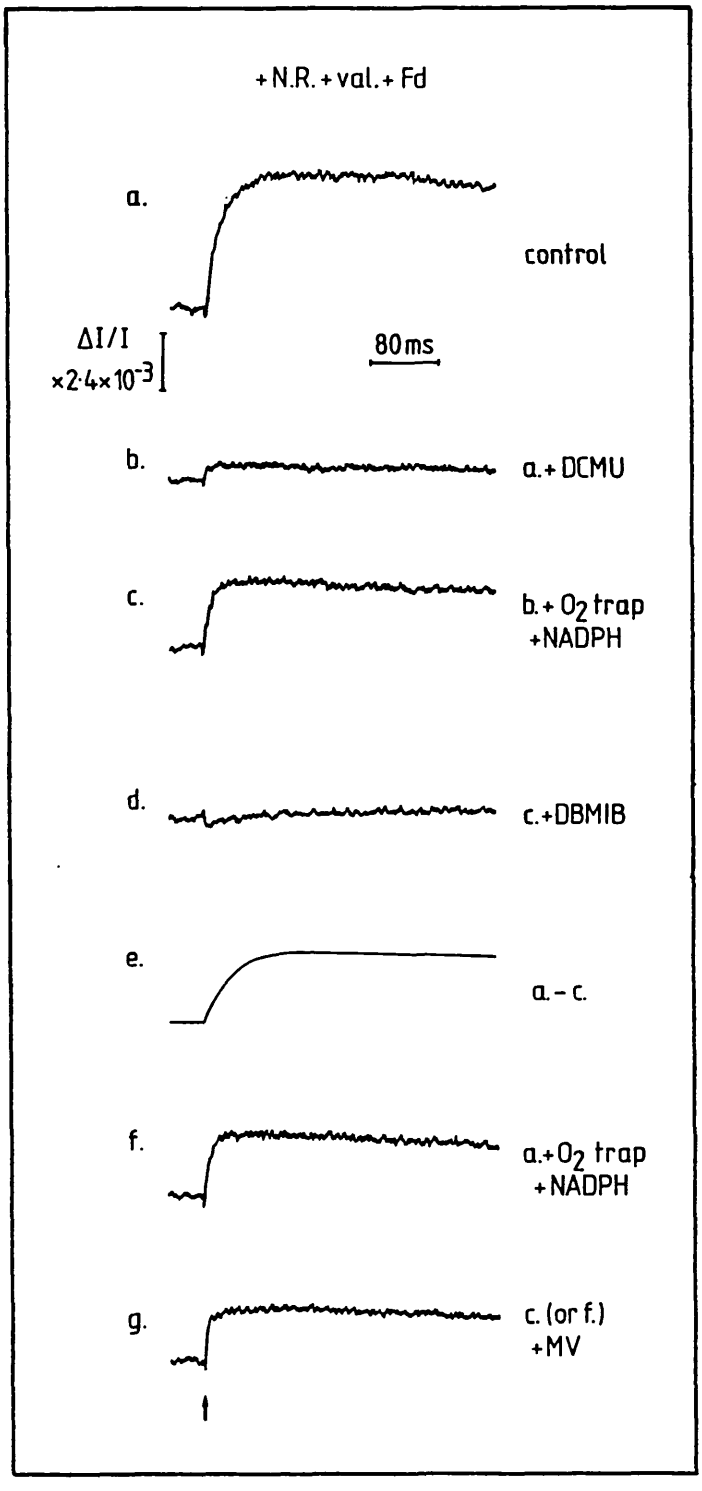


Fig. 6.6. Flash-induced proton release absorption changes recorded with the dye neutral red (N.R.), in the presence of valinomycin, at 540nm (pH 7.3). The sample was prepared as described in section 2.2.6, with stacked thylakoid membranes, and with no added inhibitor or reductant. (a) control, with no further additions ; (b) as (a) + 20mM imidazole; (c) as (a) + 2μM nigericin.

Fig. 6.7. Flash-induced proton release absorption changes recorded at 540nm. The control condition in (a) is the same as that in Fig. 6.6(a), but also in the presence of 5μM Fd. Subsequent additions are as stated in the figure, the concentrations of which are: DCMU (25μM), O_2 trap (see section 2.2.2), NADPH (0.5mM), DBMIB (15μM) and MV (50μM).


+N.R. + val. + Fd
a.
control
ΔI/I
×2·4×10⁻³
80 ms
b.
a. + DCMU
c.
b. + O2 trap
+NADPH
d.
c. + DBMIB
e.
a. – c.
f.
a. + O2 trap
+NADPH
g.
c. (or f.)
+MV

changes in the presence of dithionite. However, problems were again encountered in keeping the pH of the sample stable, this time due to the highly reducing conditions imposed by dithionite.

When ferredoxin is present as a PS1 electron acceptor, thus inducing non-cyclic conditions, the ΔA_{540} consists of an initial rapid increase followed by a slower increase, which has an approximate $t_{\frac{1}{2}}$ of 15ms, Fig. 6.7(a). It has been suggested that the rapid increase can be attributed to the oxidation of water by PS2, while the slower increase can be attributed to the oxidation of PQH_2 by PS1 (Ausländer and Junge, 1975). The following observations are in agreement with this. In the presence of DCMU, the ΔA_{540} in Fig. 6.7(a) becomes almost non-existent after a few flashes, Fig. 6.7(b), in accordance with the inhibition of electron transport. The subsequent addition of an oxygen trap and NADPH restores the ability of the DCMU-inhibited chloroplasts to release protons, Fig. 6.7(c), and also to generate phase a and phase b of the ΔA_{515}, Fig. 5.8. The proton release under the conditions of Fig. 6.7(c) is completely inhibited by the addition of DBMIB, Fig. 6.7(d).

Since the proton released by the oxidation of water is inhibited by the presence of DCMU, the remaining contribution to the neutral red response in Fig. 6.7(c) will be due to the proton release by PQH_2 oxidation. Subtracting trace (c) from trace (a), in Fig. 6.7, reveals the full extent of proton release due to water oxidation, Fig. 6.7(e): this extent matches that of the ΔA_{540} in the presence of DCMU and the Fd/NADPH couple, Fig. 6.7(c), even at relatively long times. Thus, assuming that only one proton is released, per flash, due to water oxidation, PQH_2 oxidation also appears to be associated with the release of one proton per electron transferred to P700. Similar observations have been made by Olsen et al (1980).

A feature to be noted in the subtracted trace of Fig. 6.7(e), however, is that proton release due to water oxidation apparently occurs with very slow kinetics, much slower than those expected from the rapid kinetics observed in Fig. 6.7(a). Instead, the kinetics of proton release due to PQH_2 oxidation are now very rapid, Fig. 6.7(c). This indicates that the rate of PQH_2 oxidation is rapid under these particular reducing conditions. Furthermore, in the absence of DCMU, Fig. 6.7(f), the kinetics and extent of proton release induced by the addition of the Fd/NADPH couple, are similar to those in the presence of DCMU, Fig. 6.7(c). In accordance with the observations made in Fig. 5.1(c) and the discussion of section 5.1, the Fd/NADPH couple is able to reduce the PS2 electron acceptor chemically: the proton thus released due to water oxidation will also be inhibited. The addition of 50 μM MV does not alter the neutral red response in Figs. 6.7(c) or (f), see Fig. 6.7(g): this condition would correspond to the appearance of a delayed slow rise, Fig. 5.8(b). To be noted is that all the traces in Fig. 6.7 are abolished in the presence of the permeable buffer imidazole, as in Fig. 6.6(b).

Fig. 6.8 shows a similar series of experiments to those presented in Fig. 6.7, but induced in the presence of DQH_2. The addition of DQH_2 alone to the conditions of Fig. 6.6(a) results in a rapid absorption increase, with an approximate $t_{\frac{1}{2}}$ of 12ms, Fig. 6.8(a). The maximum extent of this ΔA_{540} is comparable to that in Fig. 6.7(a). The addition of DCMU results in a deceleration in the kinetics of proton release, and a small decrease in the total extent of the ΔA_{540}, Fig. 6.8(b). In the absence of DCMU, DQH_2 does not inhibit PS2 completely, see Fig. 5.1(d). The ΔA_{540} in Fig. 6.8(a) thus probably contains a small contribution from the proton released by water oxidation, which is subsequently inhibited in the presence of DCMU.

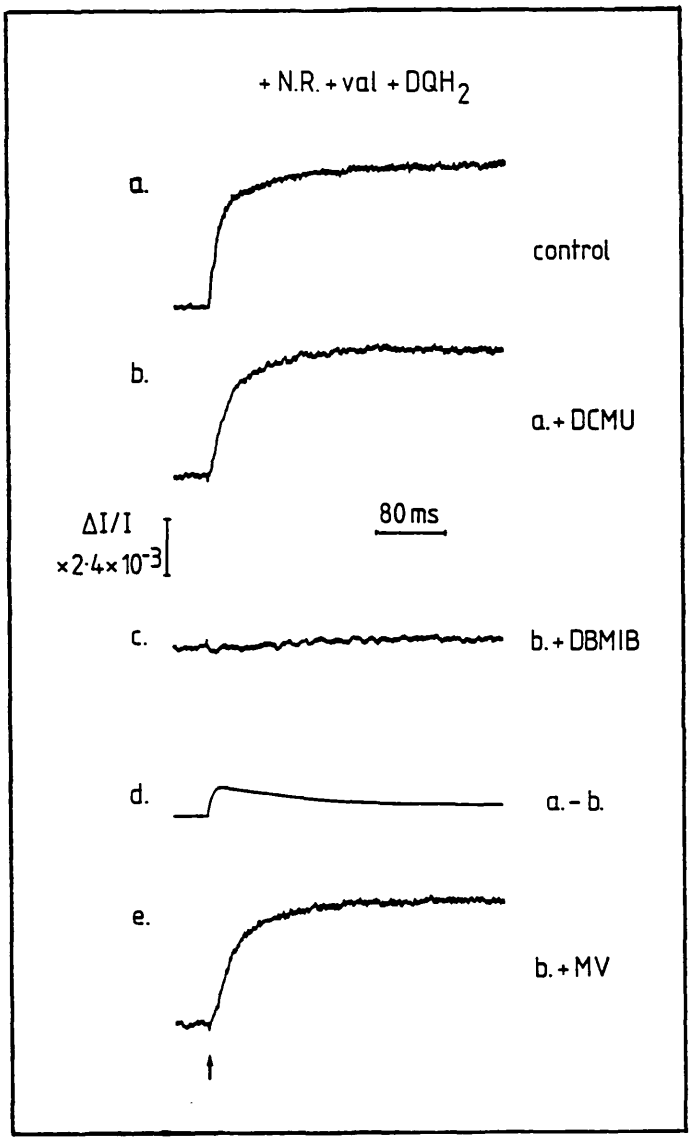


Fig. 6.8. Flash-induced proton release absorption changes recorded at 540nm. The control condition in (a) is the same as that in Fig. 6.6(a), but also in the presence of 0.5mM DQH_2. Subsequent additions are as stated in the figure, the concentrations of which are: DCMU (25μM), DBMIB (15μM) and MV (50μM).

Subtraction of trace (b) from trace (a), in Fig. 6.8, reveals the contribution from the proton due to water oxidation, Fig. 6.8(d): this exhibits the expected rapid rise kinetics. However, what percentage this is of the total contribution from the water oxidation proton is unknown. In order to estimate a possible H^+/e^- ratio with DQH_2 as reductant, it is worthwhile to compare the extent of the ΔA_{540} in Fig. 6.8(b) with that in Fig. 6.7(c): it is twice as large. It could thus be suggested that the H^+/e^- ratio for PQH_2 oxidation, under these particular reducing conditions, is 2. Again, the addition of MV does not alter the kinetics or the extent of proton release, compare Figs. 6.8(e) and (b). Furthermore, all the traces in Fig. 6.8 are abolished in the presence of imidazole.

6.4 Discussion:

The results presented in the previous chapter suggest that the generation of phase b is associated with the reoxidation of cytochrome b-563, where cytochrome b-563 appears to be involved in a Q-cycle type mechanism. The results presented in this chapter would be in support of this finding. Furthermore, they indicate an association of phase b with the transfer of protons, as is expected for a Q-cycle type mechanism.

From Figs. 6.1 and 6.2, the involvement of protons is apparent. It is such that the extent of phase b and that of the flash-induced redox reactions of cytochrome b-563 are diminished at high pH values, where the availability of protons for the reduction of PQ is limited. This not only supports the previous observation that the generation of phase b and the redox reactions of cytochrome b-563 can be closely associated, but also indicates a requirement for protons, as expected (but see later).

The kinetics of proton uptake, in the presence of reductant, Fig. 6.3(d), can be correlated with those for the occurrence of phase b, Fig. 5.11(a), under similar conditions. The pH titrations presented in Figs. 6.1 and 6.4, however, do reveal a paradox. The component responsible for proton uptake has a pK of 7.5, Fig. 6.4, while that responsible for the occurrence of phaseb has a pK of 8.7, Fig. 6.1. This might suggest that, contrary to the earlier observation, proton uptake cannot be correlated with the generation of phase b, since the components responsible for each process are different. However, the consequence of such a difference in pK values is that, although very little proton uptake is observed at pH 8.0,the full extent of phase b is still observed. The implication of this is that electron transport is still operational despite the lack of proton uptake. Such an observation is difficult to reconcile either with a typical Q- or b-cycle mechanism. Furthermore, a similar anomaly has also been noted in bacterial chromatophores (Petty et al, 1979) but without clear explanation. The pH titration in Fig. 6.4 does, however, suggest a H^+/e^- ratio of 2 at pH 7.5, in accordance with the expected uptake of $2H^+$ upon the reduction of PQ (see section 1.3.1). Furthermore, it is noted that a diffusion barrier exists which slows the uptake of protons (Ausländer and Junge, 1974): this thus limits the optimal rate of electron transfer.

Turning to the proton release measurements, it is interesting to observe that, in the absence of added reductant or inhibitor, Fig. 6.6(a), there is no rapid phase due to the water oxidation proton. This could indicate that, under these conditions, electron transport is slow, possibly due to the loss of endogenous components required for the correct redox poising of the system. The addition of ferredoxin alone, Fig. 6.7(a), is able to restore the appropriate conditions required for

the observation of rapid proton release due to water oxidation. To be noted, though, is that recent evidence suggests hindered lateral mobility of protons within the internal aqueous phase (Hong and Junge, 1983). This could explain why the water oxidation proton is not always observed as a rapid transient in the neutral red absorption trace.

In the presence of the Fd/NADPH couple, the kinetics of proton release, Figs. 6.7(c) or (f), do not match those for the generation of phase b, Fig. 5.8(a). They would instead match more closely with the kinetics of cytochrome f rereduction under similar reducing conditions, Fig. 5.9(a). Furthermore,in the presence of Fd/NADPH and MV, no delayed kinetics are observed in proton release, Fig. 6.7(g), that would correlate with the occurrence of a delayed phase b, Fig. 5.8(b). This latter result would, instead, be evidence for the discussion given in section 5.6: PQH_2 oxidation, and hence proton release, will occur despite the occurrence of a delayed phase b. The results thus presented in Fig. 6.7 would suggest that proton release is only indirectly involved in the generation of phase b.

In the presence of DQH_2 and DCMU, however, the kinetics of proton release, Fig. 6.8(b), would match those for the generation of phase b, Fig. 5.11(a), thus implicating a correlation, had it not been for the Fd/NADPH result in Fig. 6.7(g). A point worth noting, however, is that the addition of MV, in the presence of DQH_2 and DCMU, does not alter the kinetics or extent of proton release, compare Figs. 6.8(e) and (b); this suggests that proton release is not specifically associated with cyclic electron flow, under these particular reducing conditions.

The H^+/e^- ratios, as determined by proton release measurements, apparently vary with redox poise. In the presence of the Fd/NADPH couple, Fig. 6.7, the estimated H^+/e^- ratio is 1; in the case of

DQH_2, Fig. 6.8, the H^+/e^- ratio is estimated to be 2. From the discussion given in section 5.1, the Fd/NADPH couple is suggested to be a stronger reductant than DQH_2. Such a difference in H^+/e^- ratios, due to differences in redox poise, could explain the controversy that has surrounded previous measurements of H^+/e^- ratios (see section 1.3.2). However, this also leads to a paradox: although the number of protons released in the presence of the Fd/NADPH couple (and DCMU) is lower than in the presence of DQH_2 (and DCMU) the extent of phase b is similar in both cases.

CHAPTER 7

Inhibitor studies

In this final results chapter, the effect of inhibitors on the 515nm electrochromic absorption change is reported in conjunction with their effect on the cytochrome redox reactions and proton uptake/release. The conditions used are those for pseudocyclic electron flow, where DQH_2 is the reductant, see Fig. 5.11(a). Three different classes of inhibitors are used:

(1) DBMIB and UHDBT. These correspond to the type 2 inhibitors described in section 1.3.3: they have been reported to act by binding to the Rieske FeS centre and thus inhibit its reduction by PQH_2.
(2) HQNO and antimycin. These correspond to the type 1 inhibitors of section 1.3.3: they inhibit the reoxidation of the high potential cytochrome b-563.
(3) o-phenanthroline. This is thought to inhibit the oxidation of the primary acceptor Q_A, at the same site as DCMU (Satoh, 1974).

The aim of these inhibitor studies is to provide further evidence for the previous conclusions concerning (a) the involvement of cytochrome b-563 in the generation of phase b, and (b) the involvement of a Q-type cycle in photosynthetic electron transport.

7.1 Inhibitor effects on the ΔA_{515}:

Fig. 7.1 shows the effect of different inhibitors on the ΔA_{515}. The control ΔA_{515} is shown in Fig. 7.1(a) and is analogous to that shown in Fig. 5.11(a): the generation of both phase a and phase b is observed under the pseudocyclic conditions imposed. On the subsequent addition of either DBMIB (15μM), HQNO (0.2mM) or o-phenanthroline (2mM), Figs. 7.1(b)-(d), only the generation of phase b is in-

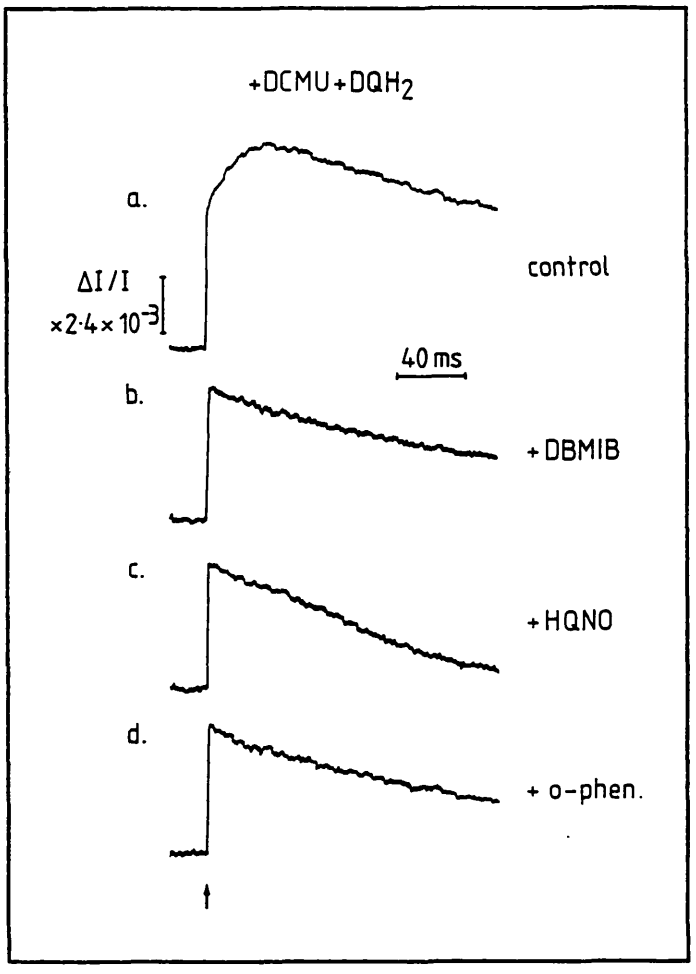


Fig. 7.1. The effect of inhibitors on the flash-induced ΔA_{515}, for stacked thylakoid membranes. Conditions are as described in section 2.2.2 for pseudocyclic electron flow, with DQH_2 (0.5mM) as reductant. (a) control, with no further additions; (b) as (a) + 15μM DBMIB; (c) as (a) + 0.2mM HQNO; (d) as (a) + 2mM o-phenanthroline (o-phen.).

hibited; the extent of phase a remains unaltered. To be noted is that, at the particular inhibitor concentrations used, uncoupling artefacts are small. The underlying mechanism by which phase b is suppressed by these various inhibitors, is different in each case due to their different sites of action: this is investigated more fully in the next section.

The effect of UHDBT or antimycin, however, appears to be twofold. Apart from their known inhibitory action on electron transfer reactions (see section 1.3.3), they also cause uncoupling, see Figs. 7.2 and 7.3. Furthermore, in the presence of UHDBT, at concentrations that do not totally inhibit phase b, a delayed slow phase is observed, Fig. 7.2. Such a delayed effect is not so apparent with antimycin at similarly low concentrations, Fig. 7.3. In the presence of DBMIB, it can be clearly observed, in Figs. 7.2 and 7.3, that the rate of decay of the ΔA_{515} is enhanced as the concentration of UHDBT, or antimycin, is increased. Concomitantly, a decrease in both the extent of phase a and that of phase b is observed. The decrease in the extent of phase a is probably due to the uncoupling effect masking its full amplitude, as described earlier in reference to Fig. 3.5(c); it is unlikely to be due to an inhibitory effect of UHDBT or antimycin on the electrogenic step in the PS1 reaction centre. It is noted that concentrations of UHDBT above 10μM apparently inhibit phase b, Fig. 7.2; in the case of antimycin, concentrations above 30μM are required, Fig. 7.3.

7.2 Inhibitor effects on cytochromes b-563 and f:

The control absorption changes of cytochromes b-563 and f are shown in Figs. 7.4(a) and 7.5(a), respectively: the conditions are

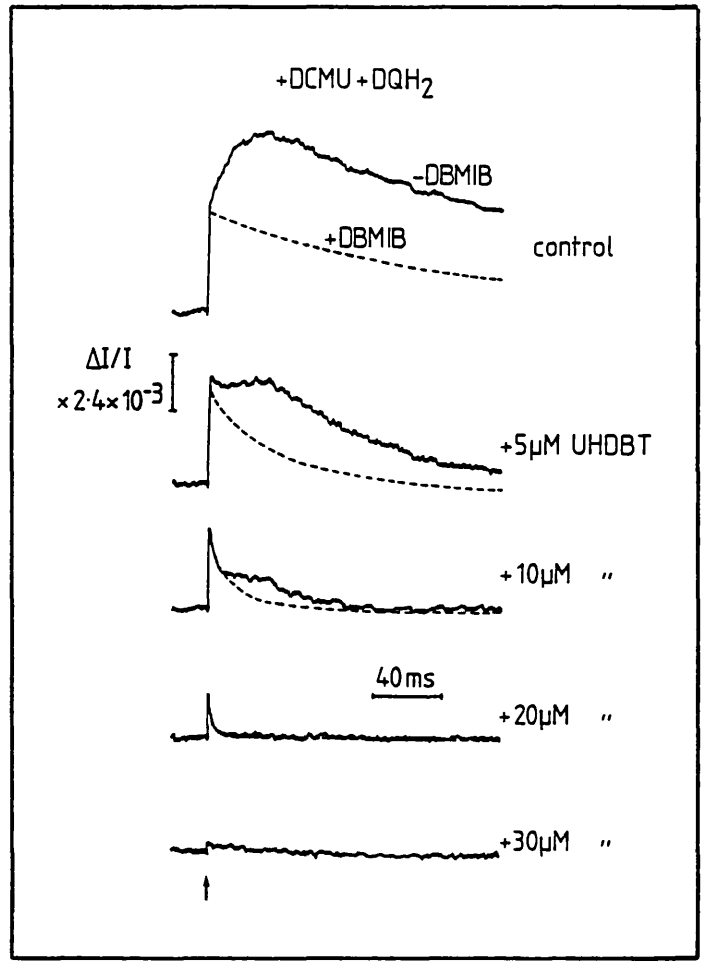


Fig. 7.2. The effect of increasing concentrations of UHDBT on the flash-induced ΔA_{515}. The control condition is as in Fig. 7.1(a), but in the absence (full line) or presence (broken line) of 15μM DBMIB.

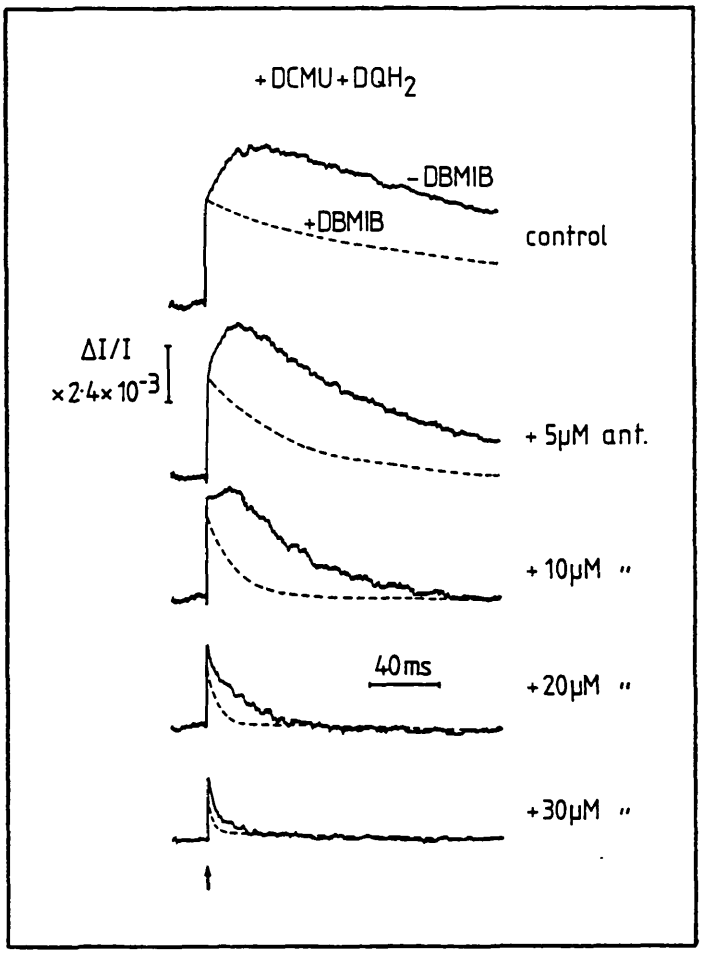


Fig. 7.3. The effect of increasing concentrations of antimycin (ant.) on the flash-induced ΔA_{515}. The control condition is as in Fig. 7.1(a), but in the absence (full line) or presence (broken line) of 15μM DBMIB.

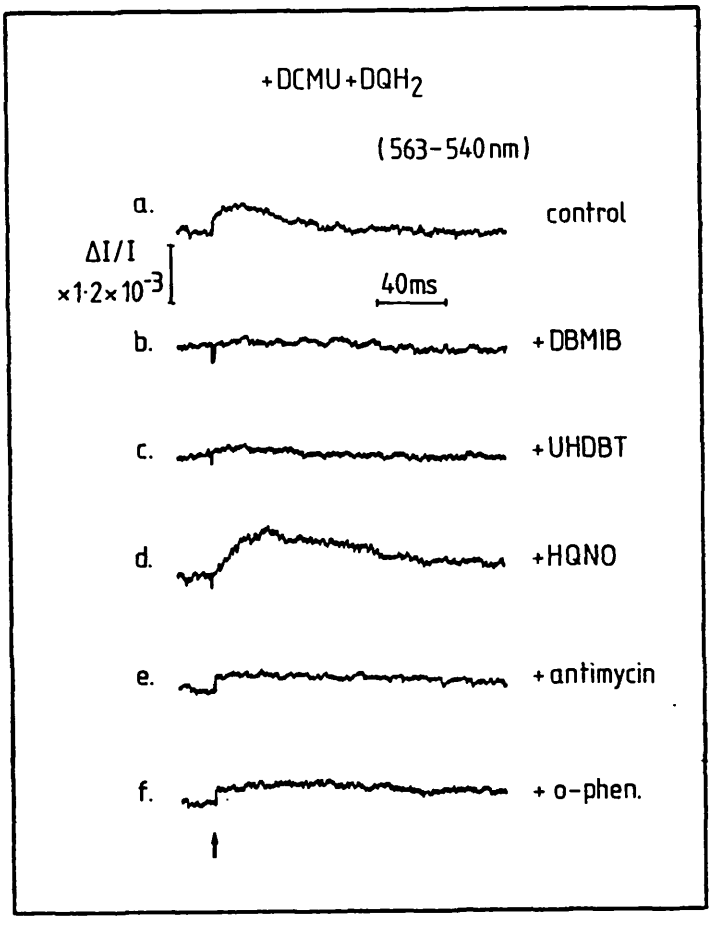


Fig. 7.4. The effect of inhibitors on the flash-induced absorption change of cytochrome b-563, as recorded at 563-540nm. Conditions are as in Fig. 7.1(a), but in the presence of valinomycin (2μM) and nigericin (2μM), see section 2.2.3. (a) control, with no further additions; (b) as (a) + 15μM DBMIB; (c) as (a) + 20μM UHDBT; (d) as (a) + 0.2mM HQNO; (e) as (a) + 40μM antimycin; (f) as (a) + 2mM o-phenanthroline.

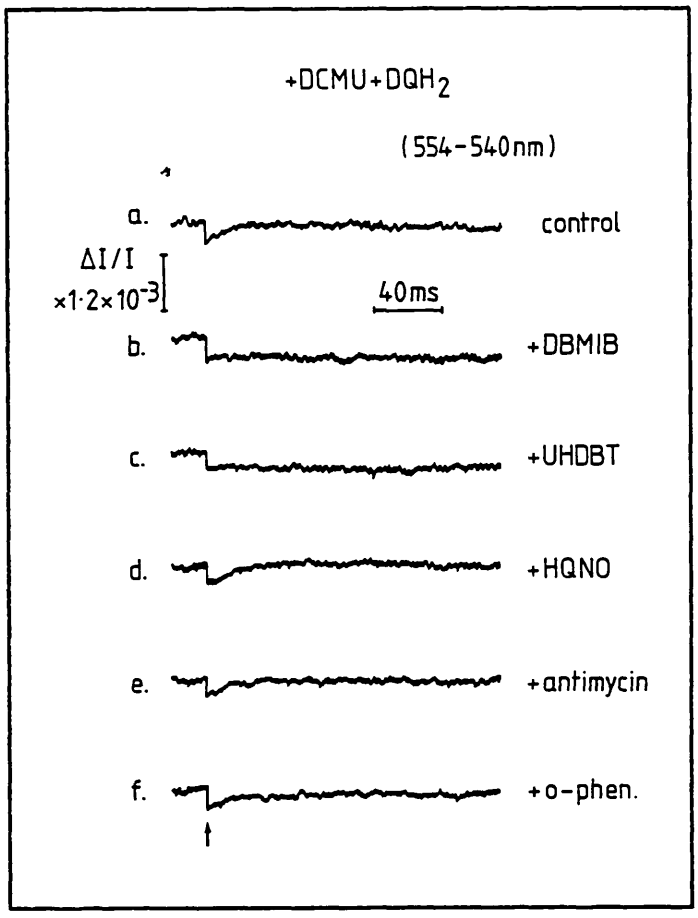


Fig. 7.5. The effect of inhibitors on the flash-induced absorption change of cytochrome f, as recorded at 554-540nm. The control condition in trace (a) is as in Fig. 7.4(a). The inhibitor concentrations are as in Fig. 7.4.

the same as those in Fig. 7.1(a). The kinetics are similar to those observed in Fig. 5.12(a): the kinetics of cytochrome b-563 reoxidation and those of cytochrome f rereduction match. A similar observation is made in bacterial chromatophores (Prince and Dutton, 1975; 1977). Both the flash-induced reduction of cytochrome b-563, Fig. 7.4(a), and the flash-induced oxidation of cytochrome f, Fig. 7.5(a), correspond to the turnover of approximately 1 molecule/4000 chlorophylls. It is noted again that all the inhibitors used in this section inhibit the generation of phase b at the concentrations employed, see section 7.1.

In the presence of DBMIB, both the flash-induced reduction, and the subsequent dark reoxidation, of cytochrome b-563 are inhibited, Fig. 7.4(b). In the case of cytochrome f, however, although its flash-induced oxidation is still observed, Fig. 7.5(b), and to the same extent as in the control, Fig. 7.5(a), its dark rereduction is very slow. Similar cytochrome absorption changes are observed in the presence of UHDBT, Figs. 7.4(c) and 7.5(c).

In the presence of HQNO, the extent of the flash-induced reduction of cytochrome b-563 is increased to twice that observed in the control, Fig. 7.4(a). Also,the rate of reduction is now apparently relatively slow, Fig. 7.4(d): it occurs with an approximate $t_{\frac{1}{2}}$ of 8ms, compared to that of 1ms in the control. The subsequent dark reoxidation of cytochrome b-563 is, however,inhibited. Cytochrome f, on the other hand, still undergoes the full extent of its flash-induced oxidation, Fig. 7.5(d), although its rereduction kinetics have slowed:

compare an approximate $t_{\frac{1}{2}}$ of 13ms in the presence of HQNO, Fig. 7.5(d), to that of 5ms in the control, Fig. 7.5(a). It would thus appear that, now, the rate of cytochrome b-563 reduction matches that of cytochrome f rereduction.

In the presence of antimycin, the cytochrome redox reactions are different to those expected: the antimycin site of inhibition is thought to be similar to that of HQNO (see section 1.3.3). The kinetics and extent of cytochrome b-563 flash-induced reduction, Fig. 7.4(e), are, instead, similar to those in the control, Fig. 7.4(a). Its dark reoxidation is, however, inhibited. The cytochrome f redox reactions are apparently unaltered in the presence of antimycin, compare Figs. 7.5(e) and 7.5(a).

In the presence of o-phenanthroline, the cytochrome absorption changes, Figs. 7.4(f) and 7.5(f), are similar to those observed in the presence of antimycin, Figs. 7.4(e) and 7.5(e).

7.3 Inhibitor effects on proton uptake/release:

Figs. 7.6 and 7.7 show the effect of certain inhibitors on proton uptake and proton release, respectively. The control traces, Figs. 7.6(a) and 7.7(a), are under the same electron transport conditions as in Fig. 7.1(a). The ΔA_{574} in Fig. 7.6(a) represents the uptake of 160pmoles of protons which, from Fig. 6.4, suggests that $2H^+$ are taken up, per flash, from the outer aqueous phase. The ΔA_{540} in Fig. 7.7(a) suggests that $2H^+$ are released, per flash, into the inner aqueous phase since its magnitude is similar to that observed in Fig. 6.8(b). A detailed analysis of proton uptake/release absorption changes is

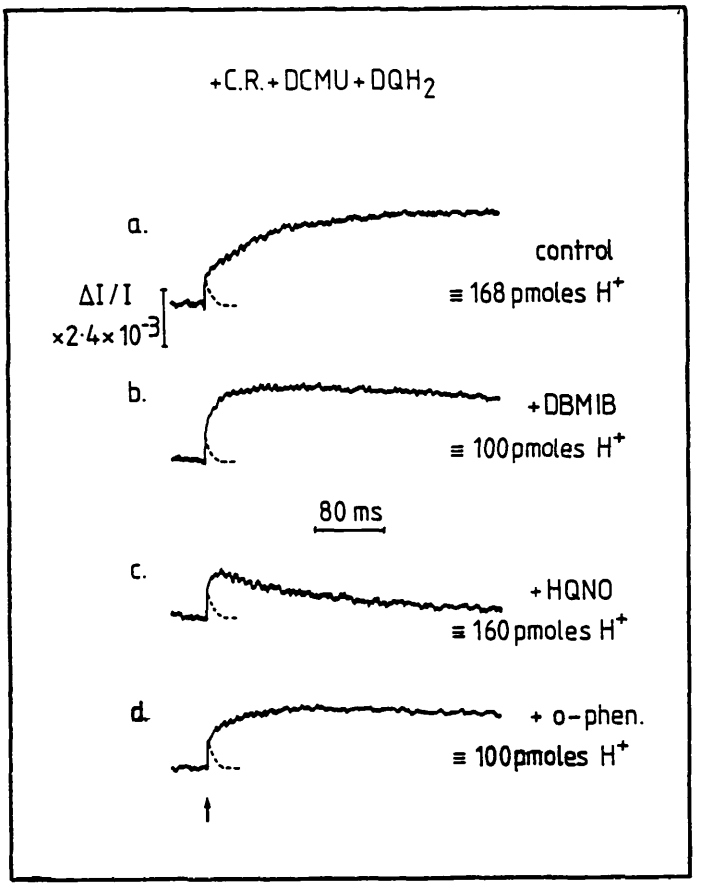


Fig. 7.6. The effect of inhibitors on the flash-induced proton uptake absorption changes, as recorded at 574nm. The sample was prepared as described in section 2.2.5, with stacked thylakoid membranes. The control condition in trace (a) is in the presence of 25μM DCMU + 0.5mM DQH_2. The inhibitor concentrations are as in Fig. 7.4. The calibrated extent of the ΔA, as determined by the method given in section 2.2.5, is also given. The dotted line in each trace represents the ΔA_{574} obtained upon the addition of 50mM tricine.

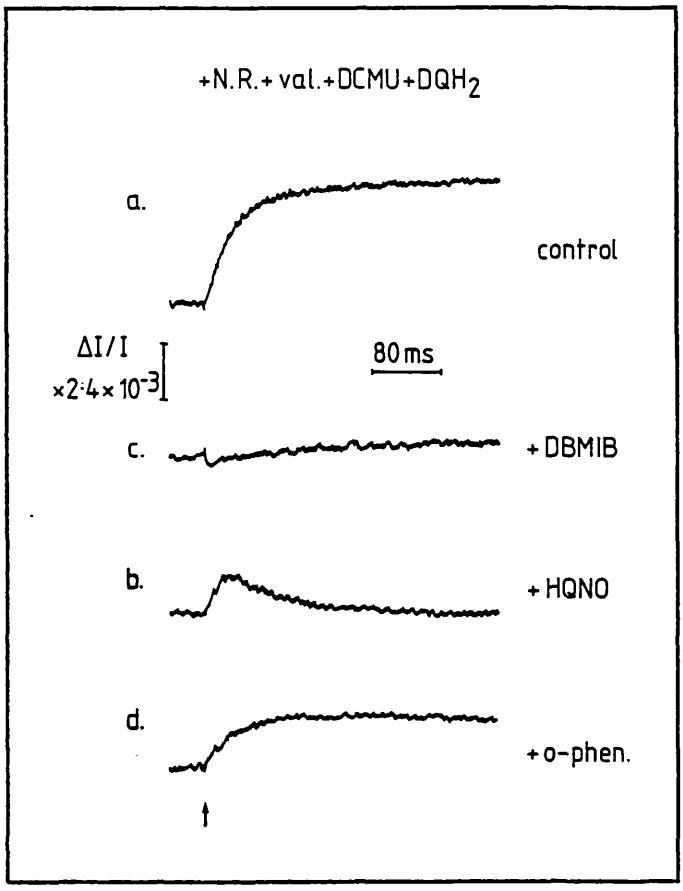


Fig. 7.7. The effect of inhibitors on the flash-induced proton release absorption change, as recorded at 540nm. The sample was prepared as described in section 2.2.6, with stacked thylakoid membranes. The control condition in trace (a) is in the presence of 25μM DCMU + 0.5mM DQH_2. The inhibitor concentrations are as in Fig. 7.4.

given in sections 6.2 and 6.3. To be noted is that, the extents of the ΔA_{574} in Fig. 7.6 are not altered upon the subtraction of that ΔA_{574} in the presence of 50mM tricine (see dotted lines in Fig. 7.6). Furthermore, the rise kinetics are only altered minimally by this procedure. Similarly, the ΔA_{540} in Fig. 7.7 are abolished in the presence of the permeating buffer imidazole, as previously shown in Fig. 6.6(b).

In the presence of DBMIB, proton uptake occurs, Fig. 7.6(b). The actual concentration of protons taken up is over half that in the control, Fig. 7.6(a); this suggests that at least $1H^+$ is taken up per flash. The rate of proton uptake is faster than in the control, although the rates of dissipation are similar. No proton release is observed in the presence of DBMIB, Fig. 7.7(b).

In the presence of HQNO, proton uptake also occurs, Fig. 7.6(c). Although the actual extent of the ΔA_{574} is smaller than the control, Fig. 7.6(a), its calibration yields the same number of protons. The kinetics of proton uptake are rapid, as in the presence of DBMIB, Fig. 7.6(b); furthermore, the dissipation of the ΔA_{574} is rapid. Fig. 7.7(c) indicates that proton release also occurs in the presence of HQNO. Assuming that the extent of the ΔA_{540} in Fig. 7.7(c) can be compared directly with that in the control, Fig. 7.7(a), this suggests that less than $1H^+$ is released. The rate of proton release is similar to that of the control, occurring with an approximate $t_{\frac{1}{2}}$ of 10ms; the dissipation of the ΔA_{540} is, instead, now rapid.

In the presence of o-phenanthroline, proton uptake again occurs, Fig. 7.6(d). Its calibrated extent is similar to that in the presence of DBMIB, Fig. 7.6(b): it is approximately half that of the control, i.e. $1H^+$ is taken up. The kinetics of proton uptake are similar to

the control, Fig. 7.6(a), as are the kinetics for the dissipation of the ΔA_{574}. Proton release is also observed to occur in the presence of o-phenanthroline, Fig. 7.7(d): its extent would suggest that only $1H^+$ is released per flash. The kinetics of proton release are slow, occurring with an approximate $t_{\frac{1}{2}}$ of 30ms; the dissipation kinetics of the ΔA_{540} are similar to those of the control.

7.4 Discussion:

The compounds used in this study all inhibit the generation of phase b. The mechanism of inhibition is, however, different for each class of inhibitor; this can be deduced from the related cytochrome and proton uptake/release absorption changes. A full analysis of these results, as is given below, would appear to favour the generation of a slow electrogenic phase coupled to a Q-cycle type mechanism.

DBMIB is a well known inhibitor of the Rieske FeS centre (see section 1.3.3); its resultant effect is to prevent the oxidation of PQH_2. The inhibition of phase b, by DBMIB, Fig. 7.1(b), thus suggests that PQH_2 oxidation is involved in the generation of phase b. This would compare with the result presented in Fig. 4.7(a) which shows that the generation of phase b correlates with the chemical reduction of a component, probably the PQ pool, with an $E_{m,7.5}$ of + 100mV.

The cytochrome absorption changes, observed in the presence of DBMIB, Figs. 7.4(b) and 7.5(b), are most easily explained by a Q-cycle type mechanism. The blocking of PQH_2 oxidation, by DBMIB, prevents the photo-reduction of cytochrome b-563; its subsequent reoxidation will thus also be inhibited, as observed in Fig. 7.4(b). Cytochrome f, however, is pre-reduced in the dark, and hence it will undergo a flash-induced oxidation, Fig. 7.5(b) . Its rereduction,

however, should be inhibited, since its supply of electrons from PQH_2 is blocked in the presence of DBMIB. Instead, a slow dark re-reduction is observed: the time lag between actinic flashes is long enough to allow the rereduction of cytochrome f by the added reducing agent, DQH_2. If a simple linear electron transport scheme were to operate, (see section 5.6), then the flash-induced reduction of cytochrome b-563 would be observed, in the presence of DBMIB, but its subsequent oxidation would be inhibited. From the cytochrome absorption changes observed in Figs. 7.4(b) and 7.5(b), three possible sites for the generation of a slow electrogenic phase can be envisaged: the reduction of cytochrome b-563, the reoxidation of cytochrome b-563 or the rereduction of cytochrome f. A clearer distinction between these possible sites is made later.

The proton uptake/release measurements in the presence of DBMIB, Figs. 7.6(b) and 7.7(b), are surprising. As might be expected, if PQH_2 oxidation is inhibited, as it is in the presence of DBMIB, proton release will not occur; this is indeed observed in Fig. 7.7(b). However, following the same argument, the uptake of protons might also be expected to be inhibited. Instead, at least $1H^+$ per flash is taken up, Fig. 7.6(b). One possible explanation is that under these particular conditions, cyclic electron flow is associated with the uptake of $1H^+$: PS1 can still turnover in the presence of DBMIB (phase a is still observed under these conditions, see Fig. 3.1(b)) and no PS1 electron acceptors are present.

UHDBT is thought to act at the same site as DBMIB (see section 1.3.3), namely at the Rieske FeS centre. The inhibition of phase b, in the presence of UHDBT is, however, not as obvious as in the pre-

sence of DBMIB: uncoupling artefacts are now quite prominent, Fig. 7.2. This thus poses the possibility that the inhibition of phase b is only an apparent effect: a similar inhibition of phase b is observed in the presence of the uncoupler valinomycin, Fig. 3.5(d). However, the cytochrome absorption changes observed in the presence of UHDBT, Figs. 7.4(c) and 7.5(c), are similar to those observed in the presence of DBMIB. This thus suggests that UHDBT and DBMIB do have a similar site of inhibition, and hence that the inhibitory effect of UHDBT on phase b is not just caused by an increased relaxation rate in the decay. To be noted, the delayed phase b observed in Fig. 7.2 is similar to that in Fig. 5.7(b).

HQNO inhibits the oxidation of the high potential cytochrome b-563 (see section 1.3.3). The inhibition of phase b, in the presence of HQNO, thus suggests the involvement of cytochrome b-563 in the generation of phase b. A similar suggestion has already been put forward in chapters 4 and 5. The cytochrome absorption changes presented in Figs. 7.4(d) and 7.5(d) support the proposed HQNO site of inhibition. In the presence of HQNO, the full extent of cytochrome b-563 flash-induced reduction is observed while its dark reoxidation is slow, Fig. 7.4(d). This indicates that HQNO only inhibits the oxidation of cytochrome b-563 and not its reduction. In this way, the true kinetics of the flash-induced reduction of cytochrome b-563 are revealed. To be noted is that the small extent of cytochrome b-563 turnover observed in the control, Fig. 7.4(a), can be most simply accounted for by the competing reduction and reoxidation reactions.

The observed flash-induced reduction of cytochrome b-563 in Fig. 7.4(d) indicates that PQH_2 oxidation still occurs in the presence of HQNO. For a Q-type cycle it can be postulated that, apart from the expected flash-induced oxidation of cytochrome f, its dark

rereduction will also occur. This is, in fact, observed in Fig. 7.5(d). Such an effect would not be expected for a simple linear electron transport scheme. The kinetics of cytochrome f dark rereduction are, however, slightly slower than those in the control, Fig. 7.5(a): it is likely that the rereduction rate of the Rieske FeS centre, and hence that of cytochrome f, is slowed, in the presence of HQNO, due to cytochrome b-563 remaining in the reduced state. To be noted, though, is that the kinetics of the flash-induced reduction of cytochrome b-563 and those of the dark rereduction of cytochrome f now match, thus favouring a Q-type cycle.

Since neither the reduction of cytochrome b-563, nor the rereduction of cytochrome f are inhibited (totally) in the presence of HQNO, they can be eliminated as possible sites for the generation of phase b, as suggested earlier in view of the DBMIB results. It is, however, possible to correlate the reoxidation of (the high potential) cytochrome b-563 with the generation of phase b.

Since both PQ reduction and PQH_2 oxidation are still able to occur in the presence of HQNO, it is expected that proton uptake and proton release also occur uninhibited. The calibrated extent of the ΔA_{574} in Fig. 7.6(c) suggests that proton uptake does indeed occur maximally, with $2H^+$ being taken up per flash. However the extent of the ΔA_{540} in Fig. 7.7(c) would suggest that only $1H^+$ is released by PQH_2 oxidation. These results are difficult to reconcile with a Q-cycle type scheme. It is, however, worthwhile noting that while the rate of proton release is slow, Fig. 7.7(c), the rate of dissipation of the ΔA_{540} is fast: this could mask the true extent of proton release.

Furthermore, in the case of the measurement of proton uptake, Fig. 7.6(c), it is observed that, although the extent of the ΔA_{574}, in the presence of HQNO, is approximately half that of the control, Fig. 7.6(a), its calibration yields the same proton concentration. This suggests that HQNO has altered the buffering capacity of the suspension. A similar effect could be induced, by HQNO, in the presence of neutral red. A direct calibration, in terms of extent, and hence number of protons released, between the ΔA_{540} in the presence of HQNO, Fig. 7.7(c), and that of the control, Fig. 7.7(a), could not, therefore be made.

Antimycin is thought to act at the same site of inhibition as HQNO. Like UHDBT, however, antimycin causes uncoupling, Fig. 7.3: this is manifested by the increased rate of decay of the ΔA_{515}. The effectiveness of antimycin to inhibit phase b is thus not as obvious as with HQNO. Furthermore the cytochrome b-563 absorption changes in the presence of antimycin are different, compare Figs. 7.4(e) and (d). The full extent of the flash-induced reduction of cytochrome b-563 is not observed, Fig. 7.4(e), as in the presence of HQNO, Fig. 7.4(d), although the inhibition of its dark reoxidation is still apparent. This observation could be taken as evidence for an alternative antimycin inhibition site. Possibly, antimycin inhibits the oxidation of the low potential b-type cytochrome, b_l in Fig. 1.6, rather than the high potential form, as would be expected. The inhibition of the reoxidation of b_l would thus inhibit the reduction and subsequent oxidation of b_h; hence the inhibition of phase b. This interpretation, however, may be complicated by the slow reoxidation kinetics of cytochrome b-563, as observed in the presence of antimycin. Such an effect could mask the full extent of the flash-induced reduction of cytochrome b-563. In bacterial chromatophores, antimycin does act like HQNO in inhibiting the oxidation of b_h (Hauska *et al*, 1983). The cytochrome

f flash-induced absorption changes, in the presence of antimycin, support the idea that antimycin only inhibits certain redox reactions of a component involved in a Q-type cycle: the cytochrome f redox reactions are observed to be unaffected, compare Figs. 7.5(e) and (a). A linear electron transport scheme can be ruled out following the earlier discussion concerning HQNO.

O-phenanthroline is thought to act at the same site of inhibition as DCMU, by competing for the Q_B binding site (see section 1.3.1). The inhibition of phase b, in the presence of o-phenanthroline, Fig. 7.1(d), is thus surprising. To be noted, is that the addition of DCMU leaves the extent of phase b unaffected, Fig. 5.1(d). The cytochrome absorption changes in the presence of o-phenanthroline, Figs. 7.4(f) and 7.5(f), are,however, very similar to those observed in the presence of antimycin, Figs. 7.4(e) and 7.5(e). This thus suggests that o-phenanthroline has a secondary site of inhibition which is within the cytochrome b_6/f complex and which is similar to that of antimycin. Namely, it inhibits the oxidation of one of the b-type cytochromes. The inhibition of phase b, by o-phenanthroline, would thus be expected in view of the earlier observations. In accordance with this predicted site of inhibition, both proton uptake and proton release are observed in Figs. 7.6(d) and 7.7(d), although only $1H^+$ is taken up or released per flash. This could indicate that, in the presence of o-phenanthroline, electron transport is slow.

To summarize, these inhibitor studies would confirm the earlier suggestions that the generation of phase b is associated with the oxidation of cytochrome b-563, and more specifically, to its high potential form. Furthermore, they indicate that this cytochrome is involved in a Q-cycle type scheme. These results also suggest possible alternative sites of inhibition for antimycin and o-phenanthroline.

CHAPTER 8

Summary and final discussion

The aim of this study has been an attempt to resolve the controversy concerning the mechanism by which the slow phase (phase b) of the flash-induced 515nm electrochromic shift is generated in chloroplasts. In this chapter, the main conclusions drawn from chapters 3,4,5,6 and 7 are summarized and interrelated. The relevance of these conclusions are discussed in terms of the current ideas on the mechanism of electron transport in the cytochrome b containing enzyme complexes.

Physical features of phase b:

The observation that phase b represents an electrical phenomenon has been well established in the literature (Velthuys, 1981; Crowther and Hind, 1980; Olsen and Barber, 1981). The results presented in chapter 3 would also appear to be in agreement with such a conclusion.

A slow "electrogenic"step has indeed been predicted both in Mitchell's Q-cycle and Wikström's b-cycle (see section 1.3.2). In the former model it is the outward movement of an electron, subsequent to that due to primary charge separation, that would generate a transmembrane potential; in the latter model it would be the inward translocation of a proton. Such an electrical event, as recorded by the electrochromically-sensitive carotenoid pigments, might be expected to exhibit a magnitude similar in extent to that of phase a due to PS1 alone, if the membrane is of uniform capacitance: both these processes represent the movement of a single charge across the membrane dielectric (albeit on different timescales). Olsen and Barber (1981) have in fact made such a correlation.

The ratio of the extent of phase a (with only PS1 active) to that of phase b, as resolved by a procedure similar to that depicted in Fig. 3.1, was found to be close to 1:1. The results presented in Fig. 3.1 are in agreement with this observation. However, in view of this, and of other experimental data, alternative interpretations for the generation of phase b have also been put forward (Olsen and Barber, 1981; Zimanyi and Garab, 1982): these only indirectly relate phase b to electron transport. To be noted, the above ratio of 1:1 for the extent of phase a (due to PS1 alone) to that of phase b, is only obtained under "optimal" conditions (e.g. as in Fig. 3.1); the observed extent of phase b is highly dependent on the membrane conductivity, see Fig. 3.5(d), and on the ambient redox potential (see chapter 4 and below).

The role of plastoquinol:

The requirement of particular reducing conditions to observe phase b is already evident from the work of a number of different groups. Either a chemical reductant is required (Bouges-Bocquet, 1977; Crowther et al, 1979; Olsen et al, 1980; also see Fig. 3.3) or specific pre-illumination with PS2 light is required (Velthuys, 1978). Crowther and Hind (1980) suggest that the chemical reduction of a component with an $E_{m,8.1}$ of -55mV is required to observe phase b. Bouges-Bocquet (1981b) has gone further to suggest that it is the reduction of a special quinone species that is required. Also, Bouges-Bocquet (1981b) observes that highly oxidizing or highly reducing conditions inhibit the generation of phase b.

The redox titration presented in Fig. 4.7(a) defines more clearly the above ambient redox potential dependence of phase b. At potentials

more positive than +150mV, phase b is either very small or not observable at all. As the potential is lowered, the extent of phase b increases such that it titrates in with an $E_{m,7.5}$ that matches that of the PQ pool (see section 4.4). A further decrease in the ambient potential and the extent of phase b decreases with an $E_{m,7.5}$ of -75mV. This latter midpoint potential would correspond to that for the chemical reduction of the high potential cytochrome b-563 located within the cytochrome b_6/f complex (Hauska et al, 1983).

Girvin and Cramer (1983) have also recently carried out redox titrations of the extent of phase b. Although they would agree that the appearance of phase b requires the chemical reduction of the PQ pool, they instead observe the full extent of phase b at potentials as low as -200mV. At these low redox potentials, cytochrome b-563 is fully reduced. Girvin and Cramer (1983) thus suggest that it is the rereduction of the flash-oxidized Rieske FeS centre, by PQH_2, which could be linked to a proton pump, that is responsible for the formation of phase b. In accordance with such a conclusion, is the earlier observation made by Bouges-Bocquet (1980b) that , in intact Chlorella cells, phase b correlates with the absorbance changes of an unknown carrier, probably an FeS centre, but not the Rieske FeS cluster. The above suggestion of Girvin and Cramer (1983) would implicate the operation of a b-cycle mechanism, see Fig. 1.6(b), in the electron transport chain. Despite an obvious discrepancy between the results presented in Fig. 4.7(a) and those of Girvin and Cramer (1983), concerning the component responsible for the generation of phase b, the results presented in chapters 5 and 7 (to be summarized below) provide a clear distinction.

Before proceeding further, however, it is worthwhile to note that, whereas originally it had been thought that cyclic electron flow was necessary to generate phase b (Crowther et al, 1979; Shahak et al, 1980), the redox titration presented in Fig. 4.7(b) shows that, in the presence of MV, a competitive electron acceptor for PS1, and under equilibrated conditions, the full extent of phase b can be titrated, as if in the absence of MV, Fig. 4.7(a). Selak and Whitmarsh (1982) have, in fact, recently shown that the full extent of phase b is observed in the presence of DQH_2 and MV (and in the absence of any redox mediators). Furthermore, the result presented in Fig. 5.11(a) is also in agreement with this. It is therefore apparent that cyclic electron flow is not an absolute requirement for the generation of phase b; a more stringent requirement is that of reduced PQ, Fig. 4.7.

Correlation of phase b with electron transport:

The spectroscopic measurements of the slow phase of the electrochromic effect and of the redox kinetics of cytochromes b-563 and f, under pseudocyclic conditions, presented in chapter 5, are not enough in themselves to predict which component is responsible for the generation of phase b and by what mechanism. The cytochrome absorption changes obtained in the presence of dithionite, Fig. 5.7(a), or DQH_2, Fig. 5.12(a), would implicate the rereduction of cytochrome f with the generation of phase b, on the basis of the similarity in kinetics. Such a correlation has previously been suggested by Crowther and Hind (1980). Also, the results presented here could be interpreted in terms of a simple linear electron transport scheme (see section 5.6). On the other hand, in the presence of Fd/NADPH, Fig. 5.9(a), the reoxidation kinetics of cytochrome b-563 would match more closely those for the generation of phase b. Furthermore, a Q-type cycle (as defined in section 1.7) would now be more appropriate. To clarify

this apparent discrepancy, both the effect of salt and the appearance of a delayed phase b, under certain conditions, have been analysed.

Changes in salt concentration alter both the extent of phase b and that of cytochrome b-563 reoxidation (see chapter 5); the kinetics and extent of the redox reactions of cytochrome f remain unaltered. Olsen and Barber (1981) have observed a similar effect of salt on the extent of phase b and have suggested a delocalization model for its generation. However, such a model could not explain the concomitant salt effect on the extent of cytochrome b-563 reoxidation. Possible explanations for this salt effect have been put forward in section 5.6. Briefly, although changes in salt concentration alter the spatial separation of the complexes within the thylakoid membrane (see sections 1.2.2 and 1.2.3), an alternative property might more appropriately explain the effect of salt on the extents of phase a, phase b and cytochrome b-563 oxidation, as observed in chapters 4 and 5.

A delay in the generation of phase b can be observed when strongly reducing reductants, under anaerobic conditions, are used in the presence of MV. The observed cytochrome absorption changes, together with the effect of salt, seem to suggest that the generation of phase b is closely related to the oxidation of cytochrome b-563, where cytochrome b-563 is involved in a Q-type cycle. This suggestion would be in accordance with the observation made earlier, from the redox titrations, Fig. 4.7, that the chemical reduction of the high potential cytochrome b-563 is responsible for the inhibition of phase b. To be noted, such a delayed phase b has not been previously reported in the literature. Furthermore, in the presence of DQH_2 and MV, no delay in the generation of phase b is induced, Fig. 5.11(a): anaerobic conditions are not necessary for this reductant.

Correlation of phase b with proton translocation:

Protons also appear to be involved in the generation of phase b. Farineau et al (1980) have observed that the kinetics of both the rise and decay of phase b are decelerated by the replacement of H_2^1O by H_2^2O. In this study, it has been shown that an increase in the concentration of protons results in a decrease in the extent of the delay in the delayed phase b and of that in the reoxidation of cytochrome b-563, under similar conditions, see Fig. 5.10. The magnitude of phase b is diminished at high pH values, Fig. 6.1, and the redox reactions of cytochrome b-563 exhibit a similar pH dependency, Fig. 6.2.

From the proton uptake/release measurements presented in chapter 6, the kinetics for the generation of phase b appear to correlate more directly with those for proton uptake than for proton release. The proton uptake results suggest that $2H^+$ are taken up per flash, at pH 7.3, Fig. 6.4. However, there is the paradox that at higher pH values, where only $1H^+$ is taken up, a maximal extent of phase b is still observed: this result is difficult to reconcile with any Q-cycle type mechanism. Such an observation, however, could indicate that one proton is specifically necessary for the generation of phase b, in a manner analogous to the bacterial system, where one of the protons taken up is antimycin-sensitive, while the second is antimycin-insensitive (Petty et al, 1979; also see Fig. 1.10). If this were the case, it could thus be envisaged that, under conditions when a delayed phase b is observed, the uptake of this proton is also delayed. To be noted, though, at very high pH values a large phase b is still observed, although no proton uptake occurs. This has also been observed in bacterial chromatophores (Petty et al, 1979) and is a further

paradox in terms of a Q-cycle type mechanism.

For proton release, and in the presence of Fd/NADPH, Fig. 6.7, the kinetics match more closely those for cytochrome f rereduction than for phase b generation. Also, under conditions where a delayed phase b is apparent, no delayed proton release is observed. In the presence of DQH_2, Fig. 6.8, the kinetics of proton release and cytochrome f rereduction again match, but they are now slow. In the literature, however, it has been suggested that it is, in fact, proton release due to PQH_2 oxidation that is responsible for the generation of phase b (Olsen and Barber, 1981; Zimanyi and Garab, 1982). The models that are subsequently proposed, however, cannot be reconciled with the observation made here, that the number of protons released by PQH_2, per flash, appears to be redox dependent: in the presence of Fd/NADPH only $1H^+$ appears to be released, while in the presence of DQH_2, $2H^+$ appear to be released. Such an observation could be described in terms of a redox dependence similar to that found for the generation of phase b, Fig. 4.7, although from this study, proton release only appears to be indirectly involved with phase b. To be noted, though, the extent of phase b in the presence of Fd/NADPH is not diminished by the same amount that the extent of proton release is, when compared to that in the presence of DQH_2.

Such a redox dependent proton release has also been observed by Crowther and Hind (1982). Using increasing concentrations of ferricyanide, they found that under non-oxidizing conditions (i.e. in the absence of ferricyanide) approximately $2H^+$ were released by PQH_2 per flash, while under mildly oxidizing conditions this value fell to $1H^+$. Although these results cannot be directly compared to those presented in chapter 6, it must be noted that, in their study, Crowther and Hind (1982) did not estimate the effect of ferricyanide on P700: increasing concentrations of ferricyanide chemically oxidize P700 and

hence the concentration of photo-oxidized P700 also decreases. Their computed changes in H^+/e^- ratios might therefore be incorrect.

The action of inhibitors within the cytochrome b_6/f complex:

The results discussed so far seem to point to a correlation between the generation of phase b and the oxidation of cytochrome b-563, where the underlying mechanism is possibly a Q-type cycle. The inhibitor studies presented in chapter 7, to be discussed briefly below, lend further support for such a conclusion.

The inhibition of phase b in the presence of DBMIB or UHDBT indicates the involvement of PQH_2 oxidation. Also inhibited are the redox reactions of cytochrome b-563 and the rereduction of cytochrome f. These results thus implicate a Q-cycle type mechanism for the reduction of cytochrome b-563.

HQNO, antimycin and o-phenanthroline also inhibit the generation of phase b, as well as the reoxidation of cytochrome b-563; they hardly affect the rereduction kinetics of cytochrome f. The consequence of these results is that cytochrome f cannot be directly implicated in the generation of phase b, as suggested by Crowther and Hind (1980). Furthermore, these results would contradict the model proposed by Girvin and Cramer (1983) in which the formation of phase b is related to the rereduction of the Rieske FeS centre. If the redox reactions of cytochrome f are unaffected in the presence of these particular inhibitors, then PQH_2 oxidation must still occur (although the actual number of protons released may be altered) and hence the Rieske FeS centre must also be able to turnover. By a similar argument, the classical b-cycle model depicted in Fig. 1.6(b), and implicated by Girvin and Cramer (1983) in the formation of phase b, can be ruled out. However, this is not

to say that protons are not closely involved in the generation of phase b, as has been discussed above.

In the presence of HQNO, apart from the inhibition of phase b, the extent of cytochrome b-563 flash-induced reduction is enhanced 2-fold, while its reoxidation is inhibited, Figs.7.1 and 7.4. This observation implicates the reoxidation of the high potential cytochrome b-563 in the generation of phase b. Since the kinetics of cytochrome b-563 reduction and cytochrome f rereduction, now match quite closely, this is further evidence for a Q-cycle type mechanism in operation. Similar observations, in the presence of HQNO, have also recently been made by Selak and Whitmarsh (1982).

The effect of inhibitors on proton uptake/release are also shown in chapter 7. For the particular conditions used here (in the absence of inhibitors) the uptake of $2H^+$ and the release of $2H^+$, per flash, has been calculated (see chapter 6). In the presence of o-phenanthroline, only $1H^+$ is taken up and $1H^+$ is released. In accordance with an earlier suggestion made in this discussion, the inhibited proton taken up could be implicated in close association with the reduction of PQ by the oxidation of the high potential cytochrome b-563, via a Q-cycle mechanism, as is observed in bacterial chromatophores (Petty et al, 1979; also see Fig. 1.10). However, the observation that $2H^+$ are still taken up in the presence of HQNO, is inconsistent with the above suggestion. Finally, the particular effect of HQNO and o-phenanthroline on the generation of phase b and on proton uptake/release, provides further evidence against the models proposed by Olsen and Barber (1981) and Zimanyi and Garab (1982): proton release still occurs due to PQH_2 oxidation, albeit with the inhibition of phase b.

A possible mechanism for the plastoquinol-plastocyanin oxidoreductase in chloroplasts:

The results presented in this thesis appear to suggest that the oxidation of the high potential cytochrome b-563 is responsible for a secondary electrogenic step, as manifested by the generation of a slow phase in the 515nm electrochromic absorption change. A modified Q-cycle, depicted in Fig. 8.1, is proposed to account for the observed electron transfer reactions. The involvement of protons in the formation of phase b, as is evident from this study, is through the redox reactions of PQ, the dark reduction of which is required to observe phase b. The implication of these results, as summarized in the model of Fig. 8.1, is that the cytochrome b_6/f complex acts as an electrogenic translocator, closely coupled to a proton pump. Evidence along these lines has, in fact, already been presented for the isolated cytochrome b_6/f complex reconstituted into phospholipid vesicles (Hurt et al, 1982).

The mechanism of electron transport, as depicted in Fig. 8.1, can be described as follows. There is a plastosemiquinone-generating site located at the inner side of the thylakoid membrane, as well as quinol/quinone binding sites located at the inner and outer sides of the membrane, Q_i and Q_o, respectively. Once plastoquinol oxidation has occurred at the Q_i site, the electron is transferred serially, through the two b-cytochromes, to the Q_o site. Full reduction of the quinone to quinol at this latter site, however, can only occur once two electrons have been stored. One electron will be provided by cytochrome b-563 (located within the cytochrome b_6/f complex). The second electron can be provided either by cyclic electron flow around PS1, an endogenous reductant or by a second turnover of the cytochrome b_6/f complex. The eventual reduction of quinone to quinol at the Q_o site is accompanied

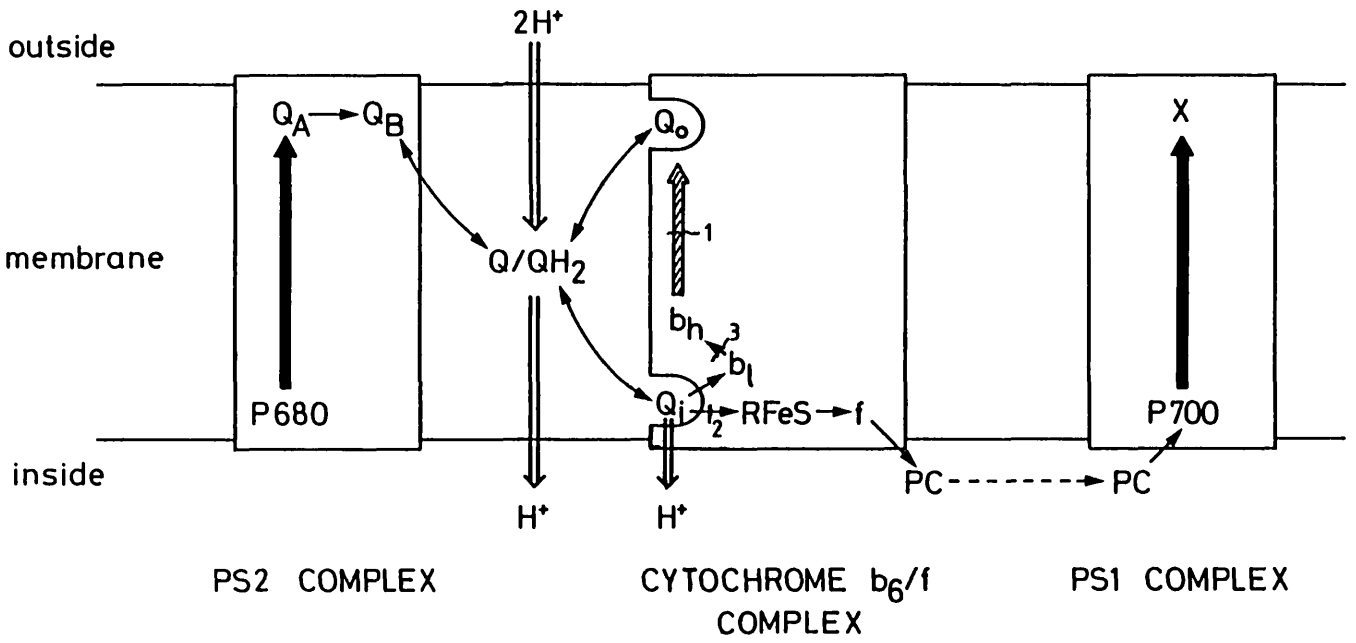


Fig. 8.1. A modified Q-cycle proposed to account for most of the data presented in this thesis. Electrogenic reactions are indicated by wide arrows (filled arrows for the most rapid photochemical steps; shaded arrows for slower electron transfer steps). Other symbols as in Fig. 1.6. The proposed sites of inhibition are: HQNO at site 1; DBMIB, UHDBT at site 2; antimycin and o-phenanthroline at site 3.

by the uptake of $2H^+$. The number of protons translocated per electron arriving at P700 is thus 2:1. The electrogenic step is linked to the oxidation of the high potential cytochrome b-563, as indicated by the work presented in this thesis. Also shown in Fig. 8.1 are the various inhibitor sites, as proposed by this study. DBMIB and UHDBT inhibit the reduction of the Rieske FeS centre; HQNO inhibits the oxidation of the high potential cytochrome b-563; antimycin and o-phenanthroline inhibit the oxidation of the low potential cytochrome b-563.

A similar model to that depicted in Fig. 8.1, has recently been proposed by Selak and Whitmarsh (1982). A variation of this model had, however, been put forward earlier by Velthuys (1979). A feature of the Velthuys model is that the two b-cytochromes are arranged in parallel within the cytochrome b_6/f complex, rather than in series. The electrogenic step is thus suggested to be linked to the oxidation of only one of the b-cytochromes, but a clear distinction as to which one, is not made. Moreover, the recent detection of the different midpoint redox potentials of the cytochrome b-563 (see section 1.2.1) is difficult to incorporate into such a model which implicates two equivalent haems. Crofts et al (1983) have, in fact, recently put forward a model, based on that proposed by Velthuys (1979), but for the bacterial electron transport chain. In the Crofts' model (1983) the b-cytochromes are now, instead, placed in series. Furthermore, this model takes into account more recent experimental data concerning the role of the ubiquinone pool in the b-cytochrome redox reactions.

The similarity between the models that can be proposed for the mechanism of electron transport in chloroplasts and in bacterial chromatophores, as well as in mitochondria (see below), derives from

the universality that has been found for their respective quinol-cytochrome c oxidoreductases (Hauska et al,1983). These oxidoreductases have recently been purified and have been found to contain similar redox components and subunit topographical arrangement. Furthermore, these isolated complexes all exhibit the phenomenon of oxidant-induced reduction of cytochrome b and when reincorporated into lipid vesicles, function as electrogenic proton translocators. The most suitable models, to date, to explain the reaction mechanism of the different quinol-cytochrome c oxidoreductases are Mitchell's Q-cycle and Wikström's b-cycle (see section 1.3.2), although the work presented here, as well as other studies, would favour variants of the Q-cycle. The similarity in the models depicted in Fig. 8.1 and Fig. 1.10, for the chloroplast and bacterial oxidoreductases, respectively, emphasize the common function of the oxidoreductases. In fact, throughout this thesis, it has been possible to draw comparisons between the chloroplast and bacterial systems.

A universal Q-cycle model has recently been suggested by Slater (1983). This is the double Q-cycle as proposed by de Vries et al (1983) for the mitochondrial oxidoreductase. One of the main arguments in favour of the Q-cycle in the mitochondrial system is the detection, by EPR, of two anionic semiquinones, $Q^{\cdot -}$, one of which is destabilized by antimycin (Ohnishi and Trumpower, 1980; also see section 1.3.1). These signals, however, have not yet been detected in the chloroplast or bacterial oxidoreductases. Perhaps the presence of excessive quinones in these complexes, has made it difficult to detect the proposed $Q^{\cdot -}$ species. A second important argument for the operation of a double Q-cycle in mitochondria is the existence of two pathways for the reduction of cytochrome b. Again, this particular feature has not yet been demonstrated in the photosynthetic systems. However, it should be noted that, the models proposed by Velthuys

(1979) and Crofts et al (1983) are, in fact, along the lines of a double Q-cycle.

It is thus apparent that further experimental evidence is required to determine the ultimate model to describe the mechanism of the quinol-plastocyanin oxidoreductase in chloroplasts. It would be nice if the mechanism were that of a double Q-cycle, as suggested by Slater (1983). In fact the chloroplast (and the bacterial) system offers the experimental advantage, over the mitochondrial system, for the study of the single turnover kinetics of the reduction of electron-carrying centres: electrons can be brought into the system by the action of a light flash directed at the photochemical reaction centres. Although a great deal of work has already been carried out using such flash-induced spectroscopic studies, further work is required in this area, of an even more detailed nature, to understand fully the delicate mechanistic properties of the electron transport chain.

REFERENCES

Allen, J.F., Bennett, J., Steinback, K.E. and Arntzen, C.J. (1981) Chloroplast protein phosphorylation couples plastoquinone redox state to distribution of excitation energy between photosystems. Nature 291, 25-29.

Anderson, J.M. (1980) Chlorophyll-protein complexes of higher plant thylakoids: distribution stoichiometry and organization in the photosynthetic unit. FEBS Lett. 117, 327-331.

Anderson, J.M.(1982) The significance of grana stacking in chlorophyll b - containing chloroplasts. Photobiochem. Photobiophys. 3, 225-241.

Anderson, J.M. and Andersson, B.(1982) The architecture of photosynthetic membranes: lateral and transverse organizations. TIBS 7, 288-292.

Anderson, J.M. and Boardman, N.K. (1966) Fractionation of the photochemical systems of photosynthesis. I. Chlorophyll contents and photochemical activities of particles isolated from spinach chloroplasts. Biochim. Biophys. Acta 112, 403-421.

Andersson, B. (1978) Separation of spinach chloroplast lamellae fragments by phase partition including the isolation of inside-out thylakoids. Thesis, University of Lund, Sweden.

Andersson, B.and Anderson, J.M. (1980) Lateral heterogeneity in the distribution of chlorophyll-protein complexes of the thylakoid membranes of spinach chloroplasts. Biochim. Biophys. Acta 593, 427-440.

Andersson, B. and Haehnel, W. (1982) Location of photosystem I and photosystem II reaction centres in different thylakoid regions of stacked chloroplasts. FEBS Lett. 146, 13-17.

Andersson, B., Akerlund, H.-E. and Albertsson, P.-A. (1981) Isolation and studies on inside-out thylakoid vesicles. in: Proc. 5th Int. Congr. Photosynth. (Akoyunoglou, G., ed.), Vol. 3, pp 55-66, Balaban Int. Sci. Serv. , Philadelphia.

Andersson, B., Anderson, J.M. and Ryrie, I.J. (1982) Transbilayer organization of the chlorophyll-proteins of spinach thylakoids. Eur. J. Biochem. 123, 465-472.

Arnon, D.I. (1949) Copper enzymes in isolated chloroplasts.Polyphenoloxidase in Beta vulgaris. Plant Physiol. 24, 1-15.

Arnon, D.I. and Chain, R.K. (1975) Regulation of ferredoxin-catalysed photosynthetic phosphorylations. Proc. Natl. Acad.Sci. USA 72, 4961-4965.

Ausländer, W. and Junge, W. (1974) The electric generator in the photosynthesis of green plants. II Kinetic correlation between protolytic reactions and redox reactions. Biochim. Biophys. Acta 357, 285-298.

Ausländer, W. and Junge, W. (1975) Neutral red, a rapid indicator for pH-changes in the inner phase of thylakoids. FEBS Lett. 59, 310-315.

Baltscheffsky, M. (1974) The effect of dibromothymoquinone on light induced reactions in chromatophores from Rhodospirillum rubrum. in: Proc. 3rd Int. Congr. Photosynth., Rehovot, Israel (Avron, M., ed.), Vol. 1, pp 799-806, Elsevier/North Holland, Amsterdam.

Barber, J. (1980) An explanation for the relationship between salt-induced thylakoid stacking and the chlorophyll fluorescence changes associated with changes in spillover of energy from photosystem II to photosystem I. FEBS Lett. 118, 1-10.

Barber, J. (1982) Influence of surface charges on thylakoid structure and function. Ann. Rev. Plant Physiol. 33, 261-295.

Barber, J. (1983a) Photosynthetic electron transport in relation to thylakoid membrane composition and organization. Plant, Cell and Environ. 6, 311-322.

Barber, J. (1983b) Membrane conformational changes due to phosphorylation and the control of energy transfer in photosynthesis. Photobiochem. Photobiophys. 5, 181-190.

Bashford, C.L., Prince, R.C., Takamiya, K. and Dutton, P.L. (1979) Electrogenic events in the ubiquinone-cytochrome b/c_2 oxidoreductase of Rhodopseudomonas sphaeroides. Biochim. Biophys. Acta 545, 223-235.

Bendall, D.S. (1982) Photosynthetic cytochromes of oxygenic organisms. Biochim. Biophys. Acta 683, 119-151.

Bennett, J. (1977) Phosphorylation of chloroplast membrane polypeptides. Nature 269, 344-346.

Berthold, D.A., Babcock, G.T. and Yocum, C.F. (1982) A highly resolved, oxygen-evolving photosystem II preparation from spinach thylakoid membranes. FEBS Lett. 134, 231-234.

Binder, R.G. and Selman, B.R. (1980) Quinones as mediators of both artificial and cyclic phosphorylation in spinach chloroplasts. Biochim. Biophys. Acta 590, 212-222.

Boardman, N.K. (1970) Physical separation of the photosynthetic photochemical systems. Ann. Rev. Plant Physiol. 21, 115-140.

Böhme, H. (1977) On the role of ferredoxin and ferredoxin-$NADP^+$ reductase in cyclic electron transport of spinach chloroplasts. Eur. J. Biochem. 72, 283-289.

Böhme, H. and Cramer, W.A. (1972) The role of cytochrome b_6 in cyclic electron transport: evidence for an energy coupling site in the pathway of cytochrome b_6 oxidation in spinach chloroplasts. Biochim. Biophys. Acta 283, 302-315.

Bouges-Bocquet, B. (1973) Electron transfer between the two photosystems in spinach chloroplasts. Biochim. Biophys. Acta 314, 250-256.

Bouges-Bocquet, B. (1977) Cytochrome f and plastocyanin kinetics in Chlorella Pyrenoidosa. II Reduction kinetics and electric field increase in the 10msec range. Biochim. Biophys. Acta 462, 371-379.

Bouges-Bocquet, B. (1980a) Kinetic models for the electron donors of photosystem II of photosynthesis. Biochim. Biophys. Acta 594, 85-103.

Bouges-Bocquet, B.(1980b) Detection of a new protein involved in the electrogenic loop of green algae. FEBS Lett. 117, 54-58.

Bouges-Bocquet, B. (1981a) Recovery of the reactants of the slow electrogenic phase in Chlorella cells and organisation of the plastoquinone pool. in: Proc. 5th Intl. Photosynth. Congr. (Akoyunoglou, G., ed.), Vol. 2, pp 19-27, Balaban Int. Sci. Serv., Philadelphia.

Bouges-Bocquet, B. (1981b) Factors regulating the slow electrogenic phase in green algae and higher plants. Biochim. Biophys. Acta 635, 327-340.

Bouges-Bocquet, B. and Delosme, R. (1978) Evidence for a new electron donor to P-700 in Chlorella pyrenoidosa. FEBS Lett. 94, 100-104.

Bowes, J.M. and Crofts, A.R. (1981) Effect of 2,5-dibromo-3- methyl-6-isopropyl-p-benzoquinone on the secondary electron acceptor B of photosystem II. Arch. Biochem. Biophys. 209, 682-686.

Braumann, T., Weber, G. and Grimme, L.H. (1982) Carotenoid and chlorophyll composition of light-harvesting and reaction centre proteins of the thylakoid membrane. Photobiochem. Photobiophys. 4, 1-8.

Bulychev, A.A. and Vredenberg, W.J. (1976) The effect of cations and membrane permeability modifying agents on the dark kinetics of the photoelectric response in isolated chloroplasts. Biochim. Biophys. Acta 423, 548-556.

Butler, W.L. (1978) Energy distribution in the photochemical apparatus of photosynthesis. Ann. Rev. Plant Physiol. 29, 345-378.

Case, G.D. and Parson, W.W.(1973) Shifts in bacteriochlorophyll and carotenoid absorption bands linked to cytochrome c-555 photooxidation in Chromatium. Biochim. Biophys. Acta 325, 441-453.

Clark, W. M. (1960) "Oxidation-reduction potentials of organic systems". Waverly Press, Baltimore, Maryland.

Cogdell, R.J., Monger, T.G. and Parson,W.W. (1975) Carotenoid triplet states in reaction centres from Rhodopseudomonas sphaeroides and Rhodospirillum rubrum. Biochim. Biophys. Acta 408, 188-189.

Conjeaud, H., Michel-Villaz, M., Vermeglio, A. and Mathis, P. (1976) Location of field-sensitive carotenoid molecules in the chloroplast membrane. Arguments from low-temperature studies. FEBS Lett. 71, 138-141.

Coombs, J. and Greenwood, A.D. (1976) Compartmentation of the photosynthetic apparatus. in: Topics in Photosynthesis (Barber, J., ed.), Vol. 1, pp 1-51, Elsevier/North Holland, Amsterdam.

Cox, R.P.(1979) Chloroplast cytochrome b-563. Hydrophobic environment and lack of direct reaction with ferredoxin. Biochem. J. 184, 39-44.

Cox, R.P. and Andersson, B. (1981) Lateral and transverse organization of cytochromes in the chloroplast thylakoid membrane. Biochem. Biophys. Res. Comm. 103, 1336-1342.

Cramer, W.A. and Butler, W.L. (1967) Light-induced absorbance changes of two cytochrome b components in the electron transport system of spinach chloroplasts. Biochim. Biophys. Acta 143, 332-339.

Crofts, A.R., Prince, R.C., Holmes, N.G. and Crowther, D. (1974) Electrogenic electron transport and the carotenoid change in photosynthetic bacteria. in: Proc. 3rd. Int. Congr. Photosynth., Rehovot, Israel (Avron, M., ed.), Vol. 2, pp 1131-1146, Elsevier/North Holland, Amsterdam.

Crofts, A.R., Crowther, D., Celis, H., Celis, S.A. and Tierney, G. (1977) Proton pumps in bacterial photosynthesis. Biochem. Soc. Trans. 5, 491-495.

Crofts, A.R., Meinhardt, S.W., Jones, K.R. and Snozzi, M. (1983) The role of the quinone pool in the cyclic electron-transfer chain of Rhodopseudomonas Sphaeroides. A modified Q-cycle mechanism. Biochim. Biophys. Acta 723, 202-218.

Crowther, D. and Hind, G. (1980) Partial characterization of cyclic electron transport in intact chloroplasts. Arch. Biochem. Biophys. 204, 568-577.

Crowther, D. and Hind, G. (1982) Stoichiometry of proton release to electron flow during plastoquinol oxidation. ARC Report.

Crowther, D., Mills, J.D. and Hind, G. (1979) Protonmotive cyclic electron flow around photosystem I in intact chloroplasts. FEBS Lett. 98, 386-390.

Deamer, D.W. and Packer, L. (1969) Light-dependent anion transport in isolated spinach chloroplasts. Biochim. Biophys. Acta 172, 539-545.

de Grooth, B.G. and Amesz, J. (1977a) Electrochromic absorbance changes of photosynthetic pigments in Rhodopseudomonas sphaeroides. I Stimulation by secondary electron transport at low temperature. Biochim. Biophys. Acta 462, 237-246.

de Grooth, B.G. and Amesz, J. (1977b) Electrochromic absorbance changes of photosynthetic pigments in Rhodopseudomonas sphaeroides.II Analysis of the band shifts of carotenoid and bacteriochlorophyll. Biochim. Biophys. Acta 462, 247-258.

de Grooth, B.G., van Gorkom, H.J. and Meiburg, R.F. (1980) Electrochromic absorbance changes in spinach chloroplasts induced by an external electrical field. Biochim. Biophys. Acta 589, 299-314.

Delosme, R., Zickler, A. and Joliot, P. (1978) Turnover kinetics of photosystem I measured by the electrochromic effect in Chlorella. Biochim. Biophys. Acta 504, 165-174.

de Vries, S., Albracht, S.P.J., Berden, J.A., Marres, C.A.M. and Slater, E.C. (1983) The effect of pH, ubiquinone depletion and myxothiazol on the reduction kinetics of the prosthetic groups of ubiquinol: cytochrome c oxidoreductase. Biochim. Biophys. Acta 723, 91-103.

Diner, B.A. and Delosme, R. (1983) Oxidation-reduction properties of the electron acceptors of photosystem II. I. Redox titration of the flash-induced carotenoid bandshift, of C550 and of the variable fluorescence yield in spinach chloroplasts. Biochim. Biophys. Acta 722, 443-451.

Dolan, E. and Hind, G. (1974) Kinetics of the reduction and oxidation of cytochromes b_6 and f in isolated chloroplasts. Biochim. Biophys. Acta 357, 380- 385.

Dutton, P.L. (1978) Redox potentiometry: Determination of midpoint potentials of oxidation-reduction components of biological electron-transfer systems. Methods in Enzymol. 54, 411-435.

Dutton, P.L. and Prince, R.C. (1978) Equilibrium and disequilibrium in the ubiquinone-cytochrome b-c_2 oxidoreductase of Rhodopseudomonas sphaeroides. FEBS Lett. 91, 15-20.

Dutton, P.L., Petty, K.M., Bonner, H.S. and Morse, S.D. (1975) Cytochrome c_2 and reaction centre Rhodopseudomonas sphaeroides GA membranes. Extinction coefficients, content, half-reduction potentials, kinetics and electric field alterations. Biochim. Biophys. Acta 387, 536-556.

Ellenson, J.L. and Sauer, K. (1976) The electrophotoluminescence of chloroplasts. Photochem. Photobiol. 23, 113-123.

Emrich, H.M., Junge, W. and Witt, H.T. (1969) Further evidence for an optical response of chloroplast bulk pigments to a light induced electrical field in photosynthesis. Z. Naturforsch. 24B, 1144-1146.

Erecinska, M., Chance, B., Wilson, D.F. and Dutton, P.L. (1972) Aerobic reduction of cytochrome b-566 in pigeon-heart mitochondria. Proc. Natl. Acad. Sci. USA 69, 50-54.

Farineau, J., Garab, G., Horvath, G. and Faludi-Daniel, A. (1980) Proton translocation in the slow rise of the flash-induced 515nm absorbance change of intact chloroplasts. FEBS Lett. 118, 119-122.

Ford, R.C. and Barber, J. (1983) Incorporation of sterol into chloroplast thylakoid membranes and its effect on fluidity and function. Planta 158, 35-41.

Forti, G., Bertole, M.L. and Zanetti, G. (1965) Purification and properties of cytochrome f from parsley leaves. Biochim. Biophys. Acta 109, 33-40.

Fowler, C.F. and Kok, B. (1976) Determination of H^+/e^- ratios in chloroplasts with flashing light. Biochim. Biophys. Acta 423, 510-523.

Gabellini, N. and Hauska, G. (1983) Characterization of cytochrome b in the isolated ubiquinol-cytochrome c_2 oxidoreductase from Rhodopseudomonas sphaeroides GA. FEBS Lett. 153, 146-150.

Gabellini, N., Bowyer, J.R., Hurt, E., Melandri, B.A. and Hauska, G. (1982) A cytochrome b/c_1 complex with ubiquinol-cytochrome c_2 oxidoreductase activity from Rhodopseudomonas sphaeroides GA. Eur. J. Biochem. 126, 105-111.

Girvin, M. and Cramer, W.A. (1983) Redox titrations of the slow electrochromic phase in chloroplasts. in: Proc. 6th Intl. Congr. Photosynth. (Sybesma, C., ed.).

Goldbeck, J.H. and Kok, B. (1979) Redox titrations of electron acceptor Q and the plastoquinone pool in photosystem II. Biochim. Biophys. Acta 547, 347-360.

Gräber, P. and Witt, H.T. (1974) On the extent of the electrical potential across the thylakoid membrane induced by continuous light in Chlorella cells. Biochim. Biophys. Acta 333, 389-392.

Gräber, P. and Witt, H.T. (1976) Relations between the electrical potential, pH gradient, proton flux and phosphorylation in the photosynthetic membrane. Biochim. Biophys. Acta 423, 141-163.

Guerrieri, F. and Nelson, B.D. (1975) Studies on the characteristics of a proton pump in phospholipid vesicles inlayed with purified complex III from beef heart mitochondria. FEBS Lett. 54, 339-342.

Haehnel, W. (1977) Electron transport between plastoquinone and chlorophyll A_1 in chloroplasts. II Reaction kinetics and the function of plastocyanin in situ. Biochim. Biophys. Acta 459, 418-441.

Haehnel, W. (1982) On the functional organization of electron transport from plastoquinone to photosystem I. Biochim. Biophys. Acta 682, 245-257.

Haehnel, W., Berzborn, R.J. and Andersson, B. (1981) Localization of the reaction side of plastocyanin from immunological and kinetic studies with inside-out thylakoid vesicles. Biochim. Biophys. Acta 637, 389-399.

Hauska, G., Reimer, S. and Trebst, A. (1974) Native and artificial energy-conserving site in cyclic photophosphorylation systems. Biochim. Biophys. Acta 357, 1-13.

Hauska, G., Hurt, E., Gabellini, N. and Lockau, W. (1983) Comparative aspects of quinol-cytochrome c/plastocyanin oxidoreductases. Biochim. Biophys. Acta 726, 97-133.

Haworth, P., Kyle, D.J., Horton, P. and Arntzen, C.J. (1982) Chloroplast membrane protein phosphorylation. Photochem. Photobiol. 36, 743-748.

Hill, R. and Bendall, F. (1960) Function of the two cytochrome components in chloroplasts: a working hypothesis. Nature 186, 136-137.

Hiyama, T. and Ke, B. (1972) Difference spectra and extinction coefficients of P700. Biochim. Biophys. Acta 267, 160-171.

Holmes, N.G. and Crofts, A.R. (1977) The carotenoid shift in Rhodopseudomonas sphaeroides: the flash induced change. Biochim. Biophys. Acta 459, 492-505.

Hong, Y.Q. and Junge, W. (1983) Localized or delocalized protons in photophosphorylation? On the accessibility of the thylakoid lumen for ions and buffers. Biochim. Biophys. Acta 722, 197-208.

Horton, P. (1983) Control of chloroplast electron transport by phosphorylation of thylakoid proteins. FEBS Lett. 152, 47-52.

Horton, P. and Croze, E. (1979) Characterization of two quenchers of chlorophyll fluorescence with different midpoint oxidation-reduction potentials in chloroplasts. Biochim. Biophys. Acta 545, 188-201.

Horvath, G., Niemi, H.A., Droppa, M. and Faludi-Daniel, A. (1979) Characteristics of the flash-induced 515 nanometer absorbance change of intact isolated chloroplasts. Plant Physiol. 63, 778-782.

Huber, S.C. and Edwards, G.E. (1977) The importance of reducing conditions for the inhibitory action of $DBMIB^+$, antimycin A and $EDAC^+$ on cyclic photophosphorylation. FEBS Lett. 79, 207-211.

Huber, H.-L., Rumber, B. and Siggel, U. (1980) Contribution of membrane potentials to energy conversion in photosynthetic membranes. Ber. Bunsenges. Phys. Chem. 84, 1050-1055.

Hurt, E. and Hauska, G. (1981) A cytochrome f/b_6 complex of five polypeptides with plastoquinol-plastocyanin-oxidoreductase activity from spinach chloroplasts. Eur. J. Biochem. 117, 591-599.

Hurt, E. and Hauska, G. (1982) Oxidant-induced reduction of cytochrome b_6 in the isolated cytochrome b_6/f complex from chloroplasts. Photobiochem. Photobiophys. 4, 9-15.

Hurt, E.C., Hauska, G. and Shahak, Y. (1982) Electrogenic proton translocation by the chloroplast cytochrome b_6/f complex reconstituted into phospholipid vesicles. FEBS Lett. 149, 211-216.

Izawa, S. and Pan, R.L. (1978) Photosystem I electron transport and phosphorylation supported by electron donation to the plastoquinone region. Biochem. Biophys. Res. Comm. 83, 1171-1177.

Jackson, J.B. and Crofts, A.R. (1969) The high energy state in chromatophores from Rhodopseudomonas sphaeroides. FEBS Lett. 4, 185-189.

Jackson, J.B. and Crofts, A.R. (1971) The kinetics of light-induced carotenoid changes in Rhodopseudomonas sphaeroides and their relation to electrical field generation across the chromatophore membrane. Eur. J. Biochem. 18, 120-130.

Jackson, J.B. and Dutton,P.L. (1973) The kinetic and redox potentiometric resolution of the carotenoid shifts in Rhodopseudomonas sphaeroides chromatophores: their relationship to electric field alterations in electron transport and energy coupling. Biochim. Biophys. Acta 325, 102-113.

Joliot, P. and Delosme, R. (1974) Flash-induced 519nm absorption change in green algae. Biochim. Biophys. Acta 357, 267-284.

Junge, W. (1974) Structural features of the primary charge separation across the functional membrane of photosynthesis in green plants. in: Proc. 3rd. Intl. Congr. Photosynth., Rehovot, Israel (Avron, M., ed.), Vol. 1, pp 273-286, Elsevier/North Holland, Amsterdam.

Junge, W. (1977) Membrane potentials in photosynthesis. Ann. Rev. Plant Physiol. 28, 503-536.

Junge, W. and Ausländer, W. (1973) The electric generator in photosynthesis of green plants. I. Vectorial and protolytic properties of the electron transport chain. Biochim. Biophys. Acta 333, 59-70.

Junge, W. and Witt, H.T. (1968) On the ion transport system of photosynthesis. Investigations on a molecular level. Z. Naturforsch. 23B, 244-254.

Junge, W., Ausländer, W., McGeer, A.J. and Runge, T. (1979) The buffering capacity of the internal phase of thylakoids and the magnitude of the pH changes inside under flashing light. Biochim. Biophys. Acta 546, 121-141.

Jurinsic, P., Govindjee and Wraight, C.A. (1978) Membrane potential and microsecond to millisecond delayed light emission after a single excitation flash in isolated chloroplasts. Photochem. Photobiol. 27, 61-71.

Katoh, S., Shiratori, I. and Takamiya, A. (1962) Purification and some properties of spinach plastocyanin. J. Biochem. 51, 32-40.

Kröger, A. and Klingenberg, M. (1973) Further evidence for the pool function of ubiquinone as derived from the inhibition of the electron transport by antimycin. Eur. J. Biochem. 39, 313-323.

Kuhn, H. (1979) Photoprocesses in monolayer assemblies. in: Light-induced charge separation in Biology and Chemistry (Gerischer, H. and Katz, J.J., eds.), pp 151-169, Verlag Chemie, Weinheim.

Larkum, A.W.D. and Bonner, W.D. (1972) Light-induced absorbance changes of P518 in intact chloroplasts. Biochim. Biophys. Acta 256, 396-408.

Leung, K.H. and Hinkle, P.C. (1975) Reconstitution of ion transport and respiratory control in vesicles formed from reduced coenzyme Q-cytochrome c reductase and phospholipids. J. Biol. Chem. 250, 8467-8471.

Liptay, W. (1969) Electrochromism and Solvatochromism. Angew. Chem. Int. Ed. Eng. 8, 177-188.

Malkin, R. (1978) Oxidation-reduction potential dependence of the flash-induced 518nm absorbance change in chloroplasts. FEBS Lett. 87, 329-333.

Malkin, R. and Aparicio, P.J. (1975) Identification of a g = 1.90 high-potential iron-sulphur protein in chloroplasts. Biochem. Biophys. Res. Comm. 63, 1157-1160.

Malkin, R. and Barber, J. (1979) On the function of the fluorescence quenchers in chloroplasts and their relation to the primary electron acceptor of photosystem II. Arch. Biochem. Biophys. 193, 169-178.

Mangel, M., Berns, D.S. and Ilani, A. (1975) Dependence of photosensitivity of bileaflet lipid membranes upon the chlorophyll and carotenoid content. J. Membrane Biol. 20, 171-180.

Matsuura, K., Ishikawa, T. and Nishimura, M. (1980) Correlation of membrane-potential-sensing carotenoid to pigment-protein complex II in Rhodopseudomonas sphaeroides. Biochim. Biophys. Acta 590, 339-344.

McCarty, R.E. and Carmeli, C. (1982) Proton translocating ATPases of photosynthetic membranes. in: Photosynthesis (Govindjee, ed.), Vol. 1, pp 647-695, Academic Press.

Meinhardt, S.W. and Crofts, A.R. (1982) The site and mechanism of action of myxothiazol as an inhibitor of electron transfer in Rhodopseudomonas sphaeroides. FEBS Lett. 149, 217-222.

Melis, A. and Harvey, G.W. (1981) Regulation of photosystem stoichiometry, chlorophyll a and chlorophyll b content and relation to chloroplast ultrastructure. Biochim. Biophys. Acta 637, 138-145.

Michels, P.A.M. and Konings, W.N. (1978) The electrochemical proton gradient generated by light in membrane vesicles and chromatophores from Rhodopseudomonas sphaeroides. Eur.J. Biochem. 85, 147-155.

Mills, J.D., Crowther, D., Slovacek, R.E., Hind, G. and McCarty, R.E. (1979) Electron transport pathways in spinach chloroplasts. Reduction of the primary acceptor of photosystem II by reduced nicotinamide adenine dinucleotide phosphate in the dark. Biochim. Biophys. Acta 547, 127-137.

Mitchell, P. (1961) Coupling of phosphorylation to electron and hydrogen transfer by a chemi-osmotic type of mechanism. Nature 191, 144-148.

Mitchell, P. (1976) Possible molecular mechanisms of the protonmotive function of cytochrome systems. J. Theor. Biol. 62, 327-367.

Mullet, J.E. and Arntzen, C.J. (1981) Identification of a 32-34 kilodalton polypeptide as a herbicide receptor protein in photosystem II. Biochim. Biophys. Acta 635, 236-248.

Mullet, J.E., Burke, J.J. and Arntzen, C.J. (1980) Chlorophyll proteins of photosystem I. Plant Physiol. 65, 814-822.

Nakatani, H.Y. and Barber, J. (1977) An improved method for isolating chloroplasts retaining their outer membranes. Biochim. Biophys. Acta 461, 510-512.

Oettmeier, W., Masson, K., Soll, H.J. and Johanningmeier (1982) Photoaffinity labelling of plastoquinone binding sites. in: 2nd Eur. Bioenerg. Conf., EBEC Reports, Vol. 2, pp 219-220, L.B.T.M.-C.N.R.S., Villeurbanne.

Ohnishi, T. and Trumpower, B.L. (1980) Differential effects of antimycin on ubisemiquinone bound in different environments in isolated succinate-cytochrome c reductase complex. J. Biol. Chem. 255, 3278-3284.

O'Keefe, D.P. and Dutton, P.L. (1981) Cytochrome b oxidation and reduction reactions in the ubiquinone-cytochrome b/c_2 oxidoreductase from Rhodopseudomonas sphaeroides. Biochim. Biophys. Acta 635, 149-166.

O'Keefe, D.P., Prince, R.C. and Dutton, P.L. (1981) The interaction of the reaction centre secondary quinone with the ubiquinone-cytochrome c_2 oxidoreductase in Rhodopseudomonas sphaeroides chromatophores. Biochim. Biophys. Acta 637, 512-522.

Olsen, L.F. and Barber, J. (1981) Origin of the slow component of the electrochromic shift: A charge delocalisation model. FEBS Lett. 123, 90-94.

Olsen, L.F. and Cox, R.P. (1979) Light-induced proton transport by chloroplasts suspended in fluid media at sub-zero temperatures: kinetics and stoichiometry. Eur. J. Biochem. 95, 427-432.

Olsen, L.F., Telfer, A. and Barber, J. (1980) A flash spectroscopic study of the kinetics of the electrochromic shift, proton release and the redox behaviour of cytochromes f and b-563 during cyclic electron flow. FEBS Lett. 118, 11-17.

Packham, N.K., Berriman, J.A. and Jackson, J.B. (1978) The charging capacitance of the chromatophore membrane. FEBS Lett. 89, 205-210.

Packham, N.K., Packham, C., Mueller, P., Tiede, D. and Dutton, P.L. (1980) Reconstitution of photochemically active reaction centres in planar phospholipid membranes. Light-induced electrical currents under voltage-clamped conditions. FEBS Lett. 110, 101-106.

Papa, S., Lorusso, M. and Guerrieri, F. (1975) Mechanism of respiration-driven proton translocation in the inner mitochondrial membrane. Analysis of proton translocation associated with oxidation of endogenous ubiquinol. Biochim. Biophys. Acta 387, 425-440.

Parson, W.W. and Ke, B. (1982) Primary photochemical reactions. in: Photosynthesis (Govindjee, ed.), Vol. 1, pp 331-385, Academic Press.

Petty, K.M. and Dutton, P.L. (1976a) Properties of the flash-induced proton binding encountered in membranes of Rhodopseudomonas sphaeroides: a functional pK on the ubisemiquinone? Arch. Biochem. Biophys. 172, 335-345.

Petty, K.M. and Dutton, P.L. (1976b) Ubiquinone-cytochrome b electron and proton transfer: A functional pK on cytochrome b_{560} in Rhodopseudomonas sphaeroides membranes. Arch. Biochem. Biophys. 172, 346-353.

Petty, K.M., Jackson, J.B. and Dutton, P.L. (1977) Kinetics and stoichiometry of proton binding in Rhodopseudomonas sphaeroides chromatophores. FEBS Lett. 84, 229-303.

Petty, K., Jackson, J.B. and Dutton, P.L. (1979) Factors controlling the binding of two protons per electron transferred through the ubiquinone and cytochrome b/c_2 segment of Rhodopseudomonas sphaeroides chromatophores. Biochim. Biophys. Acta 546, 17-42.

Prince, R.C. and Dutton, P.L. (1975) A kinetic completion of the cyclic photosynthetic electron pathway of Rhodopseudomonas sphaeroides: cytochrome b-cytochrome c_2 oxidation-reduction. Biochim. Biophys. Acta 387, 609-613.

Prince, R.C. and Dutton, P.L. (1977) Single and multiple turnover reactions in the ubiquinone-cytochrome b-c_2 oxidoreductase of Rhodopseudomonas sphaeroides. The physical chemistry of the major electron donor to cytochrome c_2 and its coupled reactions. Biochim. Biophys. Acta 462, 731-747.

Prince, R.C., Baccarini-Melandri, A., Hauska, G.A., Melandri, B.A. and Crofts, A.R. (1975) Asymmetry of an energy transducing membrane. The location of cytochrome c_2 in Rhodopseudomonas sphaeroides and Rhodopseudomonas capsulata. Biochim. Biophys. Acta 387, 212-227.

Prince, R.C., Linkletter, S.J.G. and Dutton, P.L. (1981) The thermodynamic properties of some commonly used oxidation-reduction mediators, inhibitors, and dyes, as determined by polarography. Biochim. Biophys. Acta 635, 132-148.

Radmer, R. and Cheniae, G. (1977) Mechanisms of oxygen evolution. in: Topics in Photosynthesis (Barber, J., ed.), Vol. 2, pp 303-348, Elsevier/North Holland, Amsterdam.

Reich, R. and Sewe, K.-U. (1977) The effect of molecular polarization on the electrochromism of carotenoids. I. The influence of a carboxylic group. Photochem. Photobiol. 26, 11-17.

Rich, P.R. (1981) A generalized model for the equilibration of quinone pools with their biological donors and acceptors in membrane -bound electron transfer chains. FEBS Lett. 130, 173-178.

Rich, P.R. and Bendall, D.S. (1979) A mechanism for the reduction of cytochromes by quinols in solution and its relevance to biological electron transfer reactions. FEBS Lett. 105,189-194.

Rich, P.R. and Bendall, D.S. (1980a) The redox potentials of the b-type cytochromes of higher plant chloroplasts. Biochim. Biophys. Acta 591, 153-161.

Rich, P.R. and Bendall, D.S. (1980b) The kinetics and thermodynamics of the reduction of cytochrome c by substituted p-benzoquinols in solution. Biochim. Biophys. Acta 592, 506-518.

Roberts, H., Choo, W.M., Smith, S.C., Marzuki, S., Linnane, A.W., Porter, T.H. and Folkers, K. (1979) The site of inhibition of mitochondrial electron transfer by coenzyme Q analogues. Arch. Biochem. Biophys. 191, 306-315.

Robinson, H.H. and Yocum, C.F. (1980) Cyclic photophosphorylation reactions catalyzed by ferredoxin, methyl viologen and anthraquinone sulphonate. Biochim. Biophys. Acta 590, 97-106.

Rumberg, B. (1977) Field changes. in: Encyclopedia of Plant Physiology, New Series, Vol. 5, Photosynthesis I (Trebst, A. and Avron, M., eds.), pp 405-415, Springer-Verlag,Berlin.

Saphon, S., Jackson, J.B. and Witt, H.T. (1975) Electrical potential changes,H^+ translocation and phosphorylation induced by short flash excitation in Rhodopseudomonas sphaeroides chromatophores. Biochim. Biophys. Acta 408,67-82.

Satoh, K. (1974) Action of derivatives of 1,10-phenanthroline on electron transport in chloroplasts. Biochim. Biophys. Acta 333, 127-135.

Satoh, K. (1981) Further characterization of the photosystem II chlorophyll a-protein complex purified from digitonin extracts of spinach chloroplasts-polypeptide composition. in: Proc. 5th Int. Congr. Photosynth. (Akoyunoglou, G., ed.), Vol. 3, pp 55-66, Balaban Int. Sci. Serv., Philadelphia.

Schapendonk, A.H.C.M. and Vredenberg, W.J. (1977) Salt-induced absorbance changes of P515 in broken chloroplasts. Biochim. Biophys. Acta 462, 613-621.

Schapendonk, A.H.C.M. and Vredenberg, W.J. (1979) Activation of the reaction II component of P515 in chloroplasts by pigment system I. FEBS Lett. 106, 257-261.

Schapendonk, A.H.C.M., Vredenberg, W.J. and Tonk, W.J.M. (1979) Studies on the kinetics of the 515nm absorbance changes in chloroplasts. Evidence for the induction of a fast and a slow P515 response upon saturating light flashes. FEBS Lett. 100, 325-330.

Schliephake, W., Junge, W. and Witt, H.T. (1968) Correlation between field formation, proton translocation and the light reactions in photosynthesis. Z. Naturforsch. 23B, 1571-1578.

Schlodder, E. and Witt, H.T. (1980) Electrochromic absorption changes of a chloroplast suspension induced by an external electric field. FEBS Lett. 112, 105-113.

Schmidt, S., Reich, R. and Witt, H.T. (1971a) Electrochromism of chlorophylls and carotenoids in multilayers and in chloroplasts. Naturwissen. 58, 414-415.

Schmidt, S., Reich, R. and Witt, H.T. (1971b) Electrochromic measurements in vitro as a test for the interpretation of field indicating absorption changes in photosynthesis. in: Proc. 2nd. Int. Congr. Photosynth., Stresa, Italy (Forti, G., Avron, M. and Melandri, A., eds.), Vol. 2, pp 1087-1095, Junk, W., The Hague.

Schröder, H., Muhle, H. and Rumberg, B. (1971) Relationship between ion transport phenomena and phosphorylation in chloroplasts. in: Proc. 2nd.Int. Congr. Photosynth., Stresa, Italy (Forti, G., Avron, M. and Melandri, A., eds.), Vol. 2, pp 919-930, Junk. W., The Hague.

Seely, G.R. (1973) Energy transfer in a model of the photosynthetic unit of green plants. J. Theor. Biol. 40, 189-199.

Selak, M.A. and Whitmarsh, J. (1982) Kinetics of the electrogenic step and cytochrome b_6 and f redox changes in chloroplasts. Evidence for a Q-cycle. FEBS Lett. 150, 286-292.

Sewe, K.-U. and Reich, R. (1977) The effect of molecular polarization on the electrochromism of carotenoids. II Lutein-chlorophyll complexes: the origin of the field-indicating absorption change at 520nm in the membranes of photosynthesis. Z. Naturforsch. 32C, 161-171.

Shahak, Y., Crowther, D. and Hind, G. (1980) Endogenous cyclic electron transport in broken chloroplasts. FEBS Lett. 114, 73-78.

Shahak, Y., Crowther, D. and Hind, G. (1981) The involvement of ferredoxin-$NADP^+$ reductase in cyclic electron transport in chloroplasts. Biochim. Biophys. Acta 636, 234-243.

Slater, E.C. (1983) The Q cycle, an ubiquitous mechanism of electron transfer. TIBS 8, 239-242.

Slovacek, R.E. and Hind, G. (1978) Flash spectroscopic studies of cyclic electron flow in intact chloroplasts. Biochem. Biophys. Res. Comm. 84, 901-906.

Slovacek, R.E., Crowther, D. and Hind, G. (1979) Cytochrome function in the cyclic electron transport pathway of chloroplasts. Biochim. Biophys. Acta 547, 138-148.

Stiehl, H.H. and Witt, H.T. (1969) Quantitative treatment of the function of plastoquinone in photosynthesis. Z. Naturforsch. 24B, 1588-1598.

Strichartz, G.R. and Chance, B. (1972) Absorbance changes at 520nm caused by salt addition to chloroplast suspensions in the dark. Biochim. Biophys. Acta 256, 71-84.

Stuart, A.L. and Wasserman, A.R. (1973) Purification of cytochrome b_6. A tightly bound protein in chloroplast membranes. Biochim. Biophys. Acta 314, 284-297.

Surkov, S.A. and Konstantinov, A. (1980) Dibromothymoquinone interaction with the CoQ-cytochrome b locus of the mitochondrial respiratory chain. Further evidence for the Q-cycle. FEBS Lett. 109, 283-288.

Symons, M., Swysen, C. and Sybesma, C. (1977) The light-induced carotenoid absorbance changes in Rhodopseudomonas sphaeroides. An analysis and interpretation of the band shifts. Biochim. Biophys. Acta 462, 706-717.

Takamiya, K. and Dutton, P.L. (1977) The influence of transmembrane potentials of the redox equilibrium between cytochrome c_2 and the reaction centre in Rhodopseudomonas sphaeroides chromatophores. FEBS Lett. 80, 279-284.

Thornber, J. (1975) Chlorophyll-proteins: light-harvesting and reaction centre components of plants. Ann. Rev. Plant Physiol. 26, 127-158.

Thornber, J.P. and Barber, J. (1979) Photosynthetic pigments and models for their organization in vivo. in: Topics in Photosynthesis (Barber, J., ed.), Vol.3, pp 27-70, Elsevier/North Holland, Amsterdam.

Thorne, S.W., Horvath, G., Kahn, A. and Boardman, N.K. (1975) Light-dependent absorption and selective scattering changes at 518nm in chloroplast thylakoid membranes. Proc. Natl. Acad. Sci. USA 72, 3858-3862.

Trebst, A. Harth, E. and Draber, W. (1970) On a new inhibitor of photosynthetic electron-transport in isolated chloroplasts. Z. Naturforsch. 25B, 1157-1159.

Trebst, A., Wietoska, H., Draber, W. and Knops, H.J. (1978) The inhibition of photosynthetic electron flow in chloroplasts by the dinitrophenylether of bromo- or iodo-nitrothymol. Z. Naturforsch. 33C, 919-927.

Trebst, A., Reimer, S., Draber, W. and Knops, H.J. (1979) The effect of analogues of dibromothymoquinone and of bromonitrothymol on photosynthetic electron flow. Z. Naturforsch. 34C, 831-840.

Tributsch, H. (1972) Reaction of the excited chlorophyll molecules at electrodes and in photosynthesis. Photochem. Photobiol. 16, 261-269.

Trumpower, B.L. (1981) Function of the iron-sulphur protein of the cytochrome b-c_1 segment in electron-transfer and energy-conserving reactions of the mitochondrial respiratory chain. Biochim. Biophys. Acta 639, 129-155.

van den Berg, W.H., Prince, R.C., Bashford, C.L., Takamiya, K., Bonner, W.D. and Dutton, P.L. (1979) Electron and proton transport in the ubiquinone cytochrome b-c_2 oxidoreductase of Rhodopseudomonas sphaeroides. Patterns of binding and inhibition by antimycin. J. Biol. Chem. 254, 8594-8604.

Velthuys, B.R. (1978) A third site of proton translocation in green plant photosynthetic electron transport. Proc. Natl. Acad. Sci. USA 75, 6031-6034.

Velthuys, B.R. (1979) Electron flow through plastoquinone and cytochromes b_6 and f in chloroplasts. Proc. Natl. Acad. Sci. USA 76, 2765-2769.

Velthuys, B.R. (1980) Electron and proton transfer events in chloroplasts during a short series of flashes. FEBS Lett. 115, 167-170.

Velthuys, B.R. (1981) Electron-dependent competition between plastoquinone and inhibitors for binding to photosystem II. FEBS Lett. 126, 277-281.

Velthuys, B.R. and Amesz, J. (1974) Charge accumulation at the reducing side of system 2 of photosynthesis. Biochim. Biophys. Acta 333, 85-94.

von Jagow, G. and Engel, W.D. (1980) A model for the cytochrome b dimer of the ubiquinol : cytochrome c oxidoreductase as a proton translocator. FEBS Lett. 111, 1-5.

von Jagow, G. and Engel, W.D. (1981) Complete inhibition of electron transfer from ubiquinol to cytochrome b by the combined action of antimycin and myxothiazol. FEBS Lett. 136, 19-24.

Vredenberg, W.J. and Tonk, W.J.M. (1974) On the coupling of electrical events at the membranes of energized chloroplasts in intact plant leaf cells.FEBS Lett. 42, 236-240.

Webster, G.D., Cogdell, R.J. and Lindsay, J.G. (1980) Identification of the carotenoid present in the B-800-850 antenna complex from Rhodopseudomonas capsulata as that which responds electrochromically to transmembrane electric fields. Biochim. Biophys. Acta 591, 321-330.

Wikström, M.K.F. and Berden, J.A. (1972) Oxidoreduction of cytochrome b in the presence of antimycin. Biochim. Biophys. Acta 283, 403-420.

Wikström, M. and Krab, K. (1980) Respiration-linked H^+ translocation in mitochondria: stoichiometry and mechanism. Curr. Top. Bioenerg. 10, 51-101.

Wikström, M., Krab, K. and Saraste, M. (1981) Proton-translocating cytochrome complexes. Ann. Rev. Biochem. 50, 623-655.

Witt, H.T. (1971) Coupling of quanta,electrons, fields, ions and phosphorylation in the functional membrane of photosynthesis. Results by pulse spectroscopic methods. Q. Rev. Biophys. 4, 365-477.

Witt, H.T. (1975) Primary acts of energy conservation in the functional membrane of photosynthesis. in: Bioenergetics of Photosynthesis (Govindjee, ed.), pp 493-554, Academic Press.

Witt, H.T. (1979) Energy conversion in the functional membrane of photosynthesis. Analysis by light pulse and electric pulse methods. The central role of the electric field. Biochim. Biophys. Acta 505, 355-427.

Witt, H.T. and Zickler, A. (1974) Vectorial electron flow across the thylakoid membrane. Further evidence by kinetic measurements with an electrochromic and electrical method. FEBS Lett. 39, 205-208.

Witt, H.T., Schlodder, E. and Gräber, P.(1976) Membrane-bound ATP synthesis generated by an external electric field. FEBS Lett. 69, 272-276.

Wolff, C. and Witt, H.T. (1969) On metastable states of carotenoids in primary events of photosynthesis. Registration by repetitive ultra-short-flash photometry. Z. Naturforsch. 24B, 1031-1037.

Wolff, C., Buchwald, H.-E., Ruppel, H., Witt, K. and Witt, H.T. (1969) Rise time of the light induced electrical field across the functional membrane of photosynthesis.Z. Naturforsch. 24B, 1038-1041.

Wollman, F.-A. and Bennoun, P. (1982) A new chlorophyll-protein complex related to photosystem I in Chlamydomonas reinhardii. Biochim. Biophys. Acta 680, 352-360.

Yamazaki, I. and Ohnishi, T. (1966) One-electron-transfer reactions in biochemical systems. I. Kinetic analysis of the oxidation-reduction equilibrium between quinol-quinone and ferro-ferricytochrome c. Biochim. Biophys. Acta 112, 469-481.

Yu, C.-A. and Yu, L. (1981) Ubiquinone-binding proteins. Biochim. Biophys. Acta 639, 99-128.

Zannoni, D., Prince, R.C., Dutton, P.L. and Marrs, B.L. (1980) Isolation and characterization of a cytochrome c_2- deficient mutant of Rhodopseudomonas capsulata. FEBS Lett. 113, 289-293.

Zickler, A., Witt, H.T. and Boheim, G. (1976) Estimation of the light-induced electrical potential at the functional membrane of photosynthesis using a voltage-dependent ionophore. FEBS Lett. 66, 142-148.

Zimanyi, L. and Garab, G. (1982) Configuration of the light induced electric field in thylakoids and its possible role in the kinetics of the 515nm absorbance change. J. Theor. Biol. 95, 811-821.